Protection of Centriole Engagement in Mitosis by Alternatively Spliced Shugoshin1 Isoforms in Complex with Protein Phosphatase 2A

DISSERTATION

Zur Erlangung des Grades
- Doktor der Naturwissenschaften (Dr. rer. nat.) -
an der Bayreuther Graduiertenschule für Mathematik und Naturwissenschaften (BayNat)

Vorgelegt von
Lisa Mohr, M.Sc.
aus Schweinfurt

Bayreuth, April 2016

Die vorliegende Arbeit wurde in der Zeit von März 2011 bis Dezember 2015 in Bayreuth am Lehrstuhl für Genetik unter der Betreuung von Herrn Prof. Dr. Olaf Stemmann angefertigt.

Vollständiger Abdruck der von der Bayreuther Graduiertenschule für Mathematik und Naturwissenschaften (BayNAT) der Universität Bayreuth genehmigten Dissertation zur Erlangung der akademischen Grades eines Doktors der Naturwissenschaften (Dr. rer. nat.).

Dissertation eingereicht am	11. April 2016
Zulassung durch das Leitungsgremium:	21. April 2016
Wissenschaftliches Kolloquium:	21. Juni 2016

Amtierender Direktor: Prof. Dr. Stephan Kümmel

Prüfungsausschuss:

Prof. Dr. Olaf Stemmann (Erstgutachter)
Prof. Dr. Stefan Geimer (Zweitgutachter)
Prof. Dr. Benedikt Westermann (Vorsitz)
Prof. Dr. Gerrit Begemann

TABLE OF CONTENTS

SUMMARY

Maintaining genome stability requires the chromosome cycle to be coordinated with the centrosome cycle. The challenges of this choreography might partly be met by dual use of the multi-protein complex cohesin in both sister chromatid cohesion and centriole pairing ("engagement"). Chromatin-bound cohesin is removed from chromosome arms by the prophase pathway but protected at centromeres by shugoshin 1 (Sgo1) and associated protein phosphatase 2A (PP2A) until cohesin's Scc1 subunit is proteolytically cleaved at the metaphase to anaphase transition and sister chromatids separate. Intriguingly, recent data by our and other groups suggested that prophase pathway signaling and separase's proteolytic activity also bring about centriole disengagement and, moreover, that Sgo1 is counteracting this licensing step of later centrosome duplication.

It was reported that an alternatively spliced isoform of Sgo1 localizes and functions at centrosomes rather than centromeres. Inspired by this initial study, I used stable Hek293 cell lines that inducibly expressed one of various Sgo1 isoforms from siRNA-resistant transgenes. This allowed me to deplete all endogenous Sgo1 variants by RNAi and replace them by individual isoforms. Localization studies of various isoforms of Sgo1 identified a peptide encoded by an alternatively spliced exon, which not only directs human Sgo1 to centrosomes but at the same time also abrogates its association with centromeres. This centrosomal targeting signal of human Sgo1 (CTS) is transferrable as it specifically directs mCherry to centrosomes. Mutation of just three consecutive amino acids within the corresponding peptide inactivates both the pro-centrosomal as well as the anti-centromeric targeting effect. Importantly, localization closely correlates with function as revealed by rescue experiments: Whereas centromere-associated isoforms of Sgo1 protect only sister chromatid cohesion, centrosomally bound variants exclusively preserve centriole engagement. The latter function of Sgo1 is dependent on the interaction with PP2A, as centrosome-associated Sgo1 variants with a mutated PP2A binding site are compromised in their ability to support centriole engagement. Premature centriole disengagement caused by Sgo1 depletion was consistently rescued by expression of a fusion protein consisting of the regulatory subunit of PP2A and the CTS. Sgo1

seems to directly counteract the prophase pathway at the centrosomes, analogous to its role at the chromosomes, since artificially abrogating the prophase pathway rescued the Sgo1 knockdown phenotypes. It is known that the final trigger of centriole disengagement is cleavage by separase. Therefore, I checked for removal of remaining cohesin from the centrosomes over time. Cohesin disappeared from the centrosomes only upon activation of separase in anaphase, which correlated with the timing of centriole disengagement in late mitosis.

Sgo2, the second vertebrate shugoshin, has an essential cohesin protective function in meiosis but why it is also expressed in mitosis remains largely enigmatic. Although Sgo2 does not contain a CTS, it was observed to also localize to the centrosome. A knockdown/rescue assay revealed that Sgo2, like Sgo1, contributes to the preservation of centriole engagement. Like at meiotic chromosomes, this newly discovered role of Sgo2 at mitotic centrosomes also depends on the recruitment of PP2A.

My findings unequivocally demonstrate that Sgo1's centromeric function to protect cohesin from the prophase pathway by recruiting PP2A is conserved on centrosomes. As the protector of chromatid cohesion and centriole engagement Sgo1 is a key regulator for faithful mitosis.

ZUSAMMENFASSUNG

Um die Genomstabilität aufrecht zu erhalten, muss der Chromosomenzyklus mit dem Centrosomenzyklus koordiniert werden. Diese Choreographie wird unter anderem durch die zweifache Verwendung des Multiproteinkomplex Cohesin sowohl beim Zusammenhalt der Schwesterchromatiden als auch bei der Kopplung der Centriolen erreicht. Von den Chromosomenarmen wird Cohesin durch den Prophase-Weg entfernt. An den Centromeren hingegen beschützt Shugoshin 1 (Sgo1) zusammen mit assoziierter Protein Phosphatase 2A (PP2A) Cohesin. Erst am Übergang von Metaphase zu Anaphase wird die Scc1 Untereinheit von Cohesin proteolytisch gespalten wodurch die Schwesterchromatiden endgültig voneinander getrennt werden. Interessanterweise weisen neuste Daten unserer und anderer Gruppen darauf hin, dass Prophase-Weg und proteolytische Aktivität von Separase außerdem die Entkopplung von Centriolen, dem Lizensierungsschritt der späteren Centrosomenduplikation, verursachen und dass Sgo1 dem entgegenwirkt.

Eine alternativ gespleißte Isoform von Sgo1 lokalisiert ans Centrosom und nicht ans Centromer und wirkt auch dort. Inspiriert von dieser initialen Studie verwendete ich stabile Hek293 Zelllinien, die induzierbar eine der verschiedenen Sgo1 Isoformen siRNA-resistent exprimierten. Das erlaubte mir, alle endogenen Sgo1 Varianten mit Hilfe von RNAi zu depletieren und durch einzelne Isoformen zu ersetzen. Durch Lokalisationsstudien der Sgo1-Isoformen wurde ein Peptid identifiziert, welches nicht nur centrosomale Rekrutierung vermittelt, sondern zugleich auch die centromerische Lokalisation verhindert. Diese CTS (für *centrosomal targeting signal of human Sgo1*), die von einem alternativ gespleißten Exon kodiert wird, ist übertragbar, da sie in der Lage ist, mCherry an die Centrosomen zu rekrutieren. Mutation von nur drei aufeinanderfolgenden Aminosäuren innerhalb der CTS inaktiviert sowohl die pro-centrosomale, als auch die anti-centromerischen Lokalisierungs-Effekt. Wie Rettungsexperimente zeigten, korreliert die Lokalisation der Sgo1 Isoformen direkt mit ihrer Funktion: Die Centromer-assoziierte Sgo1 Isoform beschützt ausschließlich Kohäsion der Schwesterchromatiden, wohingegen centrosomal gebundene Varianten ausschließlich die Kopplung der Centriolen aufrechterhalten. Es zeigte

sich, dass hierfür die Interaktion von Sgo1 mit PP2A essentiell ist, da die Centrosom-assoziierten Sgo1-Varianten, deren PP2A-Bindungsstelle mutiert ist, nicht mehr in der Lage sind die Kopplung der Centriolen zu beschützen. Außerdem rettete die Expression eines Fusionsproteins bestehend aus der regulatorischen Untereinheit von PP2A und der CTS die durch Sgo1-Knockdown verursachte vorzeitige Entkopplung der Centriolen. Sgo1 scheint zudem an den Centrosomen, wie auch den Chromosomen, direkt dem Prophase-Weg entgegenzuwirken, da die künstliche Inhibierung des Prophase-Wegs die Sgo1 Knockdown-Phänotypen rettet. Es war bekannt, dass der endgültige Auslöser der Entkopplung der Centriolen die Spaltung durch Separase ist. Daher überprüfte ich die Entfernung von Cohesin von den Centrosomen über die Zeit: Cohesin verschwand von den Centrosomen nur nach Aktivierung von Separase in Anaphase, was mit dem Entkoppeln der Centriolen am Ende der Mitose korreliert.

Sgo2, das zweite Shugoshin in Vertebraten, hat eine essentielle Schutzfunktion von Cohesin in Meiose. Es ist allerdings noch unbekannt, weshalb es auch in Mitose exprimiert wird. Obwohl Sgo2 keine CTS trägt, lokalisiert es an die Centrosomen. Ein Knockdown/Rettungs-Versuch zeigte, dass Sgo2, wie Sgo1, zur Erhaltung der Centriolenkopplung beiträgt. Diese neu entdeckte Rolle von Sgo2 ist an mitotischen Centrosomen, wie auch an meiotischen, abhängig von der Rekrutierung von PP2A. Meine Ergebnisse zeigen eindeutig, dass die centromerische Funktion von Sgo1, Cohesin vor dem Prophase-Weg durch Rekrutierung von PP2A zu schützen, am Centrosom konserviert ist. Als Beschützer von Chromatid-Kohäsion und Centriolenkopplung ist Sgo1 somit ein wichtiger Regulator fehlerfreier Mitose.

1. INTRODUCTION

1.1. The cell cycle

The cell cycle's purpose is to pass on the genetic information of a cell to the next generation. In order to create two identical daughter cells, the DNA must be replicated with high fidelity and evenly distributed among the daughter cells, so that each cell inherits one complete genome. Replication and segregation of DNA are the two main phases of the chromosome cycle. The duplication of one- to two-chromatid chromosomes occurs during S phase (S for synthesis). In mitosis, the sister chromatids are separated from each other before the cytoplasm is divided in cytokinesis. Mitosis and cytokinesis together make up the M phase. To generate two identical and functioning daughter cells, in addition to the chromosomes, the mass of proteins and organelles also has to be duplicated. This happens in most eukaryotic cells in the so-called Gap-phases (G1 phase between M and S phase and G2 phase between S phase and mitosis). G1, S and G2 phases together are referred to as interphase.

Protein phosphorylations and dephosphorylations as well as proteasomal degradation are the most common mechanisms by which the cell cycle is driven and the transition from one to the next phase is regulated. The activity of the cyclin-dependent kinase 1 (Cdk1) for example, is necessary in order to enter into mitosis, while its subsequent inactivation by degradation of cyclin B is a prerequisite for mitotic exit and entry into G1 phase (reviewed in Murray, 2004). To ensure that all processes of the previous phase have been completed before the next phase is initiated, the cell cycle is tightly regulated. Therefore, the cell possesses various so-called checkpoints, at which, when necessary, the cell cycle can be stopped, for example because of DNA damage or nutrient deficiency (reviewed in Kastan and Bartek, 2004).

1.2. Mitosis

Error-free segregation of chromatids into newly forming daughter cells is one of the most critical steps of mitosis, as mistakes can lead to aneuploidy (reviewed in (Venkatesan et al., 2015). The processes occurring in mitosis have to follow a strict order. Mitosis is divided in prophase, prometaphase, metaphase, anaphase and telophase (figure 1). In prophase chromosomes begin to condense, the nuclear membrane dissolves, and the centrosomes move apart to form the mitotic spindle. This spindle apparatus consists of three types of microtubules (MTs): The polar MTs connect the two poles, as they are overlapping in the middle of the spindle and connected by motor proteins. Astral MTs interact with the cell cortex, which allows the positioning of the spindle in the cell. After disintegration of the nuclear envelope, the kinetochore MTs (k-fibers) associate with the chromosomes via large protein structures on top of the centromeres, called kinetochores (prometaphase). In order to segregate sister chromatids properly, the two kinetochores of each chromosome have to be attached to MTs emanating from opposite poles of the mitotic spindle (see 1.5.6). To ensure proper chromatid segregation, the cell employs a control mechanism, the so-called spindle-assembly checkpoint (SAC, see 1.4.2). The SAC prevents mitotic progression until all kinetochores are properly attached to the spindle and chromosomes are aligned in the so-called metaphase plate. If this is the case, the SAC is switched off, the cohesion between the sister chromatids is dissolved and chromatids move apart (anaphase). They are pulled to the opposite spindle poles by shortening of k-fibers (anaphase A), as well as pushed apart as the motor proteins of overlapping polar MTs elongate the spindle (anaphase B). In telophase, the chomatids reach the spindle poles and start to decondense. A new nuclear envelope forms around the two separated chromosome masses. Finally, the cell membrane is constricted by a contractile ring of actin and myosin filaments between the emerging nuclei, which divides the cytoplasm and thus completes the cell division by cytokinesis.

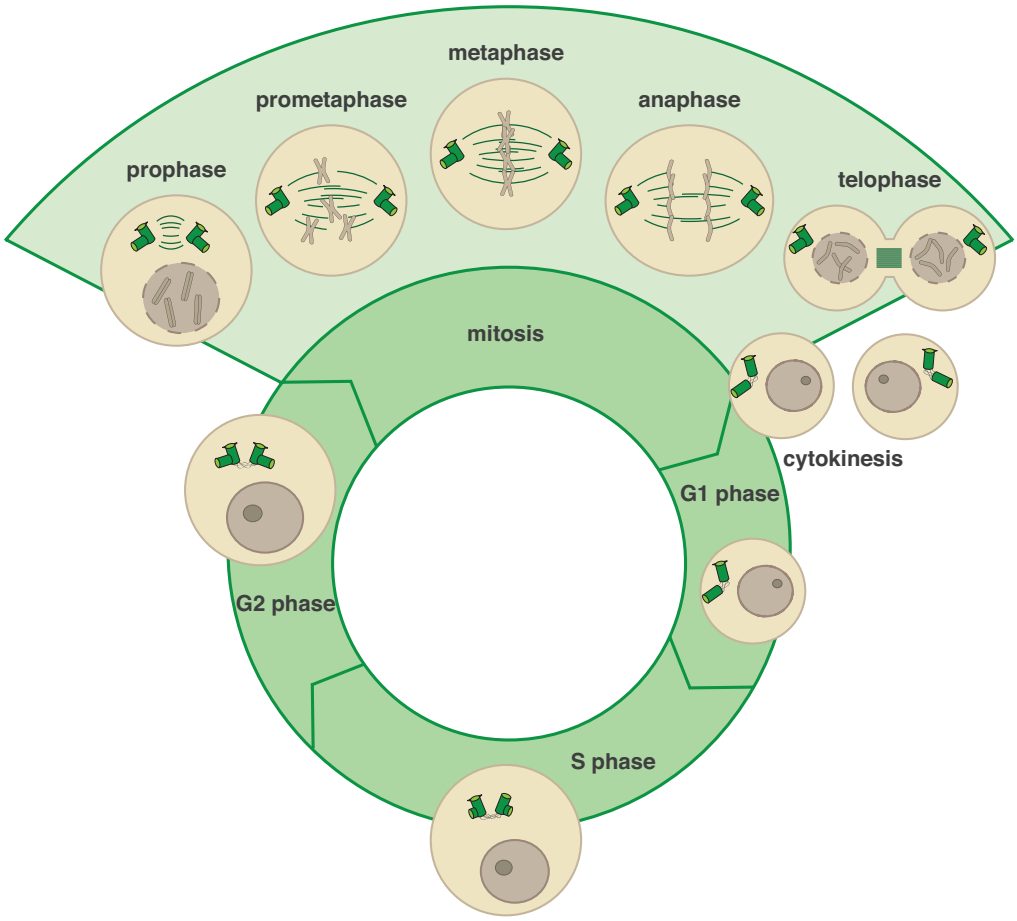

figure 1. The eukaryotic cell cycle. The cell cycle is divided in interphase (consisting of G1, S and G2 phase; G for gap and S for synthesis) and M phase (consisting of mitosis and cytokinesis). In S phase, the chromatids are duplicated (replication). In mitosis, chromatids (depicted in brown) become attached to the mitotic spindle (depicted in green) and equally distributed into the two daughter cells. For details see text.

1.3. Sister chromatid cohesion

1.3.1. The cohesin ring complex

Sister chromatids are held together from the time of their synthesis in S phase until their separation at the metaphase to anaphase transition. This cohesion is mediated by the multi-subunit complex cohesin, consisting of a tripartite ring structure composed of Smc1 (structural maintenance of cohesion), Smc3 and Scc1 (sister chromatid cohesion) plus associated proteins like SA1/2 and Pds5A/B (figure 2). The polypeptide chains of the Smc proteins fold back onto themselves at a central hinge region, thereby forming long anti-parallel coiled-coil domains (Haering et al., 2002; Melby et al., 1998). Smc1 and Smc3 strongly interact with each other via their hinge domains. N- and C-terminus of each Smc subunit together form a globular ATPase

domain (Arumugam et al., 2003; Melby et al., 1998). Scc1, a member of the kleisin family, binds to Smc3 via its N-terminus and to Smc1 via its C-terminus. The ring-complex has a diameter of about 45 nm and entraps both sister chromatids topologically within its ring structure (Gruber et al., 2003; Haering et al., 2002). SA1/2 (Scc3 in yeast) is peripherally associated with Scc1 and performs regulatory tasks (Zhang et al., 2008). Pds5 serves as a binding-platform for either Wapl or sororin in a mutually exclusive manner (Nishiyama et al., 2010; see 1.3.4).

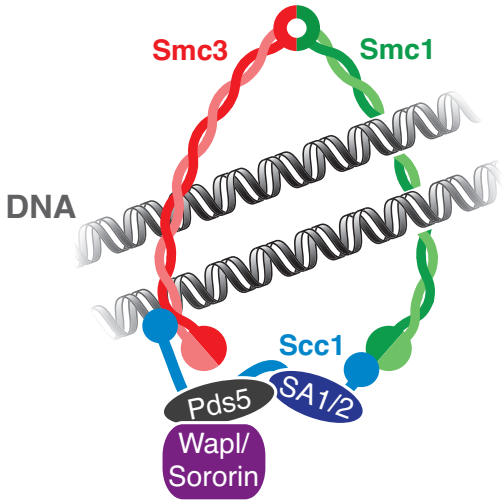

figure 2. The cohesin ring complex. Smc1, Smc3 and Scc1 form a ring that entraps both sister chromatids. Associated proteins are Pds5, which binds either Wapl or sororin, and SA1/2. Figure modified from (Buheitel and Stemmann, 2013). For details see text.

1.3.2. Loading of cohesin and establishment of cohesion

In vertebrates, the loading of cohesin onto DNA is already initiated in telophase (Losada et al., 1998, G1 in yeast, Kogut et al., 2009). As first identified in yeast, cohesin is loaded by the Scc2/Scc4 complex/kollerin (Ciosk et al., 2000; Nasmyth, 2011). This complex can also be found in humans (here the Scc2 ortholog is called Nipped-B like or NIPBL) and it was furthermore shown that loss of either subunit leads to loss of sister chromatid cohesion (Krantz et al., 2004; Tonkin et al., 2004; Watrin et al., 2006). How kollerin mediates the loading of cohesin is not completely understood yet. Kollerin has been shown to transiently interact with cohesin, thereby stimulating the ATPase domains of the Smc head domains (Hu et al., 2011; Ladurner et al., 2014; Weitzer et al., 2003). ATP hydrolysis is required to transiently open cohesin at the Smc1/Smc3 gate, which allows topological loading of cohesin onto

DNA (Buheitel and Stemmann, 2013; Gruber et al., 2006). Cohesin interaction with DNA is highly dynamic in G1 phase as loading by kollerin is constantly counteracted by removal of the ring by the action of Wapl, which binds to Pds5 (Gerlich et al., 2006; Kueng et al., 2006). It should be noted that according to a new study in yeast, the opening of the Scc1-Smc3 gate might facilitate both, loading and unloading of cohesin onto and off DNA (Murayama and Uhlmann, 2015).

Stable association of cohesin with DNA and establishment of cohesion occur in S phase, when the second chromatid is synthesized. During replication, Smc3 is acetylated by the acetyltransferase Eco1 (ESCO1 and ESCO2 in vertebrates), which renders cohesin insensitive to the action of Wapl (Rolef Ben-Shahar et al., 2008; Rowland et al., 2009; Zhang et al., 2008). In humans, establishment of cohesion depends also on sororin, an antagonist of Wapl. Acetylation of Smc3 facilitates binding of sororin to Pds5, thereby dislodging Wapl from cohesin (Nishiyama et al., 2010). After replication is completed, cohesin entraps both sister chromatids over the complete length of the chromosome.

1.3.3. Resolution of cohesion

In order to segregate the chromatids at the metaphase to anaphase transition, sister chromatid cohesion has to be resolved. During vertebrate mitosis, cohesin is removed from chromatin in two steps. The bulk of cohesin, located on chromosome arms, is non-proteolytically removed already during prophase by the action of the so-called prophase pathway (Waizenegger et al., 2000; see1.3.4), while centromere-associated complexes remain protected by shugoshin 1 (Sgo1) until the metaphase to anaphase transition, when Scc1 becomes cleaved by the cysteine protease separase (Uhlmann et al., 1999; see 1.4.1).

1.3.4. The prophase pathway

The prophase pathway depends on the phosphorylation of the cohesin subunits SA2 by Plk1 and of sororin by Aurora B and Cdk1 (Hauf et al., 2005; Nishiyama et al., 2013). This destabilizes the interaction of Pds5 with sororin at mitotic entry, upon

which the latter is replaced by Wapl (Dreier et al., 2011; Liu et al., 2013b; Nishiyama et al., 2013; figure 3). Wapl then drives opening of the cohesin ring at the Smc3-Scc1 interaction site (the so-called exit gate), leading to the release of cohesin from chromosome arms (Buheitel and Stemmann, 2013; Chan et al., 2012; Eichinger et al., 2013). At the centromere, Sgo1 in complex with protein phosphatase 2A (PP2A) is recruited to cohesin (see 1.5.3 and 1.5.5) and dephosphorylates sororin and SA2, thus antagonizing mitotic phosphorylations and, by extension, the prophase pathway (Kitajima et al., 2006; Liu et al., 2013b; Riedel et al., 2006). Therefore, a knockdown of endogenous Sgo1 leads to premature loss of sister chromatid cohesion due to abrogated protection of cohesin from the prophase pathway (McGuinness et al., 2005; Tang et al., 2004). Interestingly, the Sgo1-PP2A-mediated dephosphorylation of sororin and SA2 seems to prevent the removal of cohesin by two independent mechanisms, since co-expression of non-phosphorylatable sororin and SA2 mutants have an additive effect on cohesin dissociation (Nishiyama et al., 2013). New studies suggest, that Sgo1/PP2A and the C-terminus of Wapl bind to the same region of SA2 (Hara et al., 2014; Roig et al., 2014). Therefore, phosphorylation-dependent binding of Sgo1 to cohesin in mitosis would also physically prevent the binding of Wapl. Remarkably, the biological purpose of the prophase pathway was unknown for some time, since separase seemed to be able to resolve all sister chromatid cohesion when the prophase pathway had been inactivated (Buheitel and Stemmann, 2013; Gandhi et al., 2006). But recently, it has been shown that separase can only manage to cleave this excess of cohesin for several cell divisions, since long-term depletion of Wapl leads to defects in chromosome segregation (Haarhuis et al., 2013). This effect could arise from incomplete proteolysis of cohesin by separase, making the prophase pathway indispensable to reduce the amount of cohesin that has to be cleaved by separase.

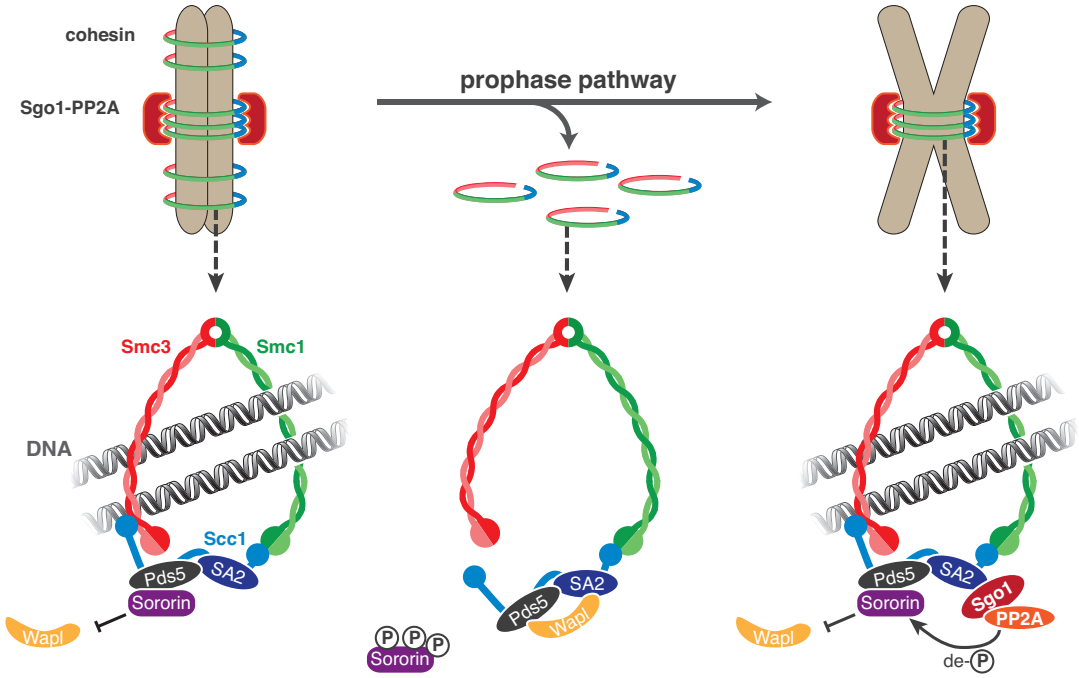

figure 3. The prophase pathway. In prophase, the cohesin rings are removed from the chromosome arms by opening of the gate between the Smc3 and Scc1 subunits of cohesin in a phosphorylation dependent manner. At the centromere however, this is counteracted by Sgo1-PP2A, which protect centromeric cohesion. For details see text.

1.4. Regulation of the metaphase to anaphase transition

1.4.1. Separase

The Sgo1-PP2A dependent protection of cohesin renders sister chromatid separation dependent on proteolytic cleavage by the cysteine endopeptidase separase. Only when kinetochores are attached to MTs of the spindle in a bipolar manner, separase becomes active and cleaves the Scc1 subunit of cohesin (Uhlmann et al., 1999). This is a critical step, since premature loss of sister chromatid cohesion or persistent cohesion results in misdistribution of the chromatids. To prevent this, separase is tightly kept in check by its mutually exclusive inhibitors securin and cyclinB/Cdk1 until the metaphase to anaphase transition (Gorr et al., 2005; Stemmann et al., 2001). For most of the cell cycle, securin binds to and inhibits separase (Yamamoto et al., 1996; Zou et al., 1999). This mechanism of inhibition has been found in all eukaryotes studied so far (Cohen-Fix et al., 1996; Funabiki et al., 1996; Leismann et al., 2000; Zou et al., 1999). How exactly securin interacts with separase, has not yet been fully elucidated. However, there are indications that the C-terminus of securin interacts with the N-terminus of separase (Holland et al., 2007; Jäger et al., 2004) and that the

catalytic site of separase (C-terminus) interacts with the middle region of securin (Csizmok et al., 2008). In addition to its role as an inhibitor, securin also has a positive effect on separase and *vice versa*. So does overexpression of separase lead to an increased amount of securin in human cells (Holland and Taylor, 2006), while, on the other hand, the protease is not only less abundant but also less active in securin knock out cells (Jallepalli et al., 2001; Pfleghaar et al., 2005). Recently it has been shown that securin associates with separase in a co-translational manner and thereby functions as a chaperone to promote correct protein folding (Hellmuth et al., 2015a). Although securin plays such an important role in separase regulation, in mice and humans it seems to be dispensable for normal mitotic progression (Mei et al., 2001; Pfleghaar et al., 2005), presumably because there is an alternative way of separase inhibition by Cdk1/cyclin B. In vertebrates, separase is phosphorylated by Cdk1 (cyclin-dependend kinase 1) dependent on cyclin B1 at S112, which enables inhibitory binding of cyclin B1 (Boos et al., 2008; Gorr et al., 2005; Stemmann et al., 2001). Hellmuth and colleagues showed recently that phosphorylation of separase primes it for isomerization by the peptidyl-prolyl isomerase Pin1, which is a prerequisite for cyclin B1 binding (Hellmuth et al., 2015b). Since the inhibitors bind to different conformational stages of separase, securin and cyclin B1 inhibition of separase are mutually exclusive. In order to activate separase, its inhibitors are ubiquitylated by an ubiquitin ligase called APC/C (anaphase promoting complex/cyclosome; Glotzer et al., 1991; Pfleger et al., 2001; Yamamoto et al., 1996) and degraded by the proteasome. Cyclin B1 carries a D-box (destruction box; RxxL) and securin has a D-box and a KEN-box, which both are recognition sites for this Cullin-RING finger E3-ubiquitin ligase (reviewed in Chang and Barford, 2014).

Separase exist in all eukaryotes, but only the last 600 amino acids are conserved (Viadiu et al., 2005). It cleaves its substrates at a conserved site (consensus ExxR). Besides Scc1, substrates of separase include Rec8 and Rad21L, which replace Scc1 in meiotic cohesin (Buonomo et al., 2000; Kudo et al., 2009 and Lisa Mohr, unpublished data), and in vertebrates it even exerts self-cleavage (Waizenegger et al., 2002). Just recently, a novel separase substrate has been found: the centrosomal scaffold protein kendrin/pericentrin B (PCNT; Lee and Rhee, 2012; Matsuo et al., 2012; see 1.6.5).

1.4.2. Control of meta- to anaphase transition

Since activation of separase is dependent on APC/C, it is crucial that the ubiquitin ligase is inhibited until the kinetochores of each chromosome are properly, i.e. amphitelically, attached to MTs (see 1.5.6). Directly after nuclear envelope breakdown (NEBD), a complex of the SAC components Mad1 and Mad2 (mitotic arrest deficient) is recruited to unattached kinetochores (Chen et al., 1998; Shannon et al., 2002). This recruitment depends on the checkpoint kinases Aurora B and Mps1 (Santaguida et al., 2010). Soluble Mad2 is found in a so-called open conformational stage (Luo et al., 2004). The binding of Mad1 to Mad 2 results in a conformational change of Mad2 to a closed stage (Luo et al., 2002). Closed Mad2 can in turn bind to and change the conformation of soluble Mad2, which then binds to Cdc20, the coactivator of the APC/C (De Antoni et al., 2005). The Mad2-Cdc20 complex binds additional checkpoint proteins BubR1 and its cofactor Bub3, thereby forming the so-called mitotic checkpoint complex (MCC; Hardwick et al., 2000; Sudakin et al., 2001). By sequestering Cdc20 as well as by direct binding to the APC/C, the MCC inhibits the ubiquitin ligase, which results in stabilization of its substrates cyclin B and securin. A recent study suggests, that the MCC becomes already assembled before NEBD in a kinetochore-independent manner in order to make the SAC response faster and more sensitive (Rodriguez-Bravo et al., 2014).

As soon as all kinetochores are properly attached and under tension, the checkpoint has to be silenced, but the mechanisms of checkpoint inactivation are only poorly understood. Several mechanisms have been proposed, such as removing SAC proteins from the kinetochores (Howell et al., 2001) or their APC/C-dependent ubiquitylation (Palframan et al., 2006; Reddy et al., 2007). Furthermore, the Mad2 inhibitor $p31^{comet}$ has been described to cause the disassembly of the MCC, which promotes the dissociation of Cdc20 (Mapelli et al., 2006; Teichner et al., 2011; Vink et al., 2006). Once Cdc20 is released, the APC/C is activated, resulting in the degradation of securin and cyclin B, which in turn activates separase. Proteolysis of Scc1 opens the cohesin ring, separates the chromatids and thereby initiates anaphase. The degradation of cyclin B furthermore inactivates Cdk1, which is necessary to prevent reactivation of the SAC (since Cdk1/cyclinB are important for checkpoint signaling; Vázquez-Novelle et al., 2014) and for mitotic exit.

1.5. Shugoshin and PP2A

1.5.1. Discovery of shugoshin

A protector of centromeric cohesion was fist discovered in *Drosophila*, where a corresponding mutant, *mei-S332*, suffered from premature loss of centromeric cohesion during meiosis I. Mei-S332 was furthermore found to localize to the centromeres during meiosis until anaphase II (Kerrebrock et al., 1992; 1995). Later screens identified related genes in budding and fission yeast (Katis et al., 2004; Kitajima et al., 2004; Marston et al., 2004; Rabitsch et al., 2004). Members of this new protein family were named shugoshins (Sgo), Japanese for guardian spirit. In 2004, Salic and coworkers found a mitotic function of shugoshin in vertebrates, where it counteracted the activity of the prophase pathway by protecting centromeric cohesin (Salic et al., 2004). While budding yeast and *Drosophila* have only one shugoshin protein, fission yeast, plants, *Xenopus laevis* and mammals possess two paralogs (Shugoshin 1 and 2; Gutiérrez-Caballero et al., 2011). In humans, Sgo1 (or SgoL1) carries mitotic functions, whereas Sgo2 (or SgoL2) plays a role in meiosis. Although they are considered to be orthologs, the members of the Sgo family are poorly conserved in their amino acid sequences, except for an N-terminal coiled-coil domain for PP2A binding and homodimerization (see 1.5.5) and a C-terminal “SGO” motif (also called Sgo C-box) for interaction with phosphorylated Histone 2A (see 1.5.3; figure 4; reviewed in Marston, 2015). Furthermore, Sgo1 has two destruction boxes (KEN- and D-boxes). The APC^{Cdh1}-dependent degradation of yeast Sgo1 occurs at the end of mitosis but is not required for separation of sister chromatids or mitotic exit (Karamysheva et al., 2009).

1.5.2. Sgo1 isoforms

In humans, there are 13 different mature transcripts of the Sgo1 gene derived from alternative splicing (ENSEMBL: ENSG00000129810). Of these, only 11 can theoretically be translated to a maximum of 7 different proteins (some mRNAs differ only in the length of their UTRs), of which 6 retain the two structural hallmarks of shugoshins, i.e. the N-terminal coiled-coil region and the conserved C-terminal Sgo C-box (figure 4). The terminology for the isoforms describes the composition of exons

in their mature mRNA (see figure 4A). A, B or C stand for the presence, partial presence or absence of exon 6, respectively, and an additional 1 indicates the absence of exon 9, while a 2 stands for its presence. So far, only three Sgo1 isoforms have been investigated: the well-characterized, centromeric Sgo1 A1, whose mRNA contains exon 6 but misses exon 9, the shorter Sgo1 C2 (sSgo1; Wang et al., 2006; 2008), with its mRNA missing exon 6 but containing exon 9, and Sgo1 B1, whose mRNA contains only part of exon 6 and lacks exon 9 (see figure 4A). The latter is only expressed in certain cancers and is considered to be a product of incorrect splicing as it localizes to the centromere but has a dominant-negative effect on cohesion (Matsuura et al., 2013).

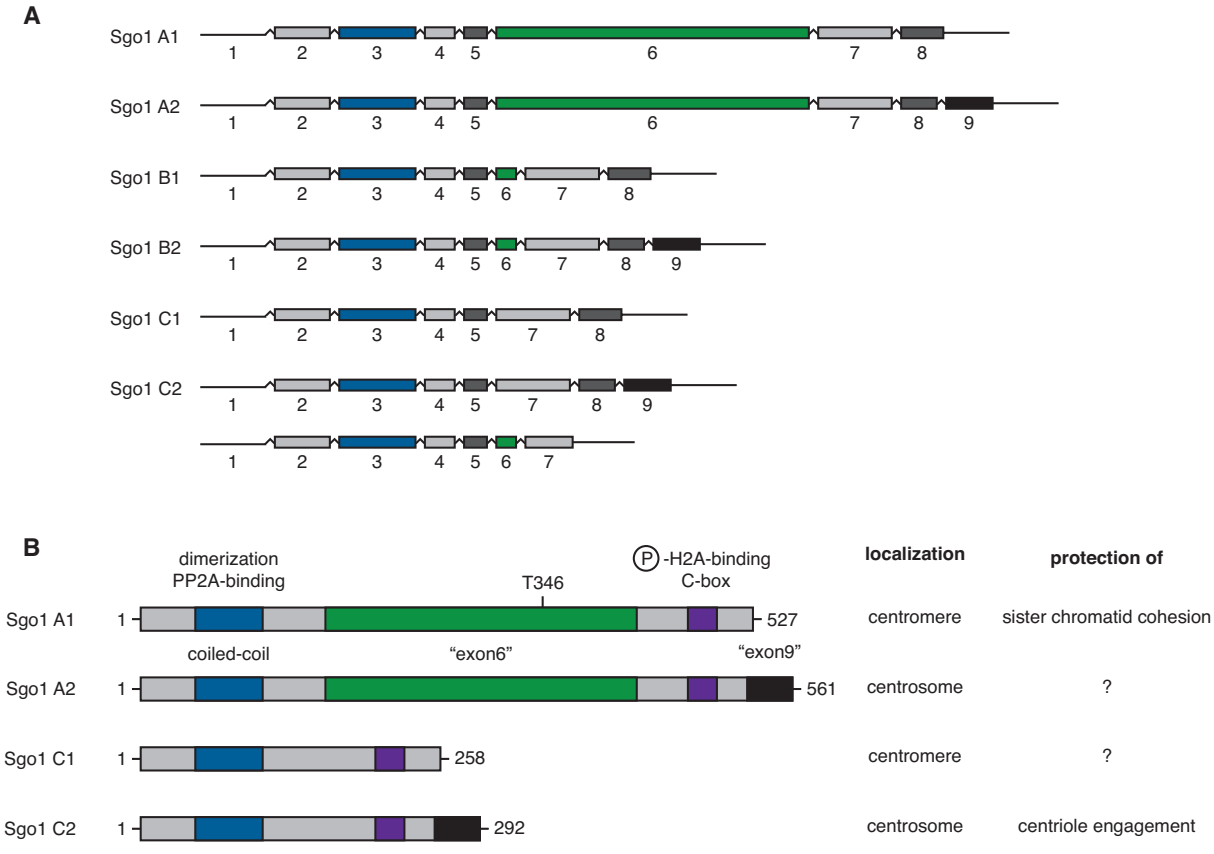

figure 4. The different splice variants of Sgo1
(A) Overview of SGO1 transcript variants. The numbers represent exons (exons 1–9). The boxes indicate the coding exons.
(B) Schematic view of Sgo1 isoforms drawn to scale. The N-terminal coiled-coil, important for dimerization and PP2A binding is shown in blue, the Sgo-C-box (phosphorylated H2A-binding site) in purple, the peptides encoded by exon 6 and exon 9 are marked green and black, respectively.

While the canonical Sgo1 A1 localizes to centromeres and protects sister chromatid cohesion, the short Sgo1 C2 (also called sSgo1) was reported to localize to

centrosomes (Tang et al., 2004; Wang et al., 2006; 2008). Since one difference between those two isoforms was the presence (A1) or absence (C2) of the peptide encoded by exon 6, it was speculated that the missing exon 6 caused the localization of Sgo1 C2 to the centrosome. Whether other isoforms had specific localizations and functions had not yet been studied. In fact, further analysis of the localization of Sgo1 A1, A2, C1 and C2 by our group revealed that, as previously described, Sgo1 A1 localizes to centromeres and Sgo1 C2 to centrosomes, while Sgo1 A2 localizes to centrosomes but not centromeres (Mohr et al., 2015). This was surprising, since Sgo1 A2 is identical to A1 except for only 40 additional amino acids at its C-terminus, which are encoded by exon 9. In contrast, Sgo1 C1, which represents C2 minus the 40 C-terminal amino acids encoded by exon 9, is found at centromeres and not centrosomes (Mohr et al., 2015). These observations suggest that not the lack of exon 6 but rather the presence of the tiny exon 9 in the mRNA might dictate a centrosomal localization of Sgo1 protein isoforms. For these reasons, the peptide encoded by exon 9 will henceforth be referred to as ‘‘centrosomal targeting signal of human Sgo1’’ (CTS).

1.5.3. Recruitment of Sgo1 to the centromere

There are two steps required for proper centromeric recruitment of Sgo1 A1. In mitosis, Bub1 kinase phosphorylates the centromeric histone 2A at T120, which is then bound by Sgo1 A1 via its Sgo C-box (Kawashima et al., 2010; Yamagishi et al., 2010). Upon Cdk1-dependent phosphorylation of Sgo1 A1 at T346, the complex is then handed over to cohesin (Liu et al., 2013b), where it interacts directly with the complex's SA2/Scc1 subunits (Hara et al., 2014). Recently it has been shown that Sgo1 interacts with RNA polymerase II, which is recruited to and promotes transcription at mitotic kinetochores (Liu et al., 2015). This interaction enables Sgo1 to reach centromeric cohesin. Interestingly, Liu and coworkers demonstrated that a Sgo C-box mutant (K492A) was able to prevent Sgo1 depletion-mediated loss of sister chromatid cohesion, while the T346A mutant was not, revealing that the direct interaction with cohesin is paramount for Sgo1’s function in mitosis (Liu et al., 2013b; 2013a). Nevertheless, the initial interaction with pH2A is important for proper centromere recruitment of Sgo1 A1, as the K492A mutant localized all over the

chromosome arms (Liu et al., 2013a). The localization of Sgo1 A1 remains dynamic during mitosis: At metaphase, bi-oriented sister kinetochores experience tension, which triggers Sgo1's redistribution from the inner centromere (via binding to cohesin) to the kinetochores (via binding to pH2A). This redistribution seems to facilitate correct chromosome segregation (Liu et al., 2013a).

1.5.4. PP2A

PP2A is an important serine/threonine phosphatase, which is involved in the regulation of many cellular processes such cell cycle progression, DNA replication, apoptosis, transcription and translation, cytoskeleton dynamics, cell metabolism (reviewed in Seshacharyulu et al., 2013) and has furthermore been linked to cell transformation and cancer (Alberts et al., 1993; Glenn and Eckhart, 1993; Ronne et al., 1991; Schönthal, 2001; Tung et al., 1985). It consists of three subunits: a structural A subunit (PP2A A), a regulatory B subunit (PP2A B) and a catalytical C subunit (PP2A C). The core dimer consists of the 65 kDa scaffolding subunit A and the 36 kDa C subunit (Guo et al., 1993). There exist two isoforms for each, the A and C subunit: PP2A Aα and -β differ in their ability to bind the various B subunits, while PP2A Cα and -β determine the localization of the enzyme. Full activity and intracellular localization is only achieved upon interaction of the PP2A A and C with one of the various PP2A B subunits, which also mediate substrate specificity. For human PP2A B, at least 26 different variants encoded by 15 different genes have been described (Zolnierowicz et al., 1994). The PP2A B subunits are classified into four different families: B (B55), B' (B56), B'' and B'''. Although they are binding to similar recognition sequences of PP2A A, the PP2A B variants are poorly conserved concerning their amino acid sequence or structure (reviewed in Lechward et al., 2001).

1.5.5. Sgo1-PP2A interaction

At the centromere, Sgo1 and -2 are interaction partners of PP2A (Kitajima et al., 2006; Riedel et al., 2006), where they protect cohesin from untimely removal (see

1.3.4 and 1.5.7). It has been shown that both PP2A and Sgo1 are needed to protect centromeric cohesion in mitosis, since knockdown of either leads to premature loss of sister chromatid cohesion (Kitajima et al., 2006; McGuinness et al., 2005; Tang et al., 2004). In 2009, Xu and colleagues uncovered the structure of the interaction site. Two Sgo proteins form a homodimeric parallel coiled coil via their N-termini, which then binds to the B'γ and Cα subunits of the PP2A holoenzyme. Based on this structure, they were able to create several mutants of Sgo1 that still dimerized but lost their ability to bind to PP2A (Xu et al., 2009). There is still a controversy, whether Sgo1 recruits PP2A to centromeres or *vice versa*. Several points speak for Sgo1-recruitment by PP2A: First, Sgo1's localization to centromeres is dramatically reduced upon depletion of PP2A A (Kitajima et al., 2005) and a PP2A-binding deficient variant of Sgo1 is neither able to localize to the centromeres, nor to prevent premature loss of sister chromatid cohesion caused by Sgo1 depletion (Tang et al., 2006). Second, even after Sgo1 depletion, PP2A can still be found localized to the centromeres (Kitajima et al., 2006). In this case however, PP2A alone is not able to prevent premature separation of sister chromatids. As already mentioned, the key element of cohesion protection is the direct interaction of Sgo1 with cohesin, where it serves as a adaptor molecule for PP2A (Liu et al., 2013a). Therefore, Sgo1 might not be required for initial recruitment of PP2A, but rather for directing it to its substrate.

1.5.6. Sgo1's role in chromosome biorientation

Besides protection of cohesin form the prophase pathway, Sgo1 promotes correct amphitelic attachment of the spindle MTs to the kinetochores (figure 5). During early mitosis, MTs connect to the kinetochores using a search and capture mechanism, which often results in incorrectly attached kinetochores (figure 5). While monotelic attachment is recognized by the SAC, merotelically or syntelically attached kinetochores are connected to MTs, but microtubule forces do not generate a tension between the kinetochores. This can be sensed by a second branch of the mitotic checkpoint, sometimes also referred to as the tension checkpoint. Lack of tension leads to centromeric recruitment of the chromosomal passenger complex (CPC) with its subunits Aurora B, INCENP, survivin and borealin. In humans, borealin gets

phosphorylated in early mitosis by Cdk1 and is then able to bind to shugoshin via its N-terminal coiled coil region, which recruits the CPC to the centromere (Tsukahara et al., 2010). Aurora B then phosphorylates components of the KMN network (for KNL1/Mis12 complex/Ndc80 complex) and CENP-E, both involved in chromosome-spindle attachment, lowering their affinity towards MTs (Kim et al., 2010; Welburn et al., 2010). The recruitment of the CPC by Sgo1 therefore corrects errors in microtubule attachment, dependent on phosphorylations by its subunit Aurora B. Thus, the role of the tension-sensitive arm of the mitotic checkpoint might simply lie in the generation of unattached kinetochores and therefore a signal for the canonical SAC. However, it has been shown in the past that Aurora B can also prevent mitotic progression directly (Santaguida et al., 2011).

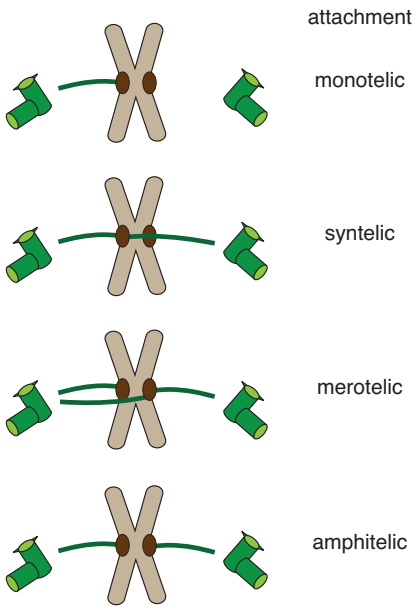

figure 5. Different types of kinetochore-microtubule attachments. Chromosomes are shown in light brown, kinetochores in dark brown, and centrosomes (spindle poles) and microtubules in green. Monotelic attachment: only one kinetochore is attached to microtubules from one spindle pole. Syntelic attachment: both kinetochores are connected to microtubules from the same spindle pole. Merotelic attachment: combination of syntelic and monotelic attachment. Amphitelic attachment: correct bipolar attachment with both kinetochores attached to opposite spindle poles.

In contrast, Foley and coworkers showed that Sgo1 also seems to promote binding of microtubules to kinetochores as it recruits PP2A with its B' subunit to the centromere. There, the phosphatase counteracts attachment-inhibiting phosphorylations by Aurora B and Cdk1 (Foley et al., 2011). Therefore, Sgo1 plays a role in both, promoting and counteracting microtubule attachment to kinetochores and with that in proper chromosome biorientation.

Interestingly, the human meiotic Sgo2 is also expressed in somatic cells and implicated in mitotic chromosome biorientation. Upon phosphorylation by Aurora B, Sgo2 recruits MCAK (mitotic centromere-associated kinesin) to the centromeres (Huang et al., 2007; Tanno et al., 2010). This kinesin is known to promote proper kinetochore-microtubule attachment by depolymerizing microtubules under the control of Aurora B (Andrews et al., 2004; Kline-Smith et al., 2004; Lan et al., 2004). However, it has been shown, that this function of Sgo2 is not essential for mitosis (Llano et al., 2008; Orth et al., 2011).

1.5.7. Meiosis and Sgo2

Sexual reproduction relies on the production of complementary gametes that together contribute all of the components necessary for normal embryonic development. In meiosis, the genome content is reduced by half because DNA replication is followed by two consecutive chromosome segregation events (meiosis I and meiosis II). Here, sister chromatids are held together by a meiosis-specific form of cohesin, in which Smc1β, Stag3 and Rec8 or Rad21L subunits replace Smc1α, SA1/2 and Scc1, respectively (Gutiérrez-Caballero et al., 2011; Klein et al., 1999; Pezzi et al., 2000; Polakova et al., 2011; Prieto et al., 2001; Revenkova et al., 2001; 2004; Watanabe and Nurse, 1999). During meiosis I, the maternal and paternal chromosomes (or "homologs") are separated. Therefore, they have to be paired at the beginning of meiosis I. Recently it has been shown that homolog recognition is mediated by cohesin with its meiosis specific subunit Rad21L (Ishiguro et al., 2014). Homolog pairing is then achieved by the formation of a structure called the synaptonemal complex, which enables reciprocal exchange between homologs by meiotic recombination (so-called chiasmata; Baudat et al., 2013). Segregation of the homologs requires each pair of sistster kinetochores to attach to microtubules from the same spindle pole (monoorientation). At this stage, sister chromatids, as well as homologs are held together by Rec8 containing cohesin (Buonomo et al., 2000; Klein et al., 1999). At the transition of metaphase to anaphase of meiosis I, separase becomes active and separates the homologs by only cleaving cohesin at the chromosome arms (Buonomo et al., 2000). The centromeric cohesin is protected by

Sgo2-PP2A, since Rec8 can only be proteolysed upon phosphorylation by Casein kinase 1 (CK1) and Dbf4-dependent Cdc7 kinase (DDK, Katis et al., 2010; Rumpf et al., 2010). This phosphorylation can only be established at the chromosome arms, while centromeric Rec8 phosphorylation is counteracted by Sgo2-PP2A, which thereby protects the cohesion of sister chromatids (Ishiguro et al., 2010; Riedel et al., 2006).

In meiosis II, similar to mitosis, sister chromatids are segregated after cleavage of centromeric cohesin by separase. For this, protection of Rec8 by Sgo2 and therefore PP2A has to be lifted. Sgo2 has been shown to colocalize with Rec8 from early meiosis I on, but also that it relocalizes to the kinetochores and with that away from Rec8 as soon as sister chromatids are bioriented and under tension in metaphase of meiosis II (Gómez et al., 2007; Lee et al., 2008). However, another study showed that PP2A still colocalized with Rec8 even after Sgo2 removal in meiosis II (Chambon et al., 2013). This led to the proposal that centromeric PP2A is inactivated by a specific inhibitor called I2PP2A. Deprotection of Rec8 might therefore dependent more inhibition of PP2A than relocalization of Sgo2.

1.6. The centrosome

Using early light microscopy of mitotic cells, Theodor Boveri first discovered centrosomes in the 1880s, but it was not before the 1950s, when electronmicroscopical studies were able to eluminate the complex structure of the organelle (Bernhard and De Harven, 1956; Sveshnikova, 1952). As microtubule-organizing centers (MTOCs) in metazoans and most unicellular eukaryotes (but not in higher land plants and yeast, Marshall, 2009), they form the spindle poles in mitosis and meiosis and function as basal bodies, which nucleate the formation of cilia. While plants don't posses specific organelles that function as MTOCs, yeast employs so-called spindle pole bodies that are embedded into the nuclear envelope and form the spindle in yeast's closed mitosis (Byers et al., 1978; Marshall, 2009).

1.6.1. Organization of the centrosome

A mature centrosome in G2-phase consists of two cylindrical centrioles, which are arranged orthogonally to each other and surrounded by the electron-dense pericentriolar material (PCM). The older centriole is called the mother centriole and differs from the younger daughter centriole in additional structural and functional features, since it possesses a set of distal and subdistal appendages. While the subdistal appendages are involved in microtubule anchoring to the centrosome (reviewed in Bornens, 2002), the distal appendages are required for the docking process with the cell membrane, which is a prerequisite for the formation of cilia (reviewed in Keeling et al., 2016). In humans, centrioles are roughly 200 nm in diameter and 500 nm in length. Inside the proximal part of their cylindrical structure, each centriole features a cartwheel structure with nine spokes that are each linked to microtubule triplets (duplets in *Drosophila* and singlets in *C. elegans*), which gives centrioles a nine-fold symmetry (figure 6A).

The PCM surrounds (part of) the centrioles and contains over 100 different proteins (Lüders and Stearns, 2007). In a recent study from the Pelletier group, more than 7000 proteins have been reported to interact with the centrosome (Gupta et al., 2015). While the PCM was long described as an “amorphous cloud”, in 2012, using 3D SIM (structured illumination microscopy), four groups could show that it is actually a highly structured toroidal assembly surrounding the mother centriole with distinct concentric layers, each consisting of a specific set of proteins (Fu and Glover, 2012; Lawo et al., 2012; Mennella et al., 2012; Sonnen et al., 2012). The protein CPAP, for example, is located at the interface between the centriole and the PCM, while pericentrin (PCNT) and Cep152 are both elongated molecules that span the PCM from the inner to the outer layers.

When the cell enters mitosis, the PCM dramatically increases in size, which is necessary for the nucleation of microtubules (see 1.6.4; reviewed in Palazzo et al., 2000).

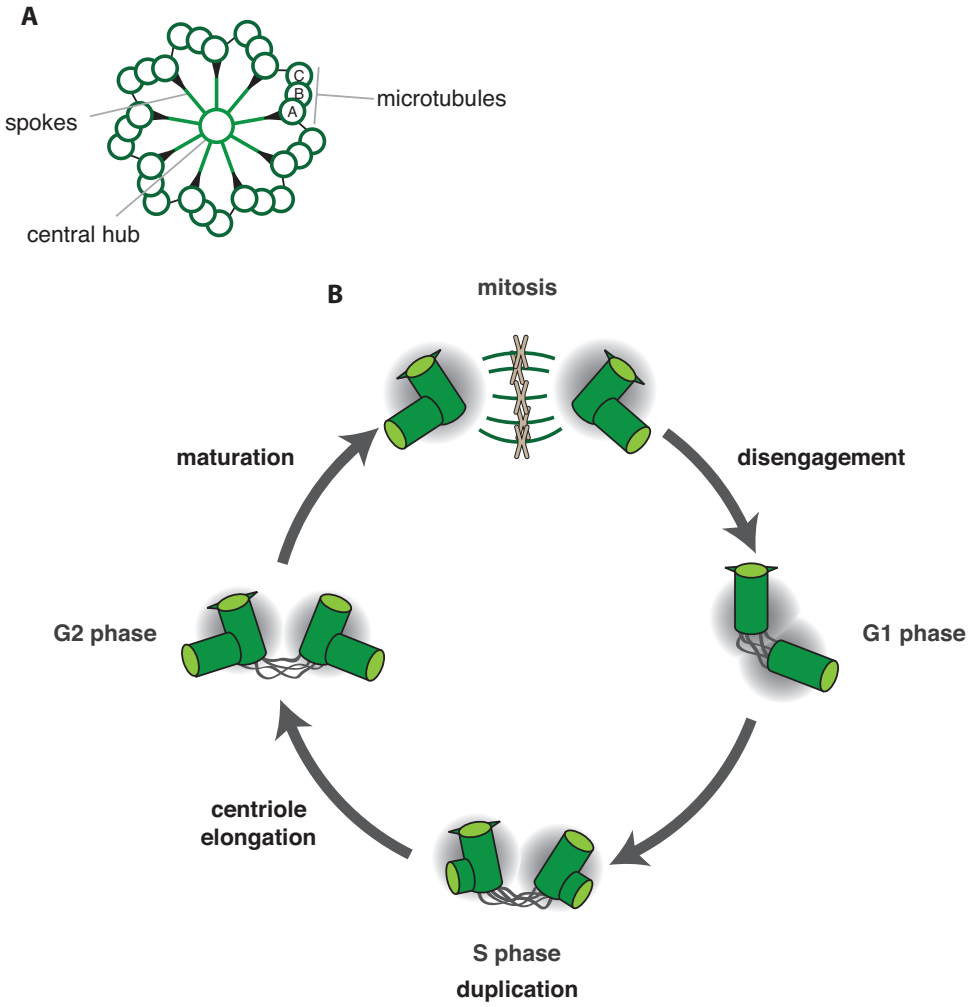

figure 6. The centrosome.
(A) Organization of a centriole, viewed from the proximal end. The nine-fold symmetry of the microtubule triplets is determined by the radial spokes emanating from the central hub.
(B) Duplication of the centrosome during the cell cycle. At the end of mitosis/early G1 phase the two centrioles (depicted in green) disengage and each centriole acquires pericentriolar material (depicted in grey). In S phase, centrioles duplicate and are elongated in the following G2 phase. At mitotic entry, the two mature centrosomes separate from each other to form the bipolar mitotic spindle in order to properly segregate the sister chromatides (depicted in brown). For details see text.

1.6.2. The centrosome duplication cycle

At the beginning of G1 phase, each cell has one centrosome consisting of two centrioles and the surrounding pericentriolar material (PCM). When the cell enters S phase, the centrioles are duplicated as daughter centrioles (at this stage also referred to as procentrioles) are newly assembled orthogonally to each of the existing mother centrioles (Kuriyama and Borisy, 1981, figure 6B). Mother and daughter centrioles are closely linked to each other, a state referred to as ‘‘engaged’’ (Tsou and Stearns, 2006). In G2 phase, the procentrioles elongate until they reach a similar length as the

mother centriole. Just before mitosis, the two fully matured centrosomes ultimately separate in order to form the two poles of the mitotic spindle apparatus. At the same time, the mother centriole begins to accumulate more PCM in order to be able to nucleate the spindle microtubules. After sister chromatid separation at the end of mitosis, the tight association of mother and daughter centriole is lost, while they remain loosely tethered by proteinaceous fibers (Bahe et al., 2005). This process known as centriole disengagement serves as a licensing step for later centriole duplication (Tsou and Stearns, 2006).

1.6.3. Centriole duplication

Like DNA replication, centriole duplication has to be limited to only once per cell cycle in order to prevent overduplication and, on account of this, multipolar spindles. The five components of the core pathway of centriole duplication have been first identified by genetic and RNAi screens in *C. elegans*: SPD-2 (spindle defective) recruits the kinase ZYG-4 (Plk4 in humans), which in turn recruits SAS-6 and SAS-5 (spindle assembly abnormal). This enables binding of SAS-4, which promotes the formation of centriolar microtubules (Dammermann et al., 2004; Delattre et al., 2006; 2004; Kemp et al., 2004; Kirkham et al., 2003; Leidel and Gönczy, 2003; Leidel et al., 2005; O'Connell et al., 2001; Pelletier et al., 2006; 2004). The duplication pathway of the centriole is highly conserved (Balestra et al., 2013; Dobbelaere et al., 2008) and the functional homologs of these factors in humans have been identified in the last years. In humans, there are three processes at the end of mitosis/beginning of G1 phase that are a prerequisite for the following duplication: 1) the centrioles have to disengage (see 1.6.5), 2) the former daughter has to acquire its own PCM (Wang et al., 2011) and 3) has to lose its cartwheel structure (Izquierdo et al., 2014). This centriole to centrosome conversion enables the new mother centriole to start duplication in S Phase (Fong et al., 2014). Then, human Cep192 and Cep152, like SPD-2 in *C. elegans*, recruit the kinase Plk4 to the centrosomes (Firat-Karalar et al., 2014; Sonnen et al., 2013). Plk4 then regulates the initiation of centriole duplication (Habedanck et al., 2005; Kleylein-Sohn et al., 2007). A prerequisite for this step is the binding of the SAS-5 homologue STIL to Plk4. This interaction activates Plk4 by inducing autophosphorylation in its activation loop. Activated Plk4 in turn

phosphorylates STIL, which can then be recruited to the centriole (Moyer et al., 2015). Furthermore, Plk4 together with STIL recruits SAS-6 to the centrioles which initiates the formation of the cartwheel orthogonally to the mother centrioles (Fong et al., 2014; Kleylein-Sohn et al., 2007). SAS-6 multimerizes to form the central hub and the 9 spokes, which are emenating outwards (Cottee et al., 2011; Kitagawa et al., 2011; Schuldt, 2011; van Breugel et al., 2011; figure 6A). STIL, which is positioned at the end of the spokes, finally recruits CPAP (homologue to *C. elegans* SAS-4), concluding the formation of the cartwheel structure. These large multimeres ultimately undergo additional stacking (Arquint et al., 2012; Sonnen et al., 2012; Tang et al., 2009; Vulprecht et al., 2012), while CPAP promotes the polymerization of centriolar A, B and C microtubules at the tip of the spokes (Kohlmaier et al., 2009; Schmidt et al., 2009; Tang et al., 2009).

It is crucial that the abundance of the proteins involved in centriole duplication is tightly regulated, as imbalances can cause serious problems. An overexpression of Plk4, for example, induces formation of flower-like centrioles with multiple procentrioles surrounding one mother centriole (Kleylein-Sohn et al., 2007) and overexpression of STIL or SAS-6 leads to overduplication (Arquint et al., 2012; Tang et al., 2009; Vulprecht et al., 2012).

But how is duplication of centrioles limited to S phase and synchronized with DNA replication? There are several factors that limit duplication of centrioles to S Phase. Like DNA replication, duplication depends on Cdk2 and its cofactor cyclin E, the latter of which is only present in late G1 and early S Phase (Matsumoto et al., 1999; Meraldi et al., 1999). Furthermore, there are several DNA (pre-)replication factors like the helicase component Mcm5, the pre-replicative complex subunit Orc1, as well as the replication licensing-inhibitor geminin present at the centrosome (reviewed in Bettencourt-Dias and Glover, 2007). Interestingly, all of these factors seem to play a role in inhibiting centrosome reduplication, as depletion of either of those factors was separately shown to cause overduplication of centrosomes by an as yet unknown mechanism (Ferguson and Maller, 2008; Ferguson et al., 2010; Hemerly et al., 2009; Lu et al., 2009; Tachibana et al., 2005). Additionally, re- and overduplication are prevented by SCF (Skp-cullin-F-box class ubiquitin ligase)-mediated degradation of Plk4 (Cunha-Ferreira et al., 2009; Holland et al., 2012; Rogers et al., 2009).

1.6.4. Centrosome maturation, disjunction and spindle formation

Duplicated centrosomes remain associated by a proteinaceous linker, consisting of rootletin and C-Nap1 (see also 1.6.5). At the G2/M transition however, the centrosomes have to move apart in order to form the mitotic spindle. Therefore, the linker is removed upon phosphorylation of rootletin and C-Nap1 by the kinase Nek2A (Bahe et al., 2005; Fry et al., 1998; Helps et al., 2000). Upstream this process is regulated by Plk1, as phosphorylation by Plk1 prevents binding of protein phosphatase 1 (PP1) to Nek2A, which until then counteracts phosphorylation of C-Nap1 (Helps et al., 2000; Mardin et al., 2011). Thereby, Plk1 promotes splitting of centrosomes, which is followed by a spatial separation. Plk1 additionally promotes the maturation of the PCM by phosphorylation of PCNT. This leads to a massive accumulation of proteins required for microtubule polymerization such as γ-tubulin, Cep192 and NEDD1, as well as PCNT and Plk1 itself, and thereby to an extension of the PMC, while its inner core retains its interphasic configuration (Lee:2011er; Lawo et al., 2012). The accumulation of proteins in the extended PCM enables the formation of γ-tubulin ring complexes (γTuRCs), giant 2.2 MDa ring shaped complexes consisting of γ-tubulin and associated γ-tubulin complex proteins (GCP2-6) (Choi et al., 2010; Teixidó-Travesa et al., 2010), (Gomez-Ferreria et al., 2007; Lüders et al., 2006; Takahashi et al., 2002; Zhu et al., 2008; Zimmerman et al., 2004). The γTuRCs then promote the formation of microtubules, the main components of the mitotic spindle. MTs are hollow tubes with a polarized structure, which are assembled from α- and β-tubulin heterodimers in a GTP-dependent manner. By longitudinal contacts between the heterodimers, they form protofilaments, which interact with each other laterally to form a tubular structure (Nogales et al., 1999; 1998). According to the widely accepted template model, the γTuRC facilitates this last step by acting as a template to assemble 13 tubulin protofilaments into a circular/tubular structure, the microtubule. It also stabilizes the microtubule by forming a cap at its so-called minus end to prevent depolymerization (Moritz et al., 2000; Wiese and Zheng, 2000). The plus ends of the MTs further polymerize and extend to ultimately form the mitotic spindle.

The separation of the spindle poles depends on these polymerizing MTs as well as the associated motor protein Eg5 (Kapoor et al., 2000; Mardin et al., 2010). This

member of the kinesin 5 subfamily forms homotetramers, which interconnect antiparallel MTs of opposite centrosomes and push them apart by plus end-directed movement (Kashina et al., 1996).

1.6.5. Centriole disengagement

It has been shown that centrioles, which were transferred form human cell culture into a cycling *Xenopus* egg extract, were only able to duplicate in the following S phase if they disengaged in the prior mitosis, while engaged centrioles had to be cycled through mitosis first, to allow for their duplication in the next S phase (Tsou and Stearns, 2006). The processes behind disengagement of the centrioles were unknown until 2009, when Tsou and colleagues surprisingly demonstrated that centriole disengagement, like separation of sister chromatids, depends on separase activity (Tsou et al., 2009). But what was the centrosomal target of separase? Interestingly, Schöckel and colleagues found that target to be the cohesin subunit Scc1, extending the parallels between separation of sister chromatids and disengagement of centrioles (Schöckel et al., 2011). They showed that overexpression of a non-cleavable Scc1 cohesin subunit prevents centriole disengagement while ectopic cleavage of an engineered variant promotes it. The same was true for artificially cleavable Smc3, whose proteolysis also led to disengagement. Several cohesin subunits (including Smc1 and -3) had already be reported to localize to the centrosome many years ago (Beauchene et al., 2010; Gregson et al., 2001; Guan et al., 2008; Kong et al., 2009; Wong and Blobel, 2008) and a recent screen confirmed this for almost all cohesin subunits (Smc1, Smc3, Scc1, SA2 and Pds5; Gupta et al., 2015). Therefore, it is tempting to speculate that the whole cohesin ring might contribute to the cohesion between mother and daughter centriole. Additionally, it was reported that separase-mediated cleavage of the PCM component PCNT at a conserved cleavage site, is also necessary and sufficient to trigger centriole disengagement (Lee and Rhee, 2011; Matsuo et al., 2012). For Scc1 it has been shown that phosphorylation by Plk1 improves its cleavage by separase at the centrosome (Agircan and Schiebel, 2014) and for PCNT cleavage it is even indispensable, since a phosphorylation-resistant mutant of PCNT was no longer cleaved by separase at all (Kim et al., 2015). Nevertheless, the

relative contributions of separase-dependent cleavage of cohesin and PCNT to centriole disengagement remain enigmatic.

After disengagement, the centioles are still held together by a proteinaceous linker, which is formed at the end of mitosis and connects the disengaged centrioles at their proximal ends: The elongated protein rootletin forms fibers, which are connected to the proximal end of the centrioles by C-Nap1 (Bahe et al., 2005; Fry et al., 1998; Yang et al., 2006).

1.6.6. Sgo1 at the centrosome

In 2006, a study by the Dai group demonstrated that a short isoform of Sgo1 (Sgo1 C2 or sSgo1) localizes to the mitotic spindle (Wang et al., 2006), and this was further shown to be dependent on Plk1 activity (Wang et al., 2008). As mentioned before (see 1.5.2), we found that not only human Sgo1 C2 but also A2 localized to the centrosomes (Mohr et al., 2015), but it still remained unclear, whether or not this fact bears any biological relevance. Since Sgo1 had previously been shown to interact with microtubules *in vitro* (Salic et al., 2004), it was initially speculated that Sgo1 C2 might regulate the stability of the spindle. However, this theory could not be verified, since Sgo1 depletion had no effect on spindle stability (Wang et al., 2008). Instead, Sgo1 was found to be involved in protecting centriole engagement, as knockdown of endogenous Sgo1 not only lead to premature loss of sister chromatid cohesion (due to abrogated cohesin-protection from the prophase pathway; McGuinness et al., 2005; Tang et al., 2004), but also to premature centriole disengagement (Schöckel et al., 2011; Wang et al., 2008; Yamada et al., 2012). Interestingly, even though alternative splicing of Sgo1 is not conserved in mice (i.e. Sgo1 C2 does not exist), Sgo1 haploinsufficient MEFs exhibited the same phenotypes (Wang et al., 2008), hinting at a conserved function of Sgo1 at the centrosomes in mice. Furthermore, localization of Sgo1 to the spindle pole was shown in *Drosophila* male meiosis (Lee et al., 2005). However, despite an increasing body of research in later years, how exactly Sgo1 functions at the centrosome in protecting centriole engagement has largely remained enigmatic.

1.7. Aim of this work

Not only have two isoforms of Sgo1, Sgo1 C2 and A2, been described to localize to the centrosome (Mohr et al., 2015; Wang et al., 2006), but knockdown of all Sgo1 isoforms leads to premature centriole disengagement in addition to premature loss of sister chromatid cohesion. To further shed light on the centrosomal functions of Sgo1, I sought to conduct Sgo1 knockdown/rescue experiments with human cell lines, which specifically express one single transgenic isoform. With these I wanted to clarify, whether the localization of centrosomal Sgo1 isoforms correlated with a function in protecting the centrioles from premature disengagement. The one region, which centrosomal Sgo1 isoforms have in common, but which is absent in centromeric isoforms, is the 40 amino acids long peptide encoded by exon 9. To better understand the recruitment of Sgo1 A2 and C2 to the centrosome I wanted to characterize this potential centrosomal targeting signal of human Sgo1 (CTS).

At the centromere, Sgo1 collaborates with PP2A, whose phosphatase activity antagonizes phosphorylations essential for the action of the prophase pathway. So far it is unknown, whether PP2A, in collaboration with Sgo1 A2 and/or C2, is also involved in protecting the centrioles from premature disengagement. Therefore, using PP2A-binding deficient variants of the centrosomal Sgo1 isoforms, I wanted to investigate, if PP2A activity was needed at the centrosomes and if the recruitment and function of PP2A to and at the centrosome depended on Sgo1.

The possible involvement of PP2A in protecting centriole engagement and the already characterized necessity of cohesin cleavage by separase to promote centriole disengagement are two striking parallels to the resolution of sister chromatid cohesion. If cohesin is really involved in the engagement of centrioles and opening of its ring (by separase) is required for disengagement at the end of mitosis, then Sgo1-PP2A may prevent premature opening of cohesin and therefore centriole disengagement by a mechanism similar to the protection of centromeric cohesin from the prophase pathway. I sought to test this hypothesis by inhibiting the prophase pathway either by depleting its key player Wapl or by chemically locking the Smc3-Scc1 gate of cohesin (which has to open in order to remove cohesin form the chromosome arms in prophase). If there is a prophase pathway at the centrosome,

these approaches should counteract Sgo1 depletion and prevent centriole disengagement.

2. RESULTS

2.1. Role of Sgo1 at the centrosomes and centromeres

2.1.1. Depletion of Sgo1 causes premature loss of sister chromatid cohesion and centriole disengagement

It has been reported previously that depletion of Sgo1 in human cell culture leads to premature loss of sister chromatid cohesion as well as precocious centriole disengagement (Schöckel et al., 2011; Tang et al., 2004; Wang et al., 2008). I recapitulated this experiment to confirm the Sgo1-depletion phenotypes. To this end, U2OS cells were thymidine-arrested in early S phase, transfected with *SGO1* or a control siRNA (*GL2*), released into G2 phase and finally arrested in prometaphase by addition of taxol. This regime allowed the quantitative synchronization of cells in mitosis, while keeping the spindle toxin-treatment as short as possible. Cells were then harvested and processed for assessment of chromatid cohesion and centriole engagement status. The Sgo1 knockdown was very efficient as judged by Western blot (figure 7A). As expected, sister chromatids were mostly separated in Sgo1 depleted cells (80%), while only 10% of cells exhibited separated chromatids in the knockdown control (figure 7B).

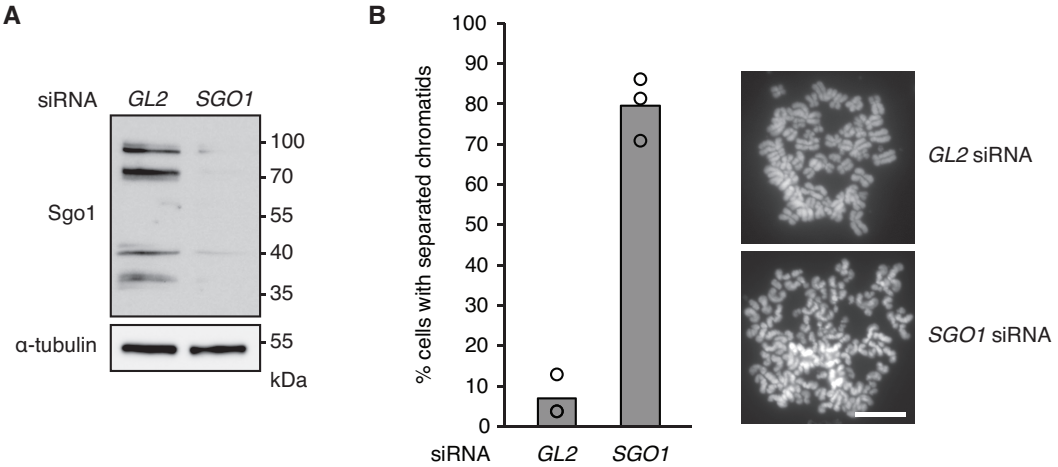

figure 7. Depletion of Sgo1 causes premature loss of sister chromatid cohesion.
(A) U2OS cells were synchronized at the G1/S boundary with thymidine. After 14 hours they were transfected with *SGO1* siRNA and 7 hours later released from thymidine, and finally, 5 hours later, arrested in prometaphase by taxol treatment for 15 hours. The Western blot shows Sgo1 knockdown efficiency. The four bands visible in the anti-Sgo1 blot represent the different variants of Sgo1.
(B) Analysis of chromosome spreads of cells from (A), scale bar: 5 µm. Each column represents averages of three independent experiments (circles, 100 cells each).

To quantify centriole (dis-)engagement, I performed immunofluorescence staining of two centrosomal proteins: The distal centriole marker centrin 2 and the proximal marker C-Nap1. The two mature, engaged centrioles of one centrosome, which can be seen from G2 until late mitosis, are tightly associated. They become disengaged in late mitosis, which means that they lose their tight association but still remain connected by rootletin fibers. With immunofluorescence microscopy (IFM) using centrin 2 and C-Nap1 antibodies the status of engagement can be visualized: For engaged centrioles, two dots of the distal centrin 2 are visible, while the two proximal C-Nap1 signals are very close to each other and cannot be resolved, hence appearing as one dot between the centrin 2 signals. The spatial separation of disengaged centrioles causes the C-Nap1 signal to split into two dots (figure 8A). I tested three different methods to quantify centriole engagement status: IFM *in situ*, on isolated centrosomes and immunofluorescence staining on chromosome spreads.

Cells treated as described above were grown on cover slips. In order to stain the centrosomes *in situ*, cells were pre-extracted with a chilled sucrose- and detergent-containing buffer, which depolymerizes the microtubules, preserves the centrosomes and permeabilizes the cell membrane to remove soluble proteins to eliminate background staining (Gregson et al., 2001). In parallel, centrosomes were pelleted by centrifugation of cell lysates through a sucrose cushion directly onto cover slips. In fixed cells (figure 8B) and on isolated centrosomes (figure 8C), the percentage of disengaged centrioles was much higher in Sgo1 depleted cells than in the control cells (85% *versus* 30% in fixed cells and 65% *versus* 15% in isolated centrosomes).

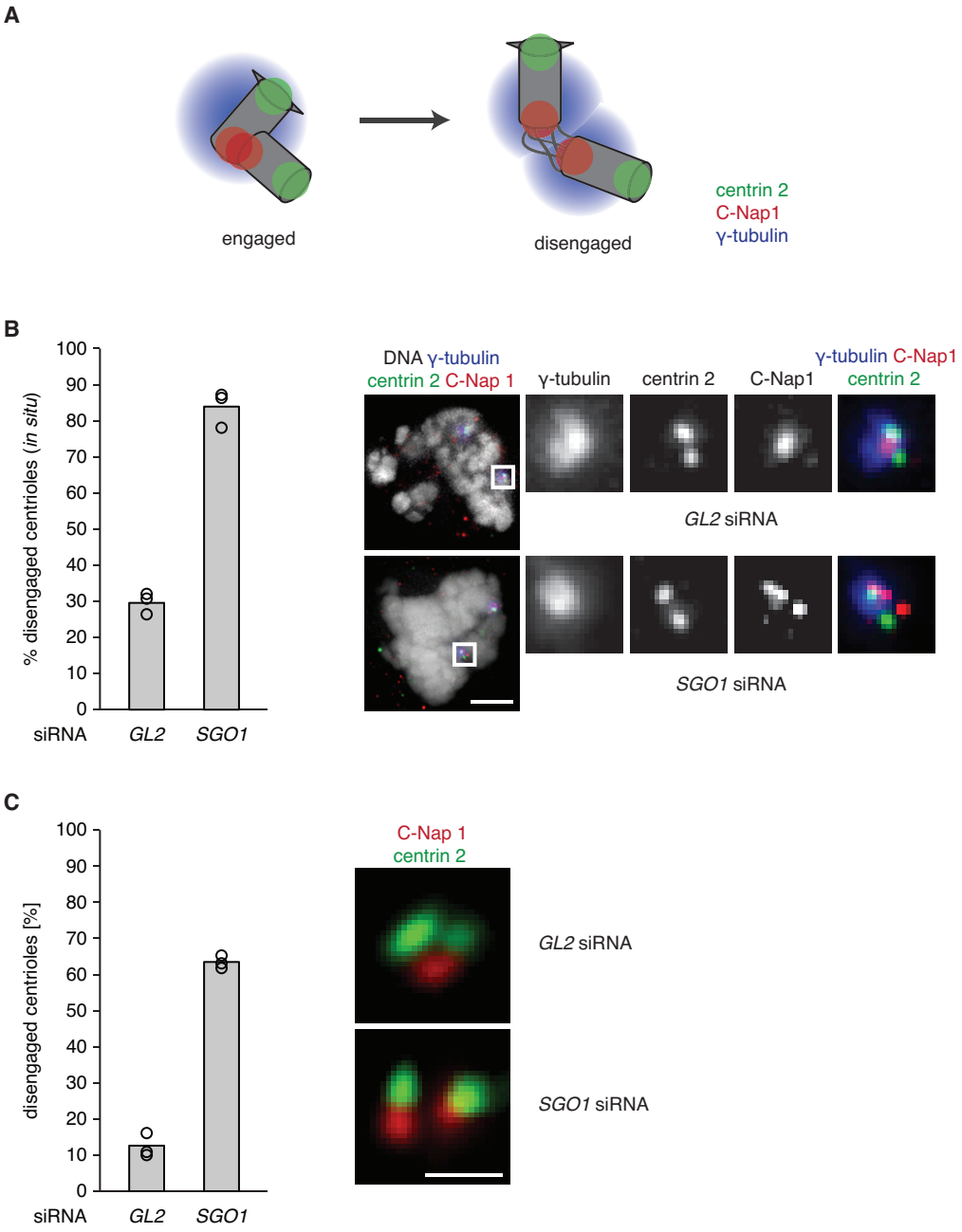

figure 8. Depletion of Sgo1 causes premature centriole disengagement.
U2OS cells were synchronized at the G1/S boundary with thymidine. After 14 hours they were transfected with *SGO1* siRNA and 7 hours later released from thymidine, and finally, 5 hours later, arrested in prometaphase by taxol treatment for 15 hours.
(A) Position of centrin 2, C-Nap1 and γ-tubulin at the centrosome. Centrin 2 is located at the distal and C-Nap1 at the proximal end of each cantriole. γ-tubulin sits in the PCM.
(B) Premature centriole disengagement caused by Sgo1 depletion can be quantified *in situ*. Cells from figure spreads were pre-extracted, fixed and stained for γ-tubulin, centrin 2 (distal centriole marker), C-Nap1 (proximal centriole marker) and DNA (Hoechst 33342). On the right centrosomes are shown at 4 fold magnification. Two centrin 2 and one C-Nap1 dot were counted as a centrosome with engaged centrioles, whereas two centrin 2 and two C-Nap1 dots were counted as disengaged, scale bar: 5 µm. Each column represents averages of three independent experiments (circles, 100 cells each).
(C) Premature centriole disengagement caused by Sgo1 depletion can be quantified on isolated centrosomes. Centrosomes were isolated from cells from figure spreads, stained for centrin 2 and C-Nap1 and analyzed by IFM, scale bar: 1 µm. Each column represents averages of three independent experiments (dots, 100 centrosomes each).

In order to examine, whether the separation of chromatids correlated with the disengagement of centrioles upon Sgo1 depletion, I performed immunofluorescence staining on chromosome spreads, which allowed me to assess the status of chromosome cohesion and centriole engagement in the same cell. When mock depleted, 90% of cells exhibited cohesed chromatids in combination with engaged centrioles. Upon Sgo1 depletion, however, cohesion of chromosomes and engagement of centrioles was lost in 85% of the cells (figure 9A and B). Interestingly, there were almost no cases of cohesed chromatids in combination with disengaged centrioles or separated chromatids in combination with engaged centrioles. Taken together, all three methods confirmed that Sgo1 depletion not only causes premature separation of chromatids but also centriole disengagement.

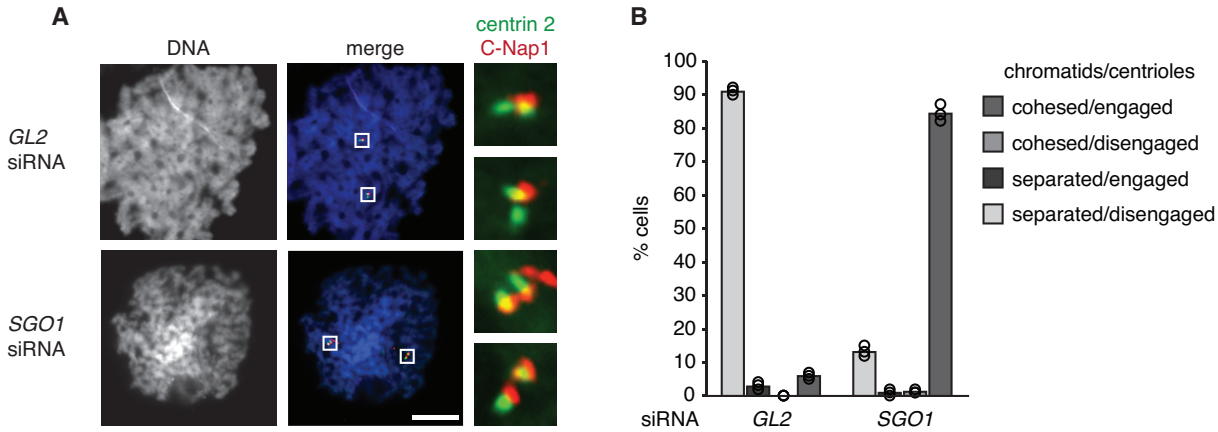

figure 9. Premature loss of sister chromatid cohesion coincides with premature centriole disengagement.
U2OS cells were synchronized at the G1/S boundary with thymidine. After 14 hours they were transfected with *SGO1* siRNA and 7 hours later released from thymidine, and finally, 5 hours later, arrested in prometaphase by taxol treatment for 15 hours.
(A) Cells were harvested and chromosomes spread, followed by (immuno)staining of centrin 2 (distal centriole marker), C-Nap1 (proximal centriole marker) and DNA (Hoechst 33342). On the right magnified centrosomes are shown, scale bar: 5 µm.
(B) Status of centriole engagement and chromatid cohesion for each cell was quantified as described above. Each column represents averages of three independent experiments (circles, 100 cells each).

In all following experiments, I examined centrosomes by isolation of centrioles followed by IFM, because discrimination between engaged and disengaged centrioles was highly reproducible and fast. It took a long time to quantify the engagement status with the other two methods, since the centrin 2 antibody unfortunately stains DNA unspecifically and only cells could be analyzed, where the centrosomes lay next to the DNA.

2.1.2. Division of labor between Sgo1 isoforms

As already mentioned in the introduction (see 1.5.2), alternative splicing gives rise to several isoforms of mammalian Sgo1. While the canonical Sgo1 A1 (and C1) localize to centromeres, Sgo1 A2 and C2 localize to centrosomes (Mohr et al., 2015; Tang et al., 2004; Wang et al., 2008; 2006). For Sgo1 A1 and C2 it was reported, that they protect from premature loss of sister chromatid cohesion and premature centriole disengagment, respectively (McGuinness et al., 2005; Schöckel et al., 2011; Tang et al., 2004; Wang et al., 2008; Yamada et al., 2012). To examine the function of these four Sgo1 isoforms, stable transgenic Hek293 cell lines were generated that inducibly express Myc-tagged variants of Sgo1 A1, A2, C1, and C2 from small interfering RNA (siRNA)-resistant transgenes. I induced the individual expression of transgenic Sgo1 A1, A2, C1, or C2 while simultaneously depleting all endogenous Sgo1 isoforms by RNAi. Following pre-synchronization in early S phase, cells were arrested in prometaphase and then analyzed (figure 10A). Transgene expression was documented by immunoblotting (figure 10B), the status of sister chromatid cohesion was assessed by chromosome spreading (figure 10C), and centriole (dis-)engagement was examined by IFM on isolated centrosomes staining centrin 2 and C-Nap1 (figure 10D). On the chromosomal level, only the canonical Sgo1 A1 was able to reduce the premature loss of sister chromatid cohesion (by 73%), while the centrosomal isoforms Sgo1 A2 and C2 had no such effect (figure 10C). Despite its reported localization to centromeres, Sgo1 C1 failed to rescue the Sgo1 depletion phenotype at the chromosomes. On the other hand, premature centriole disengagement in Sgo1-less prometaphase cells could not be rescued by the expression of Sgo1 A1 and C1 but was partially rescued by the expression of Sgo1 A2 or C2. More specifically, the two centrosomal isoforms suppressed premature centriole disengagement by 28% and 37%, respectively (figure 10D). Since these effects seemed rather small compared to the effect of Sgo1 A1 on the chromosomal phenotype (73% rescue), I asked whether both isoforms might jointly be needed at centrosomes. Therefore, I generated a doubly transgenic stable cell line that expressed Myc-tagged Sgo1 C2 and Flag-tagged Sgo1 A2 upon doxycycline addition (figure 10B). Indeed, simultaneous expression of both centrosomal isoforms had an additive effect and suppressed the centriole disengagement phenotype resulting from

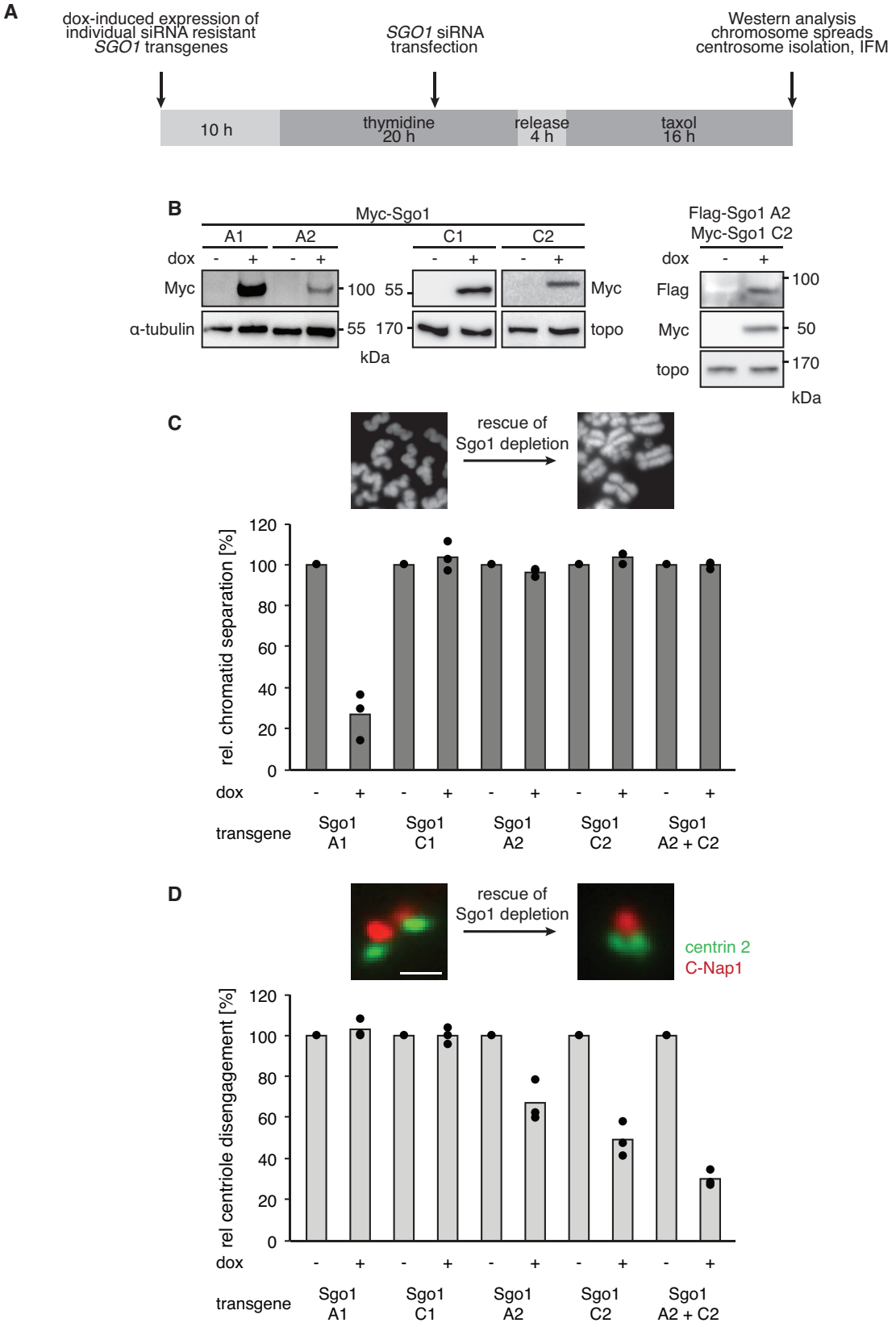

figure 10. Rescue of Sgo1-depletion phenotypes by specific Sgo1 isoforms.
(A) Experimental setup of Sgo1 knockdown-rescue experiments. At the indicated times, stable cell lines were induced by addition of doxycyline (dox) to express *SGO1* transgenes and transfected with *SGO1* siRNA to deplete all endogenous forms of Sgo1. Cells were synchronized in prometaphase by taxol addition prior to analysis by western blotting, spreading of chromosomes, isolation of centrosomes, and IFM.

figure 10 continued:
(B) Transgenic cell lines inducibly expressing siRNA-resistant Myc-Sgo1 A1, A2, C1, or C2 or both siRNA-resistant Flag-Sgo1 A2 and Myc-Sgo1 C2. The corresponding Hek293 Flp-In T-REx cell lines were treated as described in (A) and analyzed by Myc and Flag immunoblots for transgene expression. Immunodetection of α-tubulin or topoisomerase II α (topo) served as loading controls.
C) Premature loss of sister chromatid cohesion in the absence of endogenous Sgo1 is suppressed only by siRNA-resistant Sgo1 A1. Analysis of chromosome spreads.
(D) Premature centriole disengagement in the absence of endogenous Sgo1 is suppressed by siRNA-resistant Sgo1 A2 or/and C2. Centrosomes were isolated and visualized by IFM using centrin 2 and C-Nap1 antibodies. Scale bar: 1 μm.
(C and D) The stable Hek293 Flp-In T-REx cell lines were treated as described in (A). Each column represents averages of three independent experiments (circles, 100 cells or centrosomes each). The amount of chromatid separation and centriole disengagement of + dox cells was normalized to the corresponding - dox samples (set to 100%). Note that Sgo1 A1 phenotypes were quantified by Laura Schöckel.

depletion of endogenous Sgo1 by 70% (figure 10D). Thus, while centromeric Sgo1 A1 is solely responsible to preserve sister chromatid cohesion, both centrosomal isoforms, Sgo1 A2 and C2, are required to protect centriole engagement.

To better understand the role of Sgo1 on centrosomes, I sought to study possible dominant effects of long-term overexpression of individual isoforms without simultaneous depletion of the endogenous protein. For Sgo1 A1 it had already been reported that strong overexpression leads to mislocalization of Sgo1. Instead of being recruited only to the centromere, Sgo1 localized also to the chromosome arms and counteracted the prophase pathway all over the chromosomes (Liu et al., 2013). As a consequence, cohesin persisted on chromosome arms all through early mitosis until separase removed the complex from whole chromosomes at the meta- to anaphase transition. While cells can tolerate this excess of cohesin for some cell cycles, long-term inhibition of the prophase pathway ultimately leads to formation of anaphase bridges (see 1.3.4) and missegregation of chromatids (Haarhuis et al., 2013). To examine the effects of long-term overexpression of Sgo1 isoforms on centriole engagement status, I induced the expression of centrosomal Sgo1 A2 and C2, and as a control, centromeric Sgo1 A1 in the stable Hek293 cell lines. As a second control, I used parental Hek293 cells without any integrated transgene. After 7 days, transgene expression was documented by immunoblotting (figure 11A) and centrosomes of cells grown on coverslips were visualized with antibodies against centrin 2 and C-Nap1 (figure 11B). IFM revealed that samples from both control cell lines mainly featured cells harboring one or two normal centrosomes (figure 11B and C), which is the regular number for cells in G1 and G2 phase, respectively. Upon

overexpression of Sgo1 A2 and C2 however, in 50% (A2) and 28% (C2) of the cells centrosomes were marked by two C-Nap1 dots, which were surrounded by numerous centrin 2 foci. These aggregated centrosomes with a "flower-like" phenotype had previously been described by Kleylein-Sohn et al., 2007, who showed that overexpression of Plk4, the principal kinase required for centriole duplication, causes the formation of multiple daughter centrioles around one mother centriole. Thus, overexpression of centrosomal isoforms seems to disturb proper centriole duplication.

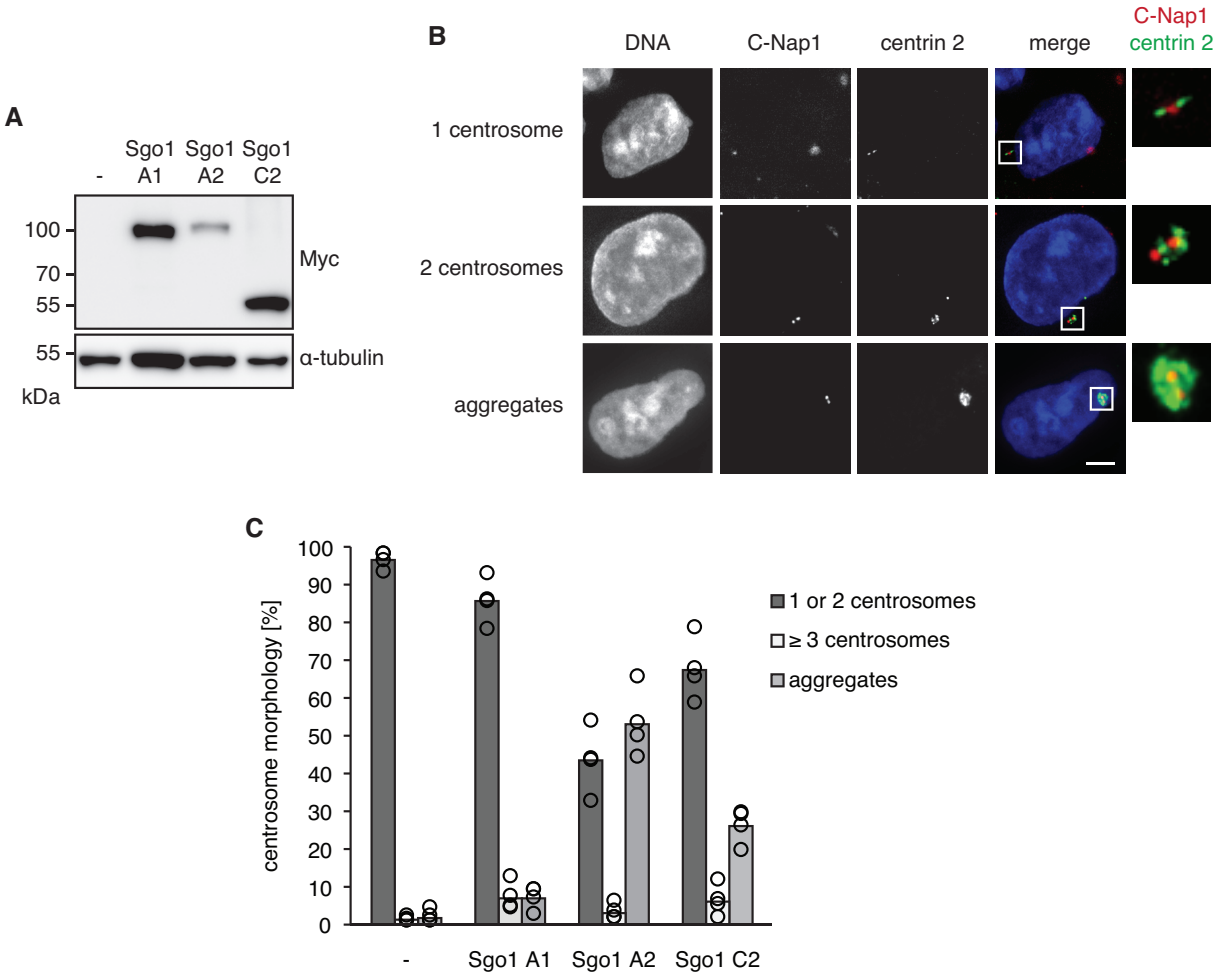

figure 11. Long-term overexpression of centrosomal Sgo1 isoforms induces aggregation of centrioles.
Transgenic cell lines inducibly expressing Myc-Sgo1 A1, A2, or C2 were induced by addition of doxycycline to express *SGO1* transgenes for 7 days.
(A) Transgene expression was analyzed by Myc immunoblot. Immunodetection of α-tubulin served as loading control.
(B) Cells from (A) were pre-extracted, fixed, and stained for centrin 2, C-Nap1 and DNA (Hoechst 33342) to assess centrosome morphology. Three different phenotypes were discriminated: the regular amount of 1 or 2 centrosomes, overduplicated centrosomes (3 or more) and aggregates of centrosomes which consist of 2 C Nap1 dots surrounded by several centrin 2 foci.
(C) Quantification of centrosome morphology as shown in (B). Each column represents averages of four independent experiments (circles, 100 cells each).

2.1.3. Chromosomal and centrosomal Sgo1 isoforms have varying expression levels in different normal and cancerous tissues

Since overexpression as well as depletion of Sgo1 causes defects in both the chromosome and the centrosome cycles, the expression of the different isoforms of Sgo1 must be tightly regulated, since both, chromosomal and centrosomal aberrations can be tied to the development of cancer (Basto et al., 2008; Lingle et al., 2002; Pihan et al., 2001 and reviewed in Chan, 2011; Hanahan and Weinberg, 2011; Santaguida and Amon, 2015). To test a possible correlation between the expression levels of the various Sgo1 variants and tumorigenesis, I performed comparative real time quantitative PCR (qPCR) using the TaqMan gene expressing assay with primers specifically recognizing either Sgo1 A1 (and C1) or A2 and C2, i.e. chromosomal or centromeric Sgo1, respectively.

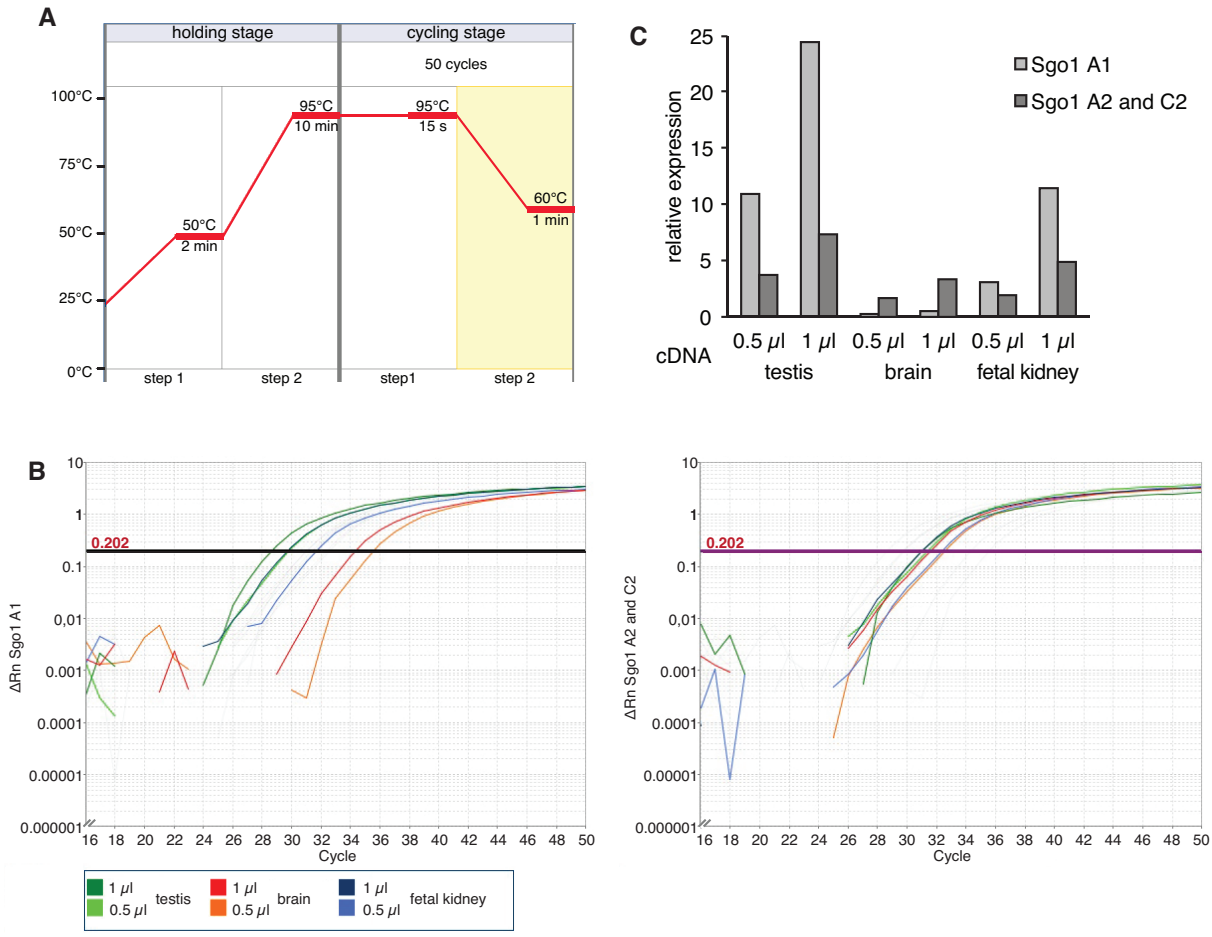

figure 12. Expression of Sgo1 variants in different tissues.
(A) The PCR was conducted after a standard protocol for TaqMan gene expression assay, modified for the Sgo1 isoform specific primers.
(B) The amplification plot shows the variation of log (ΔRn) with PCR cycle number for the qPCR with Sgo1 A1 and A2/C2 specific primers on cDNA from testis, brain and fetal kidneys. The relative

figure 12 continued: normalized reporter value (ΔRn) is defined as the measured reporter value, normalized to the signal of an internal passive reference dye (ROX), minus the Rn value of the baseline signal generated by the instrument. To compare the actual expression levels, one has to set a threshold (in this case 0.202), which is a specific value of signal intensity at which all curves begin to indicate exponential signal increase.
(C) Relative expression of Sgo1 A1 and A2/C2 in the different tissues. The relative expression is defined as $2^{-\Delta C_t}$. The cycle number, at which the signal reaches the threshold is called C_t value (for threshold cycle), from which the C_t value of the housekeeping gene (GAPDH) is subtracted, giving the ΔC_t value.

The expression level of GAPDH served as an internal standard. In preliminary experiments I established the optimal temperatures and number of cycles for the PCR reaction (figure 12A). Using human cDNAs from testis, brain and fetal kidney as templates, the fluorescence signals produced by the PCR reactions increased exponentially until they reached a plateau, which is caused by the limiting amount of primers (figure 12B). The relative expression of Sgo1 A1 and A2/C2 varied in the different tissues with the highest expression in the testis and the lowest expression in the brain (figure 12C). Note that doubling the amount of template resulted in about twice the relative expression, which verifies the fidelity of the assay. Interestingly, only in testis and fetal kidney the level of Sgo1 A1 exceeded that of Sgo1 A2 and C2. In the brain however, Sgo1 A2/C2 level was about 4 times higher than the level of Sgo1 A1. Thus, expression levels of Sgo1 isoforms seem to be tissue specific.

To investigate the expression levels of Sgo1 in different cancer tissue samples, I used a commercially available cancer tissue array containing 96 samples of cDNA, which were obtained from 8 different tissues (breast, colon, kidney, liver, lung, ovaries, prostate and thyroid gland) at different stages of cancer. In addition three non-cancerous samples were included per tissue (figure 13, stage 0). In this array, the amounts of the pre-plated cDNAs were normalized to and validated with ß-actin, which means that all relative expression levels can be directly compared. While non-cancer samples (stage 0, figure 13) exhibited relative expression levels of both isoforms between 0.5 and 2, some samples especially from lung and ovary cancers reached expression levels up to 20 times higher (figure 13E-F). These numbers are only slightly lower for colon and breast cancer samples, which reach relative expression levels of up to 16 (figure 13G-H). While the correlation is much milder, also prostate, thyroid gland, kidney and liver tissues exhibited elevated Sgo1 expression levels in their respective cancer samples (figure 13A-D).

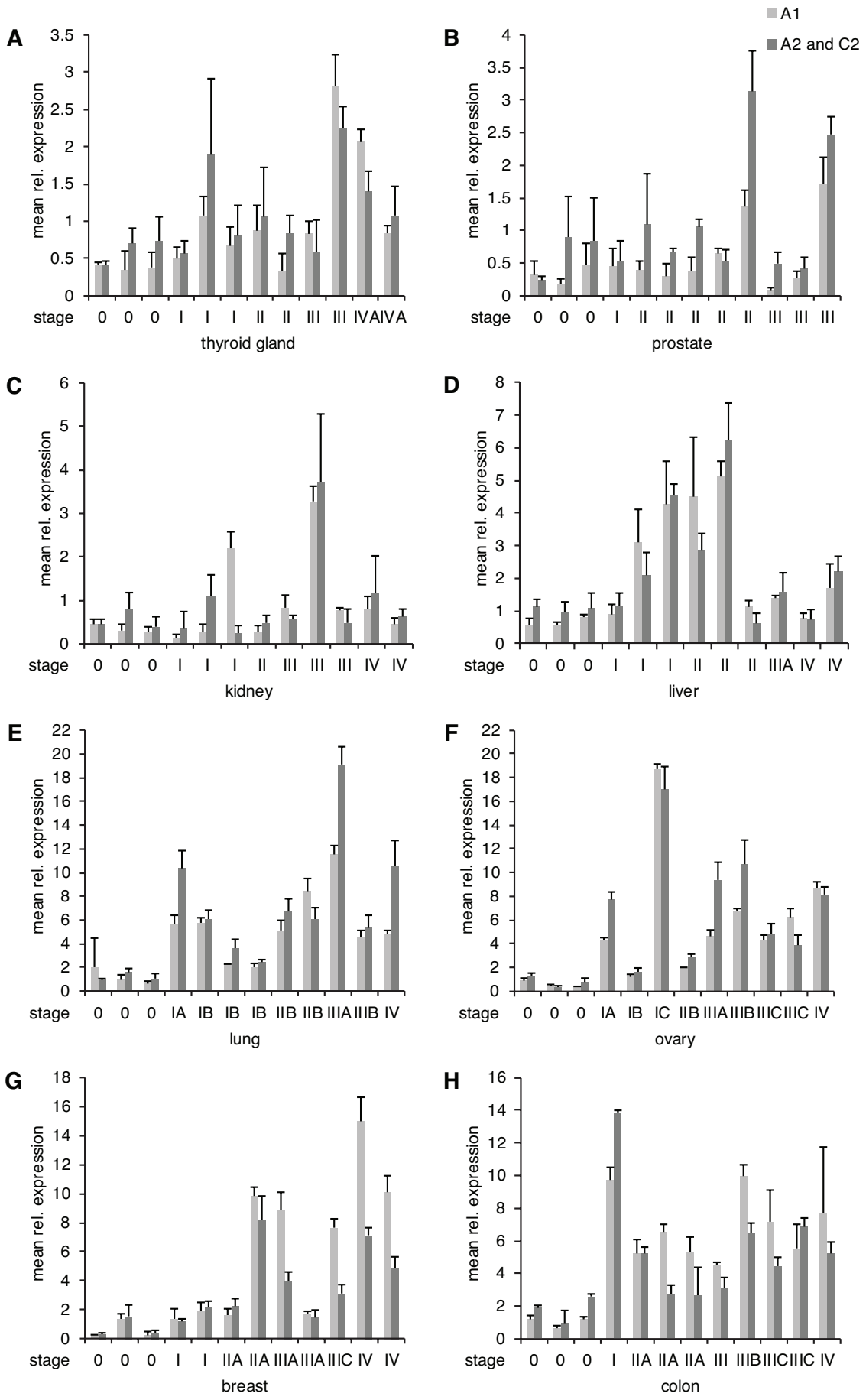

figure 13. Expression of Sgo1 variants in different cancer tissue samples.

figure 13 continued:
Measurement of the Sgo1 A1 and A2/C2 expression levels in cDNA from normal and cancer tissue samples of thyroid gland (A), prostate (B), kidney (C), liver (D), lung (E), ovaries (F), breast (G) and colon (H) using qPCR. The PCR reactions were performed as shown in figure 12A using "TissueScan" cancer tissue cDNA arrays as templates. Shown are mean relative expression levels of Sgo1 A1 and A2/C2. Each set of tissue consists of 3 samples of normal tissues (stage 0) and 9 tissue samples from different stages of cancer (stage I-IV). Every column represents averages of three independent experiments. Bars represent standard deviation.

However, while there is a clear general link between all tested cancer types and Sgo1 overexpression, there is no apparent association between discrete levels of Sgo1 overexpression and specific stages of cancer. Many cancer samples exhibited simultaneous overexpression of centromeric (A1) as well as centrosomal Sgo1 (A2/C2), a notable example being the tissue sample from ovary cancer stage IC (figure 13F). Yet interestingly, in many samples centrosomal or centromeric Sgo1 isoforms seem to be differentially up-regulated. While, for example, many breast cancer-derived samples exhibited higher expression of centromeric compared to centrosomal Sgo1 (figure 13G), in several other samples, some of which are marked by dramatic Sgo1 overexpression (namely lung cancer stages IA and IIIA, and colon cancer stage I), the centrosomal Sgo1 isoforms heavily dominated over their centromeric counterpart. Distorted proportions were also observed for many of the cancer with weaker phentypes (especially in prostate tissues), which overexpressed mainly centrosomal Sgo1. Together these results not only argue that Sgo1 A2 and C2 most likely play a role in the development of cancer but also that tumorigenesis might be linked to the differential misregulation of centrosomal *versus* centromeric Sgo1 isoforms.

2.1.4. Chromosomal Sgo1 C1 is a dominant negative isoform

Interestingly, although it localized to the centromere (Mohr et al., 2015), Sgo1 C1 was not able to prevent the premature separation of sister chromatid cohesion caused by Sgo1 depletion (figure 10C). When looking at the culture dishes of cells overexpressing the different Sgo1 isoforms, it was obvious, that more cells expressing Sgo1 C1 accumulated in mitosis, then cells expressing the other isoforms. To quantify this phenotype, I utilized flow cytometry to analyze cell cycle profiles from cells transiently overexpressing Sgo1 C1, compared to untransfected cells and to cells expressing Sgo1 A1. Expression of Sgo1 C1 indeed led to an

accumulation in G2/M, while the control samples exhibited a normal cell cycle profile (figure 14A and B). This accumulation could putatively be the result of premature sister chromatid separation, which triggers the spindle assembly checkpoint. To examine this possibility, I overexpressed Sgo1 C1 or C2 in Hek293T cells, arrested them in mitosis and spread the chromosomes. As a positive control for premature loss of sister chromatid cohesion I depleted Sgo1 (figure 14C). As predicted, cells overexpressing Sgo2 C1 suffered from premature loss of sister chromatid cohesion, comparable to the Sgo1 depleted cells, while overexpression of Sgo1 C2 did not have this effect (figure 14D). A comparable effect on sister chromatid cohesion had been reported previously for cells overexpressing Sgo1 B1, a cancer-associated isoform lacking most of the peptide encoded by exon 6 (Matsuura et al., 2013), thereby making it very similar to C1 (figure 14E).

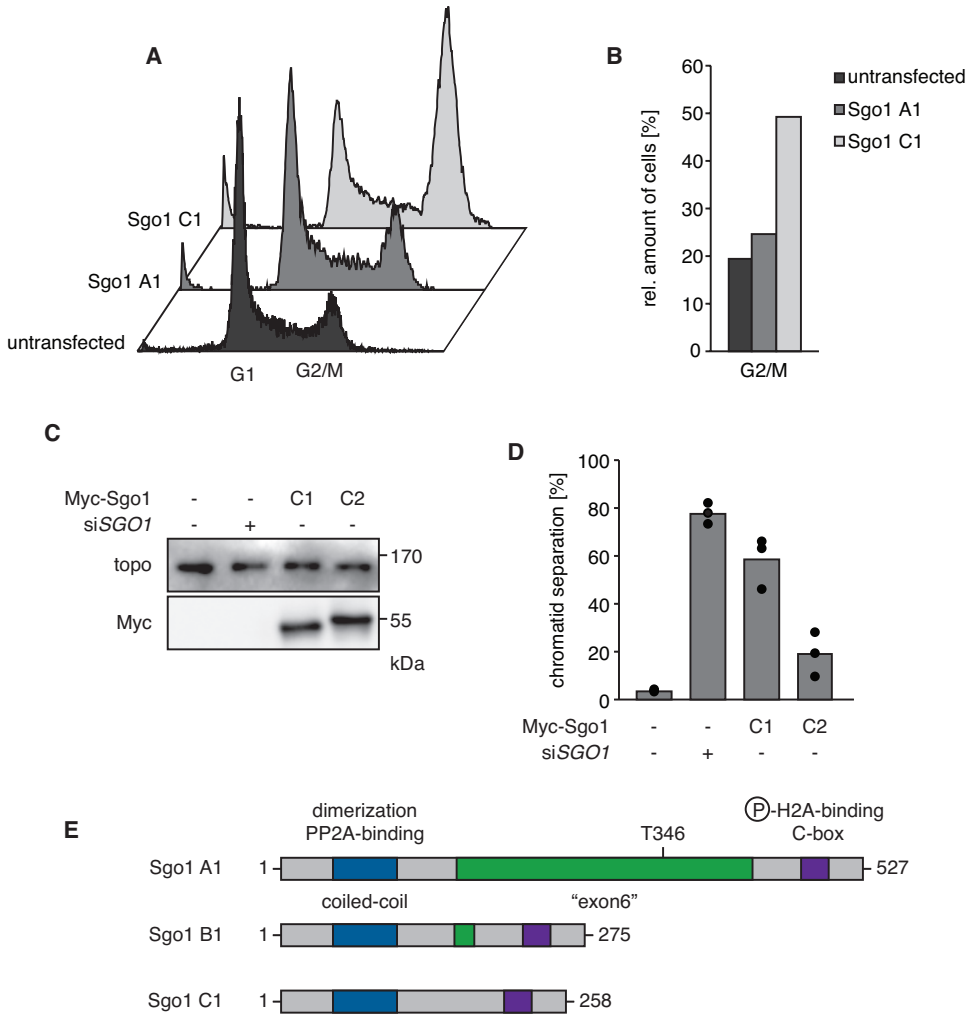

figure 14. Overexpression of Sgo1 C1 leads to arrest in mitosis due to premature loss of sister chromatid cohesion.
(A) Myc-tagged Sgo1 A1 and C1 were transiently expressed in Hek293T cells for 36 h followed by propidium iodide-staining and flow cytometry.

figure 14 continued:
(B) Each column represents the relative amount of cells of the G2/M peak from (A).
(C, D) Hek293T cells were transfected with *SGO1* siRNA or plasmids coding for Myc-Sgo1 C1 or C2. After knockdown/expression for 32 h, cells were synchronized in prometaphase by nocodazole addition prior to analysis by Western blotting (C) and spreading of chromosomes (D).
(D) Each column represents averages of three independent experiments (dots, 100 cells each).
(E) Schematic view of Sgo1 A1, B1 and C1 drawn to scale.

2.2. How are Sgo1 isoforms recruited to the centrosomes?

2.2.1. The N-terminus of Sgo1 is not a centrosomal targeting signal

In a previous study, the absence of the peptide encoded by exon 6 was considered to be responsible for centrosomal localization, since a Myc-tagged N-terminal part of Sgo1 (amino acids 1–196) reportedly localized to centrosomes in HeLa cells (Wang et al., 2008). This stood in contrast to our observations, where Sgo1 C1 (exon 6-encoded part missing) localized to the centromere and Sgo1 A2 (exon 6-encoded part present) got recruited to the centrosome, arguing for the C-terminus as the centrosomal localization signal. I tried to recapitulate the results from Wang and colleagues and expressed the aforementioned Myc-tagged N-terminal peptide in Hek293T as well as in HeLa cells. Interestingly, in Hek293T cells, the N-terminal fragment did not localize to the centrosomes (figure 15A), whereas in HeLa K cells, I was able to detect localization to the centrosomes and the spindle. Strikingly however, the centrosomal staining was lost upon depletion of endogenous Sgo1 (figure 15B). This leads to the conclusion that centrosomal recruitment of this N-terminal fragment most likely depends on dimerization with endogenous Sgo1 via the coiled-coil domain. The binding to the spindle seems to be independent of dimerization and also specific only for HeLa cells.

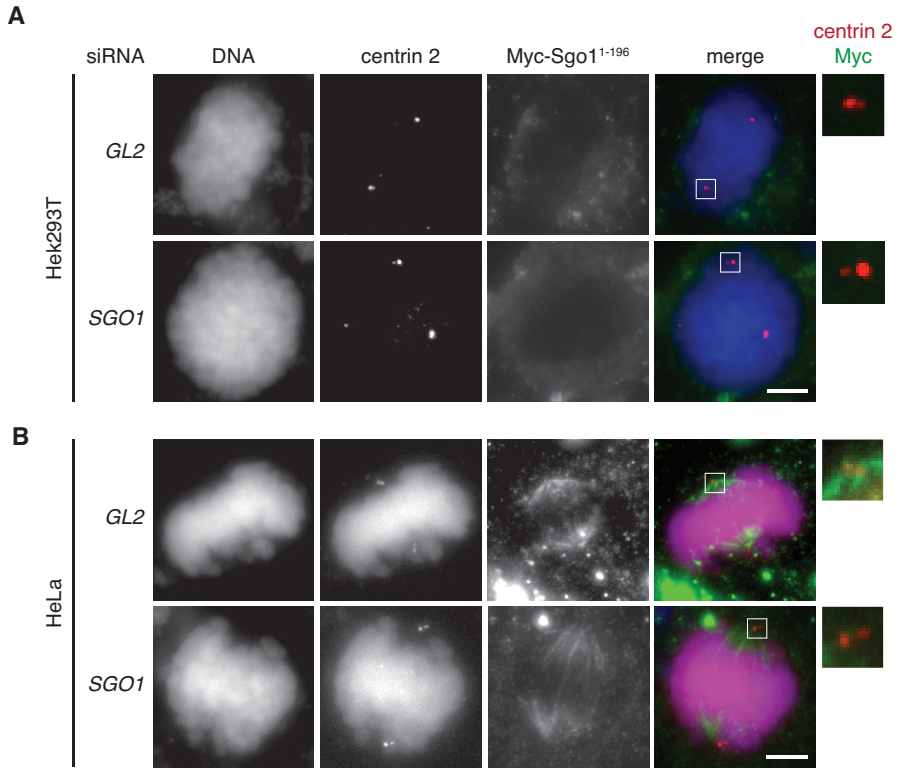

figure 15. The N-terminus of Sgo1 does not localize to the centrosome in Hek293T cells. Myc-Sgo1$^{1-196}$ was expressed in Hek293T (A) and HeLa K (B) cells for 24 h in combination with Sgo1 knockdown or mock treatment (GL2). Note that the RNAi did not affect the transgenic protein. Cells were pre-extracted, fixed and stained for centrin 2, Myc and DNA (Hoechst 33342). Note also that the centrin 2 antibody unspecifically stains DNA in HeLa K cells. On the right, centrosomes are shown at 4 fold magnification. Scale bars: 5 µm.

2.2.2. The CTS constitutes a transferrable centrosomal targeting signal

As explained above (see 2.1.2), the one region that is specific for centrosomally localized shugoshins ant therefore could serve as a corresponding targeting signal is the peptide encoded by exon 9. This putative centrosomal targeting signal of Sgo1 (CTS) consists of only 40 amino acids at the very C-terminus of Sgo1 A2 and C2 and is conserved only in humans and higher primates (figure 16A). The last seven amino acids, which are absent in orangutans, are also dispensable in humans, since Sgo1 C2 with the corresponding deletion still localized to the centrosome (bachelor's thesis Carina Schmidt, University of Bayreuth).

In order to test, whether the CTS of Sgo1 A2 or C2 might be sufficient for centrosomal localization, I expressed it in fusion with an N-terminal mCherry-tag in Hek293T cells. mCherry-CTS indeed localized to centrosomes in interphase and mitosis. Remarkably, replacing the three consecutive amino acids ILY, which are

conserved in humans and higher primates, with alanines (figure 16A) totally abrogated centrosomal localization (figure 16B).

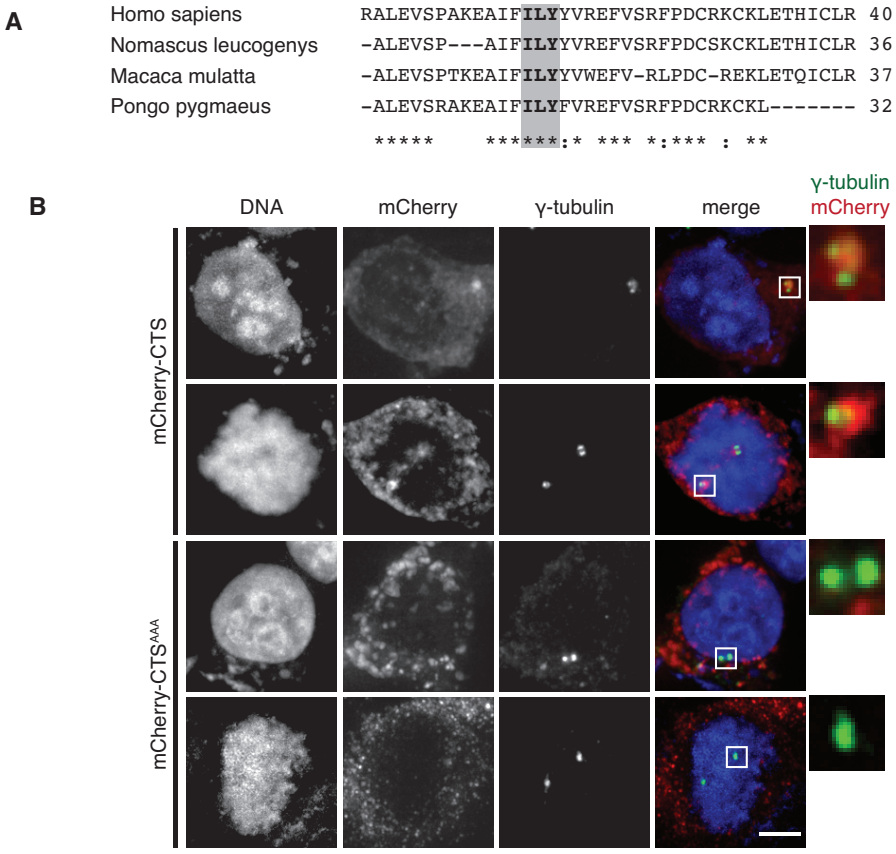

figure 16. The 40 amino acids encoded by exon 9 constitute a transferrable centrosomal targeting signal.
(A) Sequence alignment of the CTS of human Sgo1 and related sequences of gibbon, rhesus macaque and orangutan.
(B) C-terminal fusion to the CTS (centrosomal targeting signal of Sgo1), but not the ILY to AAA variant thereof, directs mCherry to centrosomes. Wild type and the AAA variant of mCherry-CTS were transiently expressed in Hek293T cells for 48 hr. To enrich for mitotic cells, pre-synchronized cells were released from a G1/S arrest 10 hr prior to pre-extraction, fixation, and staining for γ-tubulin, mCherry, and DNA (Hoechst 33342). On the right, centrosomes are shown at 4-fold magnification. Scale bar: 5 μm.

The CTS-mediated centrosomal recruitment of mCherry could be recapitulated in HeLa cells (figure 17, upper panels), strongly suggesting that the peptide constitutes an universal centrosomal targeting signal in human cells. For several centrosomal proteins, it has been reported that their recruitment is dependent on the presence of microtubules (Lee and Rhee, 2010; Zimmerman and Doxsey, 2000). The localization of mCherry-CTS, however, is independent of the presence of microtubules, as mCherry-CTS still localized to the centrosome upon nocodazole treatment (figure 17, lower panels).

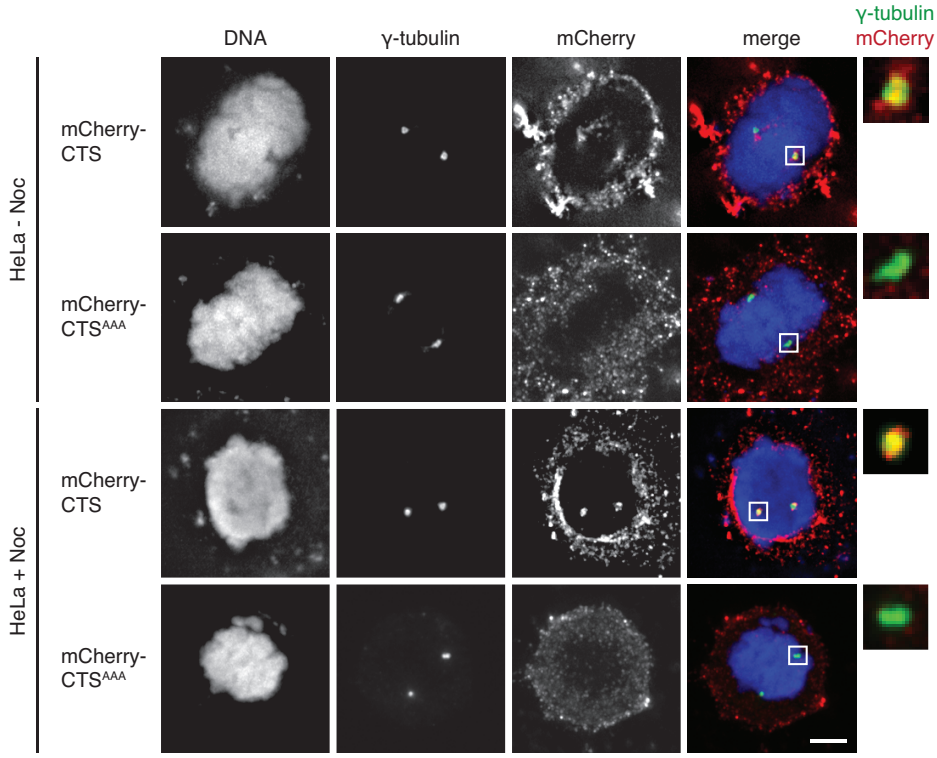

figure 17. mCherry-CTS (but not -CTS^{AAA}) is recruited to centrosomes of HeLa K cells in the absence of microtubules.
mCherry-CTS and mCherry-CTS^{AAA} were transiently expressed in HeLa K cells for 36 h. For depolymerization of microtubules, nocodazole was added 6 h prior to pre-extraction, fixation and staining for γ-tubulin, mCherry and DNA (Hoechst 33342).
Note: IFM of - Noc cells was performed by Johannes Buheitel (University of Bayreuth).

The fact that the CTS not only recruits Sgo1 A2 and C2, but also mCherry to the centrosome, strongly implies direct binding of the peptide to an as yet unknown centrosomal protein. If this was true, one would expect heavy overexpression of the CTS to outcompete endogenous Sgo1 A2 and C2 for binding to centrosomes and thereby phenocopy Sgo1 depletion. Indeed, when transiently overexpressed in fusion with a detectable tag (FKBP), wild type (WT) CTS, but not the ILY to AAA variant (AAA), triggered premature centriole disengagement in Hek293T cells (figures 18A and B).

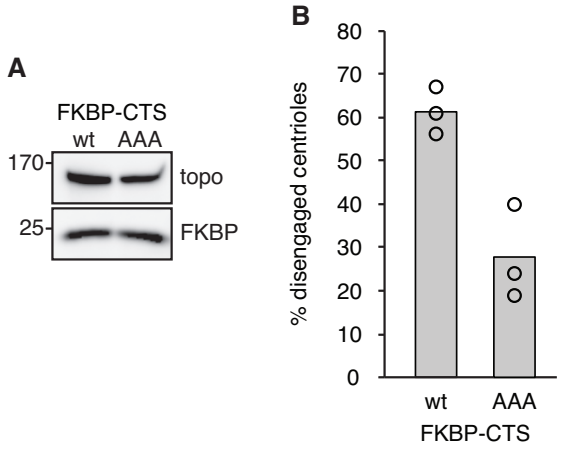

figure 18. Overexpression of the CTS induces premature centriole disengagement.
Hek293T cells were transfected with plasmids encoding FKBP-CTS (WT or AAA) 24 hr prior to addition of thymidine. Cells were then treated as described in figure 8C.
(A) Expression of transgenes was analyzed by Western blot.
(B) Centrosomes from (A) were isolated and visualized by IFM using centrin 2 and C-Nap1 antibodies. Each column represents averages of three independent experiments (circles, 100 centrosomes each).

Sgo1 A2 and C2 still contain the Sgo1 C-box, which mediates recruitment to the centromere via binding to phosphorylated Histone 2A. While binding of the CTS to a centrosomal target does explain how Sgo1 is recruited to the centrosome, it remains a mystery how it prevents centromeric recruitment of Sgo1 A2 and C2. One possibility to avoid binding to the centromere would be export out of the nucleus. The CTS contains three sequence stretches weakly resembling a Crm1/exportin1-specific NES (Güttler et al., 2010 and figure 19A). Therefore, I inhibited the exportin1 dependent nuclear export with leptomycin B (LMB) in Hek293T cells transiently expressing mCherry-CTS WT or AAA. Cells were then fixed without pre-extraction, in order to preserve the cytoplasmic/nuclear distribution of the fusion protein. The staining of survivin, a component of the chromosomal passenger complex, which is excluded from the nucleus in interphase via Crm1-dependent nuclear export, served as a control (Knauer et al., 2006 and figure 19B). As expected, survivin localized to the nucleus upon LMB treatment. For mCherry-CTS, neither the WT nor the mutant variant localized to the nucleus without LMB treatment. Addition of LMB did not result in an altered localization of the proteins (figure 19C). Therefore, the CTS of the centrosomal Sgo1 isoforms A2 and C2 does not seem to feature a functional NES, dismissing nuclear export as a putative means to negatively affect Sgo1 recruitment to the centromere.

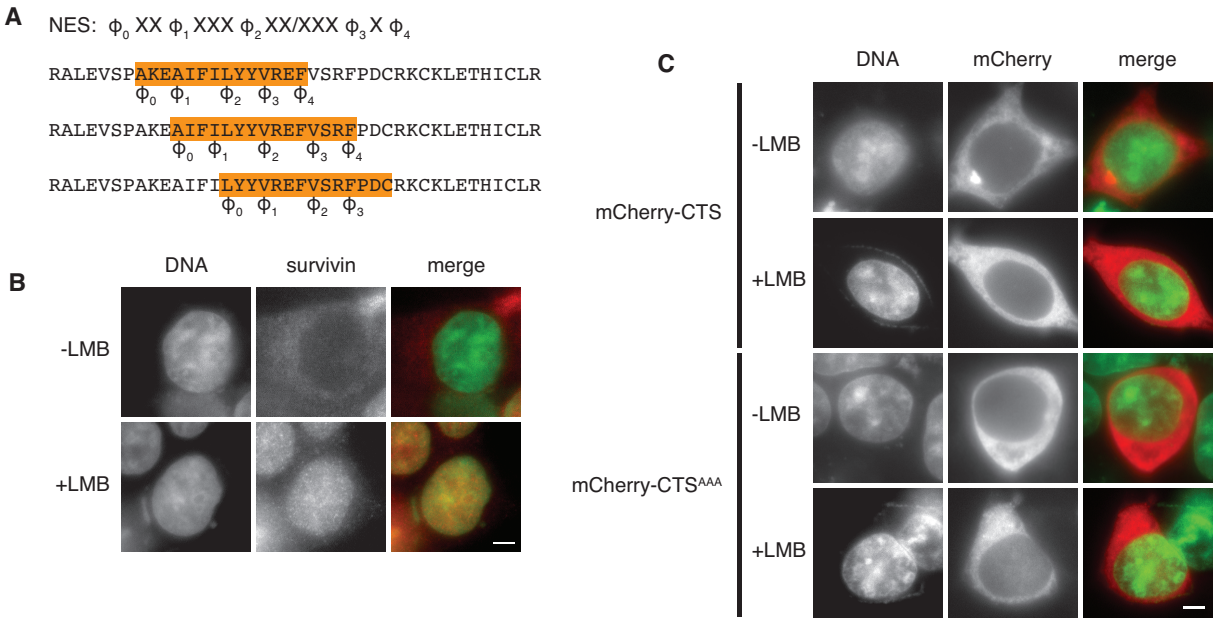

figure 19. The CTS does not contain an NES for exportin1.
(A) Consensus of an optimal nuclear export sequence (NES) as defined by (Güttler et al., 2010) with ϕ = L, I, V, F, A M and x = random amino acid. Sgo1's CTS contains three potential NES (marked in yellow).
(B) Hek293T cells were treated with leptomycin B (LMB) to inhibit exportin1-dependent nuclear export by exportin1 for 11 h. Cells were fixed and stained for survivin and DNA.
(C) Hek293T cells were transfected with plasmids encoding mCherry-CTS or mCherry-CTS^{AAA} 37 h prior to addition of leptomycin B (LMB). 11h later cells were fixed stained for mCherry with an RFP antibody and DNA (Hoechst 33342).
Note that cells were not pre-extracted in order to preserve the cytoplasmic fraction of survivin and the mCherry fusion-proteins. Scale bars: 5 μm.

2.3. Role of Sgo1 at murine centrosomes

As mentioned above (see 2.2.2), the CTS is conserved only in humans and higher primates. Nevertheless, there has been a report about a link between centriole engagement and Sgo1 in mouse cells (Wang et al., 2008). Although the murine *SGO1* gene lacks exon 9, the mechanism, which allows the CTS to mediate centrosomal recruitment, seems to be conserved, since mCherry-CTS expressed in mouse NIH 3T3 fibroblasts readily localized to the centrosome, while the corresponding ILY to AAA variant again failed to do so (figure 20A). Therefore, even if Sgo1's centrosomal targeting signal is not conserved between human and mouse, the interaction partner of the human CTS at the centrosome certainly is. It has been reported that Sgo1$^{+/-}$ mouse embryonic fibroblasts (MEFs) suffer from premature centriole disengagement (Wang et al., 2008). To further investigate a potential role of Sgo1 at centrosomes at murine centrosomes, I expressed Myc-tagged mouse Sgo1 in NIH 3T3 cells, in which it localized to both centromeres and centrosomes (figure

20B). RNAi-mediated depletion of murine Sgo1 expectedly caused premature loss of sister chromatid cohesion in NIH 3T3 cells (figure 21A).

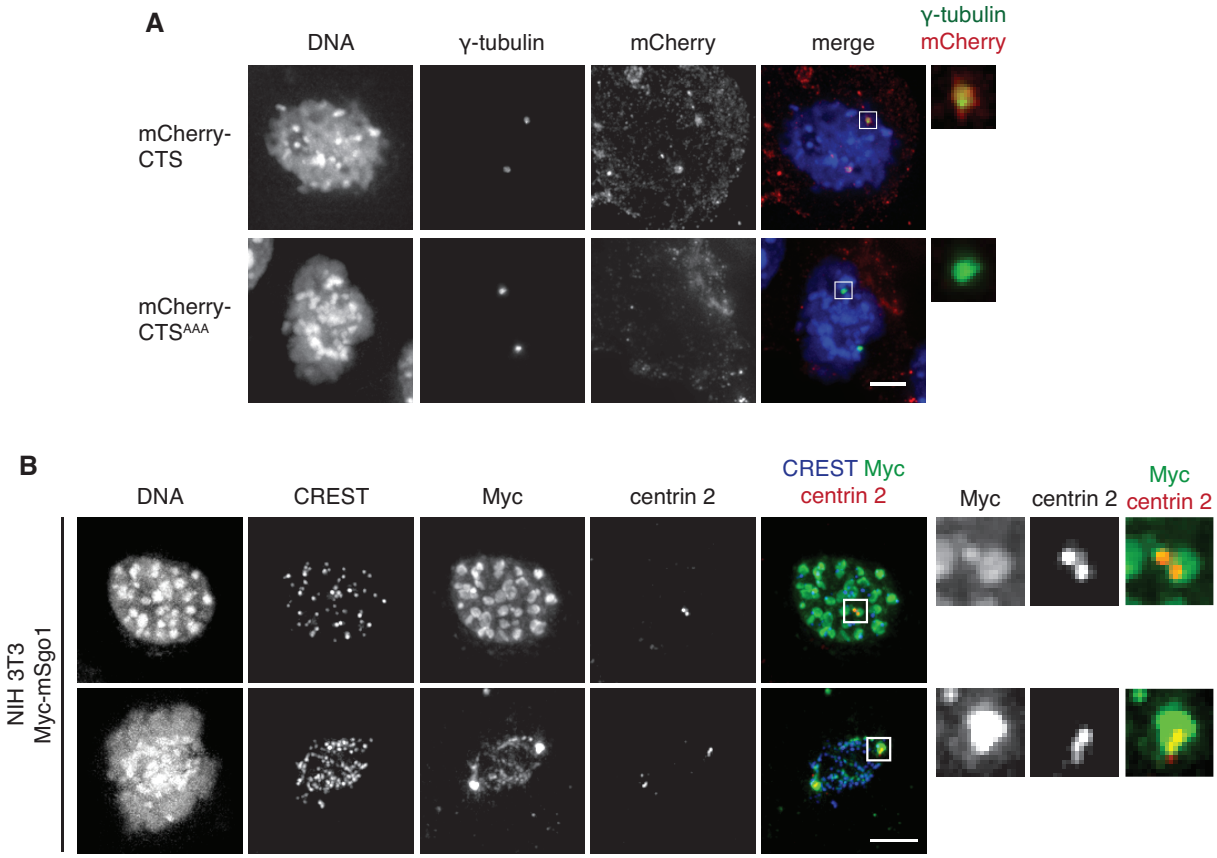

figure 20. Murine Sgo1 and mCherry-CTS localize to centrosomes in mouse cells.
(A) mCherry-CTS localizes to the centrosomes in mouse cells. mCherry-CTS and mCherry-CTS^{AAA} were transiently expressed in NIH 3T3 cells for 36 hr. Cells were fixed and stained for γ-tubulin, mCherry, and DNA (Hoechst 33342). On the right, centrosomes are shown at 4-fold magnification.
(B) Murine Sgo1 localizes to centromeres and centrosomes. Myc-tagged mSgo1 was transiently expressed in NIH 3T3 cells for 36 h. Cells were pre-extracted, fixed and stained for CREST (centromere), Myc (Sgo1 isoforms), centrin 2 (centrosomal marker) and DNA (Hoechst 33342).
Scale bars: 5 μm.

Unfortunately, the C-Nap1 antibody, raised against human C-Nap1, doesn't recognize murine C-Nap1. Therefore, to investigate the engagement status of centrioles, I used only the centrin 2 antibody on fixed cells and measured the distance between the two centrin 2 foci associated with the two centrioles of one centrosome. Upon Sgo1 depletion, this distance was doubled, which suggests that centrioles disengaged in the absence of Sgo1 (figure 21B and C). Thus, mice seem to utilize a single Sgo1 isoform to fulfill both, centromeric and centrosomal functions of shugoshin 1.

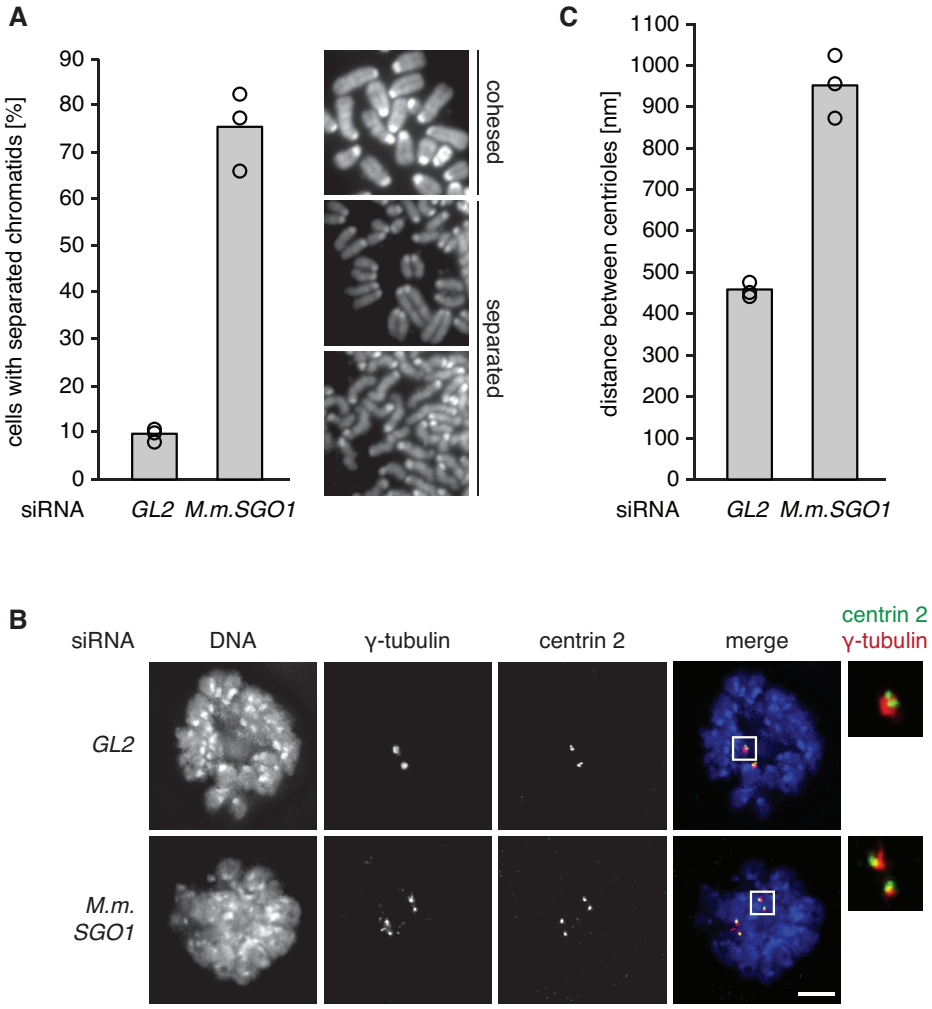

figure 21. Knockdown of murine Sgo1 causes premature sister chromatid separation and centriole disengagement.
NIH 3T3 cells were thymidine-arrested in early S phase and transfected with *M.m. SGO1* siRNA. After release, cells were synchronized in prometaphase with taxol.
(A) Status of chromatid cohesion was analyzed by spreading of chromosomes. Each column represents averages of three independent experiments (circles, 100 centrosomes each).
(B) Aliquots of cells from (A) were fixed and stained for γ-tubulin, centrin 2, and DNA (Hoechst 33342). On the right, centrosomes are shown at 4-fold magnification. Scale bar: 5 μm.
(C) To discriminate between engaged and disengaged centrioles (in the absence of a working antibody against murine C-Nap1), the distance between the two centrin 2 dots, representing the centrioles of one centrosome, was measured. Each column represents average distances from three independent experiments (circles, 100 centrosomes each).

2.4. Recruitment of PP2A by Sgo1 is essential for maintenance of centriole engagement

2.4.1. Sgo1 promotes recruitment of PP2A to the centrosomes

At centromeres Sgo1 protects cohesin by recruiting the B'α (B56) isoform of PP2A, thereby antagonizing the phosphorylation-dependent prophase pathway (Kitajima et al., 2006; Nishiyama et al., 2013; Riedel et al., 2006; Xu et al., 2009). We speculated

that the phosphatase might have a similar function for the protection of centriole engagement. Using an antibody against the catalytical PP2A-C subunit in IFM, I could indeed show that PP2A also localized to the centrosome and that this localization depended on Sgo1, as the PP2A signal is lost upon Sgo1 depletion (figure 22).

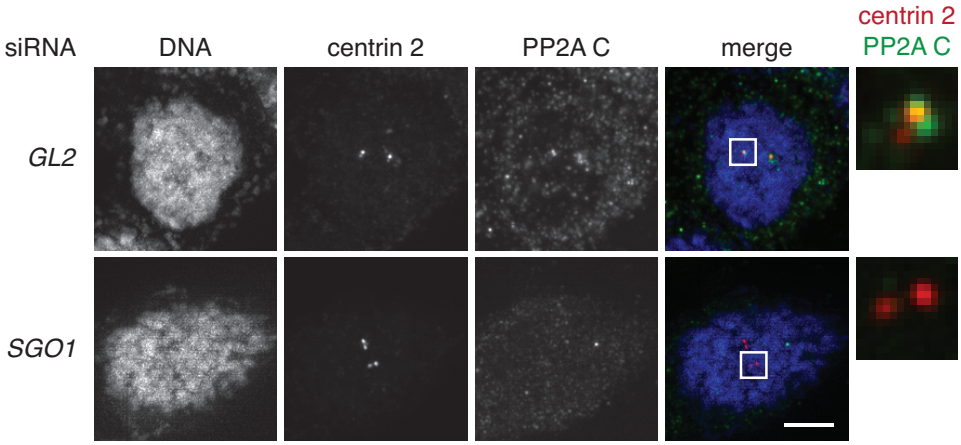

figure 22. Localization of PP2A to centrosomes depends on Sgo1.
24 h before fixation, Hek293T cells were transfected with *GL2* or *SGO1* siRNA. Cells were pre-extracted prior to fixation and stained for centrin 2, PP2A-C, and DNA (Hoechst 33342). On the right, centrosomes are shown at 4-fold magnification. Scale bar: 5 μm.

To test, whether PP2A recruitment is required for the Sgo1-mediated protection of centriole engagement, I introduced previously described compromising mutations (N61I and Y57A, K62A; Xu et al., 2009) into the PP2A binding site of Sgo1 A2 and C2 and generated inducible transgenic Hek293 cell lines. Co-immunoprecipitation experiments confirmad that both variants exhibited greatly reduced PP2A-binding in comparison to WT Sgo1 A2 and C2 (figure 23A and B).

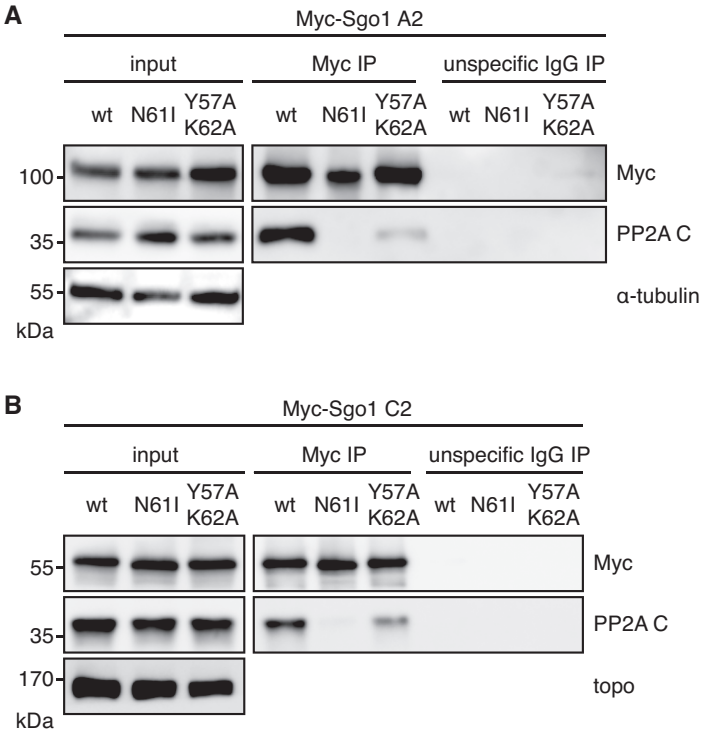

figure 23. Variants of Sgo1 A2 and C2 bearing Y57A, K62A, or N61I mutations in the N-terminal coiled-coil domain can no longer bind PP2A.
Myc-tagged variants of Sgo1 A2 (A) or C2 (B) were transiently expressed in Hek293T cells for 36 hr. Cell lysates were subjected to immunoprecipitation (IP) with anti-Myc or unspecific immuno-globulin G (IgG). Inputs and eluates were finally analyzed by western blot using the indicated antibodies.

To investigate the recruitment of Sgo1 and PP2A to the centrosome, I depleted endogenous Sgo1, induced the expression of the Myc-tagged PP2A-binding deficient Sgo1 A2 and C2 mutants in the stable Hek293 cell lines and examined the localization of the mutants and PP2A. While the PP2A-binding deficient mutants of Sgo1 A2 and C2 still localized to centrosomes (figure 24A and B), they were not able to recruit PP2A (figure 24C and D). There are contradictory reports about whether Sgo1 recruits PP2A to the centromere or the other way around (see 1.5.5). My results strongly suggest that at the centrosome PP2A is recruited by Sgo1.

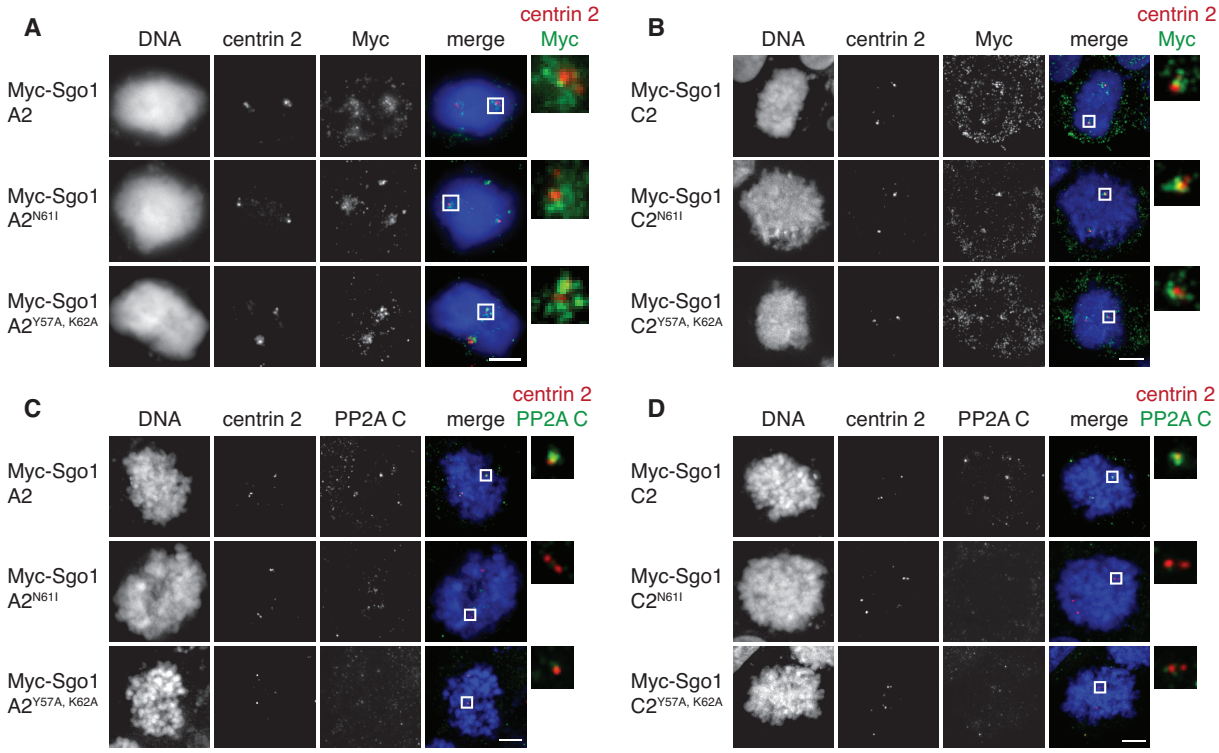

figure 24. The recruitment of PP2A to centrosomes depends on Sgo1.
(A,B) PP2A-binding deficient Sgo1 A2 (A) and C2 (B) variants still localize to the centrosomes.
(A) Expression of Myc-Sgo1 A2, A2^{N61I} or A2$^{Y57A, K62A}$ was induced with doxycycline (dox) for 48 h in stable Hek293 Flp-In T-REx cells. 24 h before fixation, cells were transfected with *SGO1* siRNA. Cells were pre-extracted prior to fixation and centrin 2 (centrosomal marker), Myc (Sgo1 isoforms) and DNA (Hoechst 33342) were visualized by IFM.
(B) Cells inducibly expressing Myc-Sgo1 C2, C2^{N61I} or C2$^{Y57A, K62A}$ were treated as described in (A). Centrin 2 (centrosomal marker), Myc (Sgo1 isoforms) and DNA (Hoechst 33342) were visualized by IFM.
(C,D) PP2A-binding deficient Sgo1 A2 (C) and C2 (D) variants do not recruit PP2A to centrosomes. Cells were treated as described in (A) and stained for centrin 2, PP2A-C and DNA (Hoechst 33342).
Scale bars: 5 μm.

2.4.2. PP2A is essential for maintaining centriole engagement in mitosis

If the protection of centriole engagement depends on Sgo1-dependent recruitment of PP2A, then PP2A-binding deficient Sgo1 variants should not be able to prevent the premature centriole disengagement caused by Sgo1 depletion. And indeed, the Sgo1 N61I and Y57A, K62A mutants were unable to prevent premature centriole disengagement in the absence of endogenous Sgo1 (figure 25). These results strongly suggest that Sgo1's function as a recruitment factor for PP2A is conserved between centromeres and centrosomes.

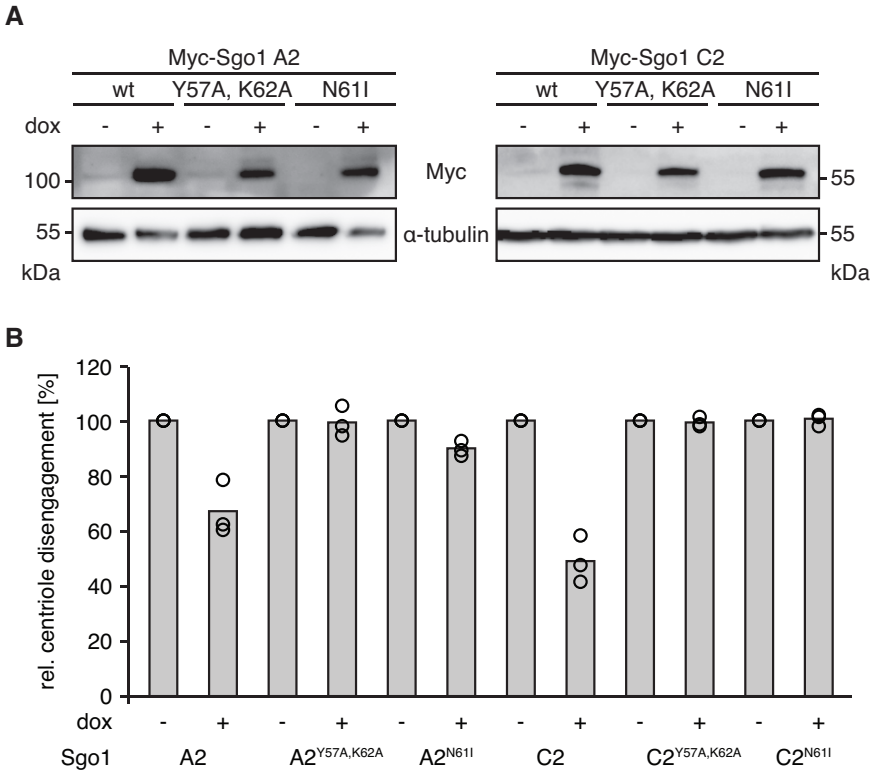

figure 25. PP2A binding-deficient variants of Sgo1 A2 and C2 fail to rescue the premature centriole disengagement caused by Sgo1 depletion.
Transgenic Hek293 cell lines inducibly expressing siRNA-resistant wild type (WT) Myc-Sgo1 A2/C2 or PP2A binding-deficient variants thereof (Y57A, K62A or N61I) were treated as described in figure 10A, before being analyzed by immunoblotting (A) and centrosome isolation followed by IFM using centrin 2 and C-Nap1 antibodies (B).
(A) Transgene expression was analyzed by Myc immunoblots. Immunodetection of α-tubulin served as loading control.
(B) Quantification of centriole disengagement. Each column represents averages of three independent experiments (circles, 100 centrosomes each). The amount of centriole disengagement of + dox cells was normalized to - dox cells (set to 100%).

To corroborate these results, I tested, whether artificially tethering PP2A to centrosomes can bypass the need for Sgo1 to protect centriole engagement. Therefore, I fused the open reading frame (ORF) of PP2A-B'α to an extended version of the CTS and used this construct to generate Hek293 cell lines stably, but inducibly, expressing the fusion protein. Upon doxycycline addition, this protein readily localized to the centrosomes (figure 26A). Crucially, assessment of centriole engagement status revealed that PP2A-B'α-CTS indeed suppressed premature centriole disengagement by 30%, while uninduced cells were not able to mitigate the Sgo1 depletion phenotype (figure 26B and C and data not shown).

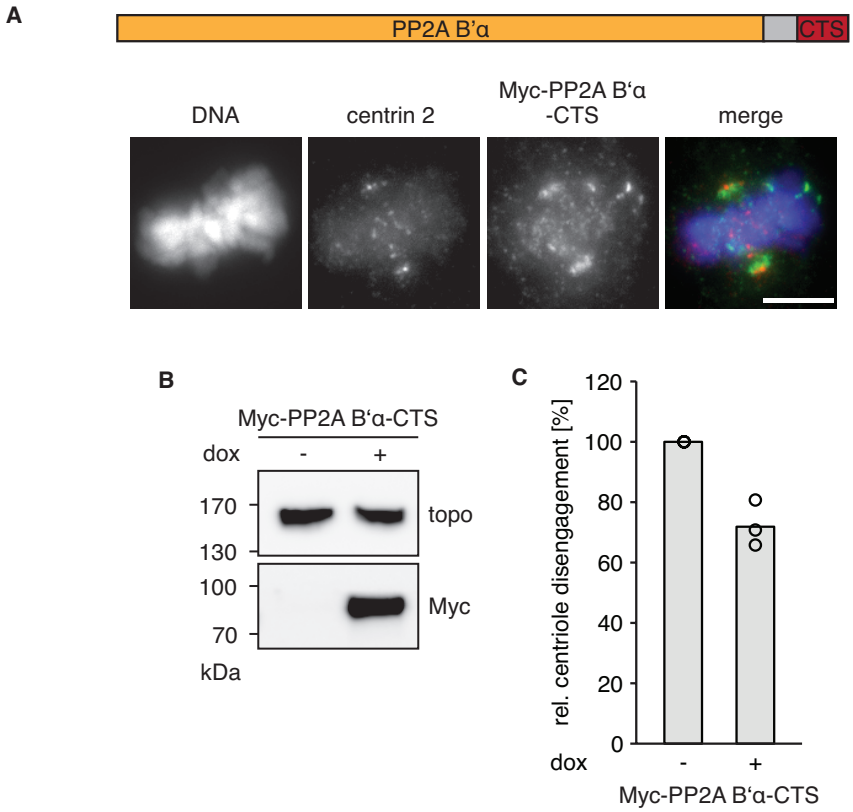

figure 26. PP2A is the actual effector protecting centrosome engagement.
(A) Schematic view of chimeric protein consisting of PP2A-B'α and the C-terminus of Sgo1 A2 (aa 493–561) drawn to scale. A transgenic cell line inducibly expressing Myc-PP2A-B'α-CTS was treated with dox to induce transgene expression for 2 days. To enrich mitotic cells, cells were first arrested in S-phase using thymidine for 20 h and then released from the arrest 11 h prior to pre-extraction and fixation. Centrin 2, Myc and DNA (Hoechst 33342) were visualized by IFM. Scale bar: 5 μm.
(B,C) Artificial recruitment of PP2A to the centrosome prevents premature centriole disengagement caused by Sgo1 depletion. The transgenic Hek293 cell line inducibly expressing Myc-PP2A-B'α was treated as described in figure 10A, before being analyzed by immunoblotting (B) and centrosome isolation followed by IFM using centrin 2 and C-Nap1 antibodies (C).
(B) Transgene expression was analyzed by a Myc immunoblot. Detection of topoisomerase IIα (topo) seved as loading control.
(C) Quantification of centriole disengagement. Each column represents averages of three independent experiments (circles, 100 centrosomes each). The amount of centriole disengagement of + dox cells was normalized to - dox cells (set to 100%).

To exclude the possibility that the observed rescue effect was caused by the higher level of PP2A rather than its tethering to the centrosome, I expressed Myc-tagged PP2A-B'α, PP2A-B'α-CTS and PP2A-B'α-CTS^{AAA} in Hek293T cells (figure 27B). Additionally, the cells were treated with nocodazole to investigate, if the localization and function of PP2A and its chimeric variants depend on microtubules. IFM revealed that only PP2A-B'α-CTS localized to the centrosomes in a Sgo1-depletion background, while the ILY to AAA variant and WT PP2A-B'α did not (figure 27A). Consistent with its localization, only PP2A-B'α-CTS partially suppressed premature

centriole disengagement by (30%), while neither the corresponding ILY to AAA variant nor WT PP2A-B'α rescued the Sgo1 depletion phenotype (figure 27C). Thus, Sgo1's centrosomal function lies in its ability to recruit PP2A, which then acts as the actual effector for the protection of centriole engagement.

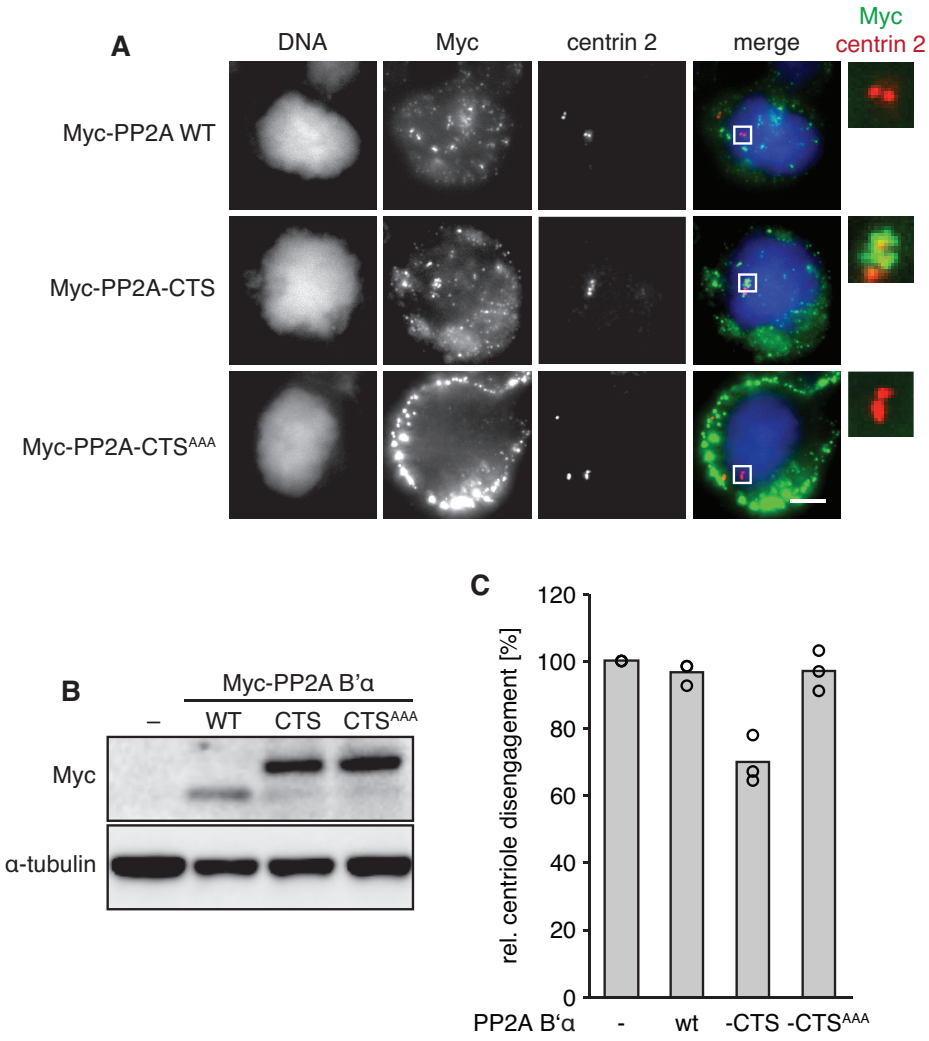

figure 27. Artificial recruitment of PP2A to the centrosome rescues premature centriole disengagement caused by Sgo1 knockdown in the absence of microtubules.
(A) A PP2A-B'α-CTS fusion protein is artificially directed to centrosomes. Myc-tagged PP2A-B'α, PP2A-B'α-CTS and PP2A-B'α-CTSAAA were transiently expressed in Hek293T cells for 48 h. To prevent recruitment via Sgo1, cells were depleted of endogenous Sgo1 by transfection of siRNA 24 h later. Microtubules were depolymerized by addition of nocodazole 16 h prior to pre-extraction and fixation. Centrin 2, Myc (PP2A variants) and DNA (Hoechst 33342) were visualized by IFM.
(B) Hek293T cells were transfected with plasmids encoding Myc-tagged PP2A-B'α, PP2A-B'α-CTS or PP2A-B'α-CTS^{AAA} and treated as described in figure 10A but finally arrested with nocodazole instead of taxol before being analyzed by immunoblotting.
(C) IFM on isolated centrosomes from (B). Each column represents averages of three independent experiments (circles, 100 centrosomes each).

2.5. Sgo2 plays a role at mitotic centrosomes

During localization studies of Sgo2 it emerged that Sgo2 located in two distinct foci next to the DNA, strongly suggesting centrosomal localization. To determine, if this was true, I analyzed the localization of Sgo2 during the cell cycle in HeLa cells with Sgo2- and γ-tubulin-specific antibodies (figure 28). In interphase Sgo2 was not detectable via IFM after pre-extraction. In early mitosis however, the protein appears to be recruited to distinct foci on chromosomes, strongly resembling a centromere-like pattern. Interestingly, from ana- to telophase, this signal is lost from DNA, but it re-emerges as two distinct foci, co-staining with the centrosomal marker γ-tubulin. This centrosomal association was eventually lost at cytokinesis. This observation, together with the fact that Sgo1 and 2 share crucial functional domains, like the C-terminal Sgo C-box (mediates recruitment to kinetochores) and the N-terminal coiled coil (dimerization, PP2A-binding), led to the question, whether Sgo2 might have a function at the centrosome in mitosis.

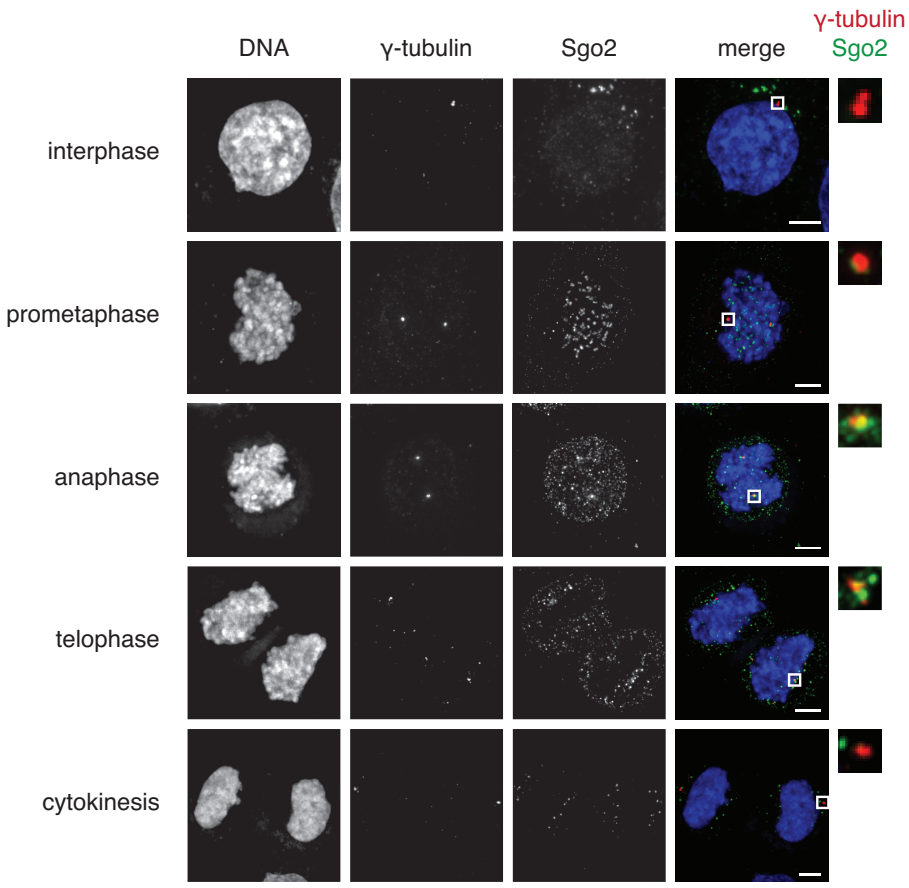

figure 28. Sgo2 localizes to the centrosomes in mitosis.
HeLa cells were pre-extracted, fixed and stained for tubulin (centrosomes), Sgo2 and DNA (Hoechst 33342). To increase the amount of mitotic cells, cells had been arrested in S phase by thymidine

figure 28 continued: addition, 20 h later released and after 11 h fixed. On the right, centrosomes are shown at 5-fold magnification, scale bars: 5 μm.

2.5.1. Sgo2 depletion leads to premature centriole disengagement

To examine a potential role of Sgo2 at the centrosome, I depleted Sgo2 and, as a control, Sgo1 in U2OS cells and arrested them in prometaphase. The status of sister chromatid cohesion was assessed by chromosome spreading and the centriole (dis-)engagement was evaluated by IFM on isolated centrosomes. As expected, sister chromatid cohesion was unaffected by Sgo2 depletion (figure 29A, see 1.5.6 introduction). On the centrosomal level, however, knockdown of Sgo2 caused premature centriole disengagement to almost the same extent as knockdown of Sgo1 (figure 29B). Combined depletion of both did not reveal a marked additive effect, suggesting that Sgo1 and Sgo2 might act in the same pathway at the centrosome.

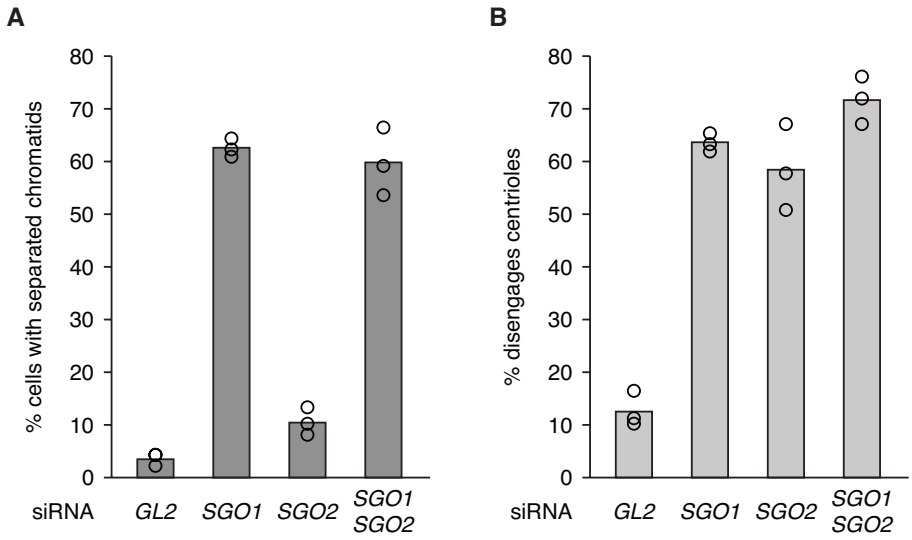

figure 29. Knockdown of Sgo2 causes premature centriole disengagement but no premature loss of sister chromatid cohesion.
U2OS cells were synchronized at the G1/S boundary with thymidine. After 14 h they were transfected with *GL2*, *SGO1*, *SGO2* or SGO1 and *SGO2* siRNA, 7 h later released from thymidine, and finally, 5 hours later, arrested in prometaphase by taxol treatment for 15 h.
(A) Analysis of chromosome spreads of cells from (A). Each column represents averages of three independent experiments (circles, 100 cells each).
(B) Centrosomes were isolated, stained for centrin 2 and C-Nap1 and analyzed by IFM. Each column represents averages of three independent experiments (circles, 100 centrosomes each).

2.5.2. Sgo2 overexpression prevents premature centriole disengagement

To further investigate Sgo2's role at the centrosome, I generated stable Hek293 cell lines that inducibly express siRNA resistant, Myc-tagged Sgo2 either in its wild type form or as a PP2A-binding deficient variant ($Sgo2^{N58I}$). When expressed in the corresponding cell lines, wild type and mutant variant of Sgo2 both localized to the centrosome (figure 30).

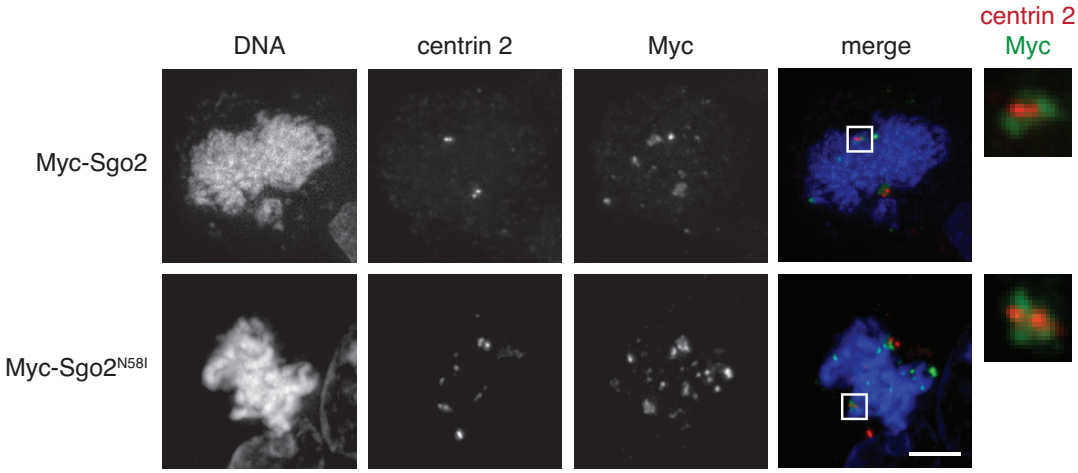

figure 30. Overexpressed Sgo2 and $Sgo2^{N58I}$ localize to centrosomes in mitosis.
Expression of Myc-Sgo2 or PP2A-binding deficient Myc-$Sgo2^{N58I}$ was induced with doxycyline for 48 hr in stable Hek293 Flp-In T-REx cells. Cells were pre-extracted prior to fixation and centrin 2 (centrosomal marker), Myc (Sgo2), and DNA (Hoechst 33342) were visualized by IFM. On the right, centrosomes are shown at 4-fold magnification. Scale bar: 5 μm.

To test, if the Sgo2 depletion phenotype at the centrosome can be rescued by overexpression of Sgo2 and if this is dependent on PP2A, I knocked down Sgo2 in the stable cell lines expressing Myc-Sgo2-WT or the N58I variant. Cells were then arrested in prometaphase and subjected to analysis by Western blotting and centrosome isolation (figure 31A). Both cell lines expressed the transgenes at similar levels (figure 31B). To verify the efficiency of the Sgo2 knockdown, cells of both cell lines were transfected with GL2 instead of Sgo2 siRNA. (figure 31C). The engagement status of the centriole was assessed by IFM, which showed that expression of wild type Sgo2 but not the PP2A-binding deficient variant prevented premature centriole disengagment caused by Sgo2 depletion (figure 31D). This not only leads to the conclusion that the centrosomal effect of Sgo2 depletion is specific but also that Sgo2's centrosomal role lies in the recruitment of PP2A.

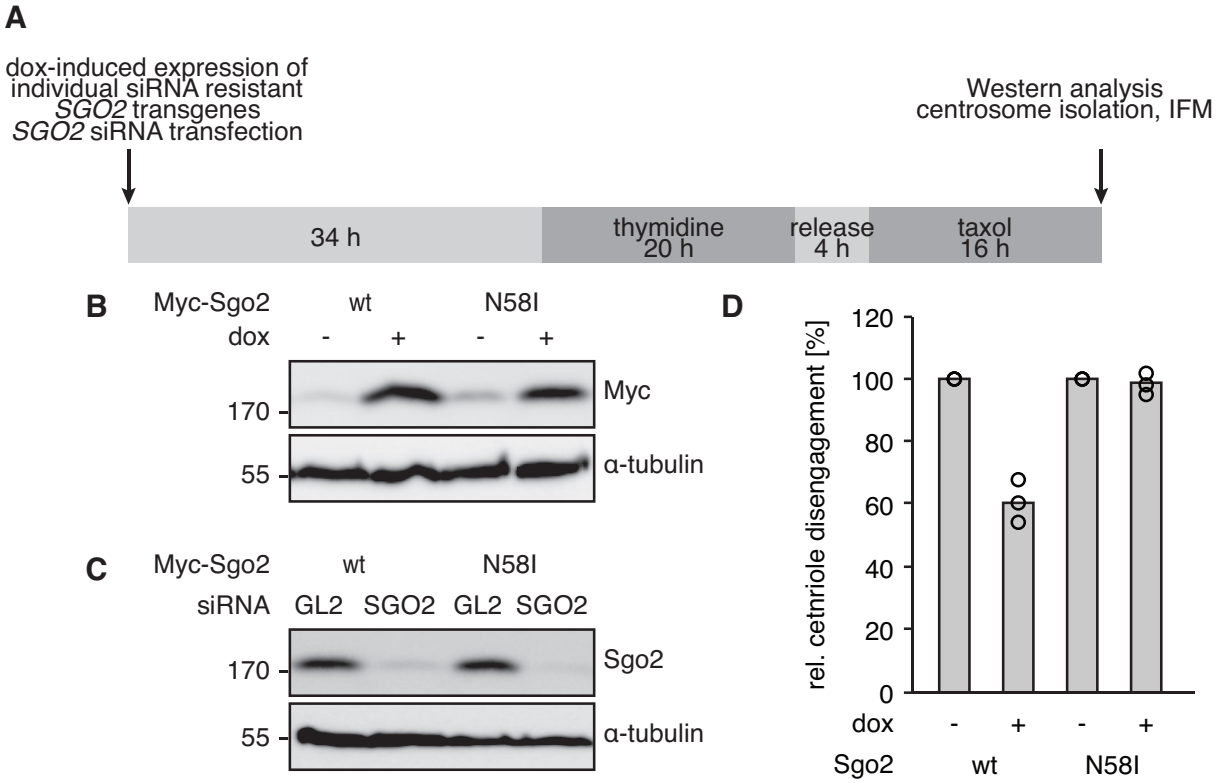

figure 31. Overexpression of siRNA-resistant Sgo2 prevents premature centriole disengagement caused by Sgo2 depletion.
(A) Experimental setup of Sgo2 knockdown-rescue experiments. At the indicated times, stable cell lines were induced by addition of doxycyline (dox) to express *SGO2* transgenes and transfected with *SGO2* siRNA to deplete all endogenous Sgo2. Cells were synchronized in prometaphase by taxol addition prior to analysis by western blotting, isolation of centrosomes, and IFM.
(B) The transgenic cell lines inducibly expressing siRNA resistant Myc-Sgo2 wild type (wt) or Myc-Sgo2^{N58I} were treated as described in (A) in the presence or absence of dox and analyzed by a Myc immunoblot for transgene expression. Immunodetection of α-tubulin served as loading control.
(C) The stable cell lines were treated as described in (A) but without dox. To test efficiency of Sgo2 depletion cells were mock (GL2) or Sgo2 depleted and Sgo2 levels were analyzed by immunoblot. Anti-α-tubulin staining served as loading control.
(D) Quantification of centriole disengagement. Each column represents averages of three independent experiments (circles, 100 centrosomes each). The amount of centriole disengagement of + dox cells was normalized to the corresponding - dox samples (set to 100%).

To test, whether Sgo1 and -2 not only work in the same pathway, but are actually redundant PP2A-recruiters at the centrosome, I asked, whether Sgo2 could also rescue a Sgo1 depletion phenotype and replace Sgo1 at the centrosome. For this experiment I used cell lines inducibly expressing Myc-tagged versions of wild type Sgo2, Sgo2 C-terminally fused to Sgo1's CTS (Sgo2-CTS) or Sgo2^{N68I}. I induced transgene expression in these cell lines, transfected them with *SGO1* siRNA and arrested the cells in prometaphase. The transgene expression was monitored by Western blot (figure 32A) and centrosomes were isolated to examine the engagement status of the centrioles (figure 32B). In the cell lines expressing wild type

Sgo2 and Sgo2-CTS centriole disengagement was reduced by 32% and 48%, respectively. The PP2A-binding deficient Sgo2 was not able to prevent premature centriole disengagement caused by Sgo1 depletion (figure 32B). In summary, Sgo1 and Sgo2 seem to be exchangeable, but loss of either one causes centriole disengagement.

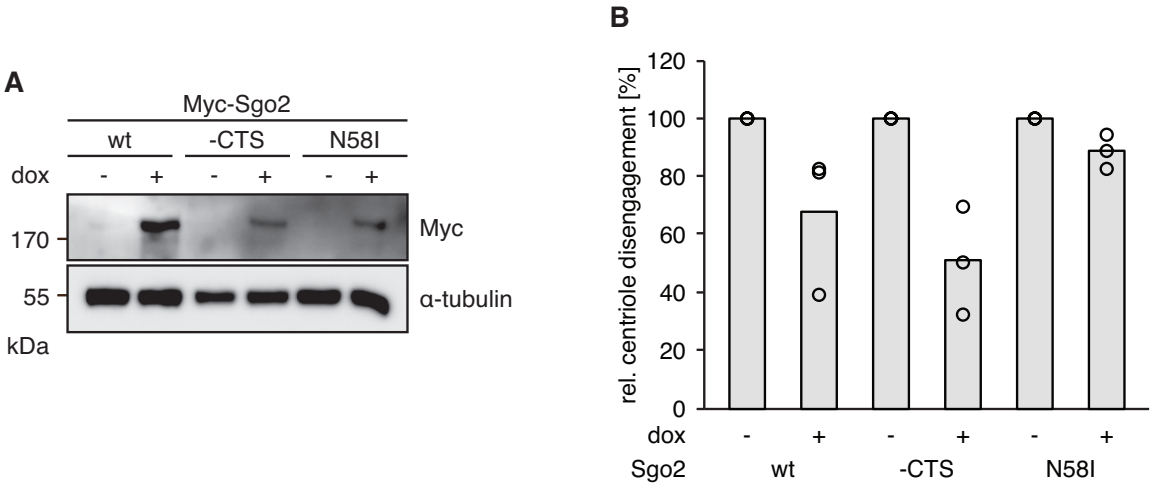

figure 32. Overexpression of Sgo2 and Sgo2-CTS rescues a Sgo1 knockdown.
(A) Transgenic cell lines inducibly express Myc-Sgo2, Myc-Sgo2-CTS or Myc-Sgo2^{N58I}. The corresponding Hek293 Flp-In T-REx cell lines were treated as described in figure 10A and analyzed by Myc immunoblot for transgene expression. Immunodetection of α-tubulin served as loading control.
(B) The stable cell lines were treated as described in figure 10A. Expression of Sgo2 of Sgo2-CTS rescues the Sgo1 depletion caused premature centriole disengagement. Centrosomes were isolated and visualized by IFM using centrin 2 and C-Nap1 antibodies. Each column represents averages of three independent experiments (circles, 100 centrosomes each). The amount of centriole disengagement in the + dox samples was normalized to the corresponding - dox samples (set to 100%).

2.6. Does Sgo1 protect cohesin from the action of the prophase pathway at the centrosomes?

At the centromere, Sgo1 A1 recruits PP2A, which counteracts the prophase pathway. My results now indicate that Sgo1 A2 and C2 together with PP2A protect centriole engagement. While this fact might imply an involvement of the prophase pathway at the centrosome, this has never been formally proven.

2.6.1. Wapl depletion prevents premature centriole disengagement caused by depletion of Sgo1

Prophase pathway signaling causes phosphorylation-dependent cohesin opening at the Smc3-Scc1 interface (Buheitel and Stemmann, 2013; Eichinger et al., 2013),

which is counteracted at centromeres by Sgo1-PP2A. Therefore, abrogating the prophase pathway by depletion of its key factor, Wapl, abolishes the need for Sgo1-mediated protection and, therefore, rescues premature loss of sister chromatid cohesion associated with Sgo1 knockdown (Gandhi et al., 2006). To explore the possibility that Sgo1-PP2A's function might be conserved on centrosomes, I tested, whether a Wapl knockdown was able to also alleviate premature centriole disengagement associated with Sgo1 depletion. Therefore, I transfected U2OS cells with siRNA against *WAPL* and/or *SGO1*, arrested the cells in prometaphase, prepared samples to analyze the efficiency of the knockdowns, and isolated the centrosomes to evaluate the engagement status of the centrioles (figure 33A). Cells depleted of Wapl alone showed a slight decrease in centriole disengagement compared to undepleted cells. The high percentage of disengaged centrioles caused by Sgo1 depletion (73%) however, was reduced to 35% in the double knockdown cells, thus arguing for conservation of Sgo1-PP2A's role as a cohesion protector between chromo- and centrosomes (figure 33B and C).

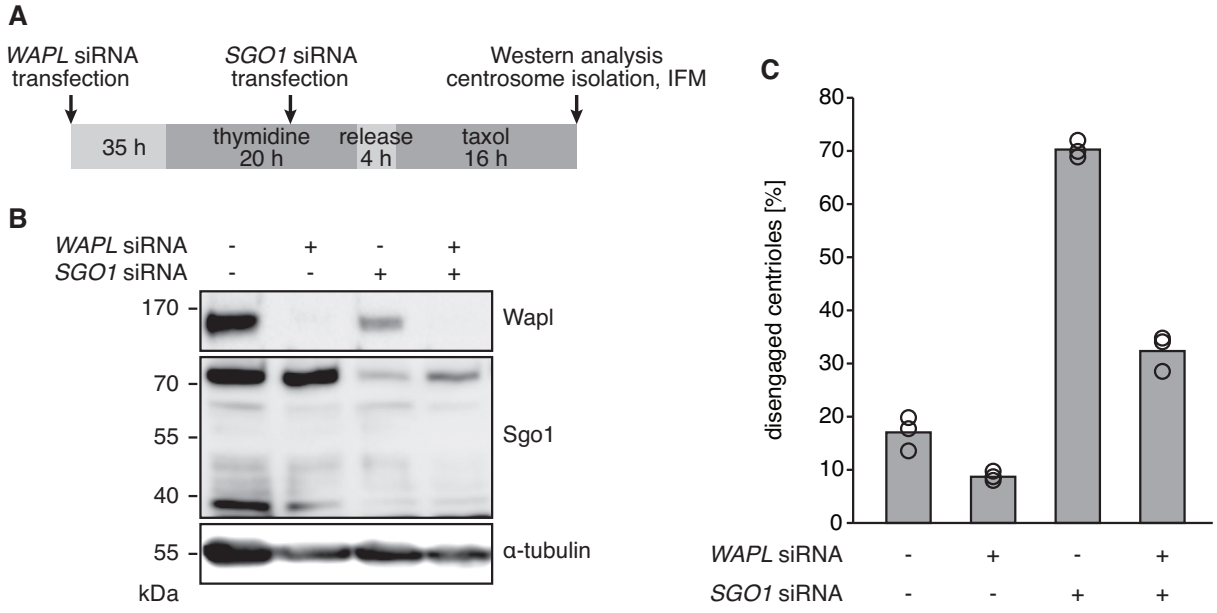

figure 33. Wapl depletion rescues premature centriole disengagement caused by Sgo1 depletion.
(A) Experimental setup of rescue of Sgo1 depletion by additional Wapl depletion. U2OS cells were depleted of Wapl by siRNA prior to synchronization in early S-phase by addition of thymidine. Cells were transfected with SGO1 siRNA, released into fresh medium and then arrested in prometaphase by taxol addition prior to analysis by Western blotting, isolation of centrosomes and IFM.
(B) U2OS cells were treated as described in (A) and analyzed by Wapl and Sgo1 immunoblots for knockdown efficiency. Immunostaining of α-tubulin served as loading control.
(C) Wapl depletion rescues premature centriole disengagement caused by Sgo1 depletion. Centrosomes were isolated and visualized by IFM using centrin 2 and C-Nap1 antibodies. Each column represents averages of three independent experiments (circles, 100 centrosomes each).

2.6.2. Sgo1 protects centrosomal cohesin from prophase pathway signaling

If the prophase pathway was acting on cohesin also at centrosomes, then artificially locking the Smc3-Scc1 gate might prevent premature centriole disengagement caused by Sgo1 depletion. I capitalized on previously generated doubly transgenic Hek293 cell lines, in which each of the three cohesin gates (Smc1-Smc3, Smc3-Scc1, or Scc1-Smc1) is tagged with FKBP and FRB (FKBP-rapamycin binding domain of mTOR) in such a way that they can individually be locked by rapamycin-induced FKBP-FRB heterodimerization (Buheitel and Stemmann, 2013). To guarantee efficient replacement of endogenous cohesin by engineered ring complexes, the induced expression of each pair of FKBP/FRB-tagged variants was combined with simultaneous depletion of the corresponding endogenous subunits by RNAi. Two days later, the cells were synchronized in early S phase. During this arrest, they were depleted of Sgo1 by siRNA transfection and later released into early G2 phase. Then, taxol and rapamycin (or DMSO as control) were added to arrest cells in prometaphase of the following mitosis and lock each of the cohesin gates in the corresponding cell line, respectively (figure 34A). Finally, the expression of the transgenes, the efficiency of the cohesin knockdowns, and the degree of sister chromatid separation and centriole disengagement were analyzed as before (figure 34B-D). Consistent with the previous finding (Buheitel and Stemmann, 2013), the loss of sister chromatid cohesion in Sgo1-depleted cells could be mitigated by closure of the Smc3-Scc1, but not by locking of the Smc1-Smc3 or Scc1-Smc1 gate (figure 34C). Interestingly, the same effect was observed at the centrosomal level: Centriole disengagement in response to Sgo1 depletion was alleviated by blocking the Smc3-Scc1 gate but not by keeping the other gates closed (figure 34D). It has been shown before that the FRB/rapamycin/FKBP-mediated closure of the Smc1-Smc3 gate is functional, despite the absence of a phenotype in this cell line (Buheitel and Stemmann, 2013). However, for the Scc1-Smc1 gate, we cannot fully exclude the possibility that the FRB/FKBP-tags of Scc1 and Smc1 are not functional, since its closure does not seem to produce phenotypes in any of our tests (Buheitel and Stemmann, 2013). Therefore, I repeated the experiments shown in figure 34 using a transgenic Hek293 cell line stably expressing an siRNA resistant SCC1-SMC1 in-

frame fusion construct, which can replace Scc1 and Smc1 functionally (Buheitel and Stemmann, 2013). Like the rapamycin-treated doubly stable cell line expressing Scc1-FRB and FKBP-Smc1, the fusion construct was not able to prevent the Sgo1 depletion phenotypes on the chromosomal and the centrosomal level (figure 35). Thus, Sgo1-PP2A is antagonizing the prophase pathway by preventing premature opening of cohesin's exit gate not only at centromeres but also at centrosomes.

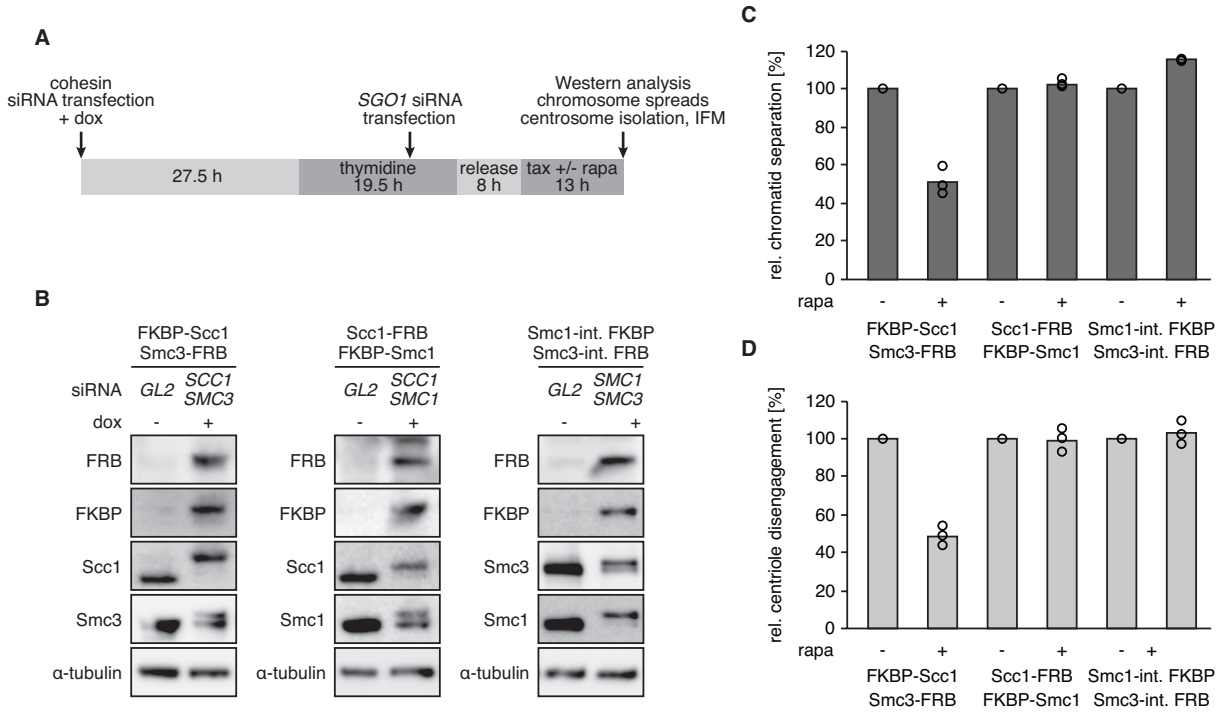

figure 34. Sgo1 protects centrosomal cohesin from prophase pathway signaling.
(A) Experimental setup of Sgo1 knockdown rescue. Expression of transgenes was induced in doubly stable cell lines transfected with cohesin and *SGO1* siRNAs as indicated. Cells were synchronized in prometaphase, supplemented with rapamycin (rapa) to close individual cohesion gates, and finally analyzed by western blotting, spreading of chromosomes, and IFM on isolated centrosomes.
(B) Three doubly transgenic cell lines inducibly co-expressing FKBP-Scc1 and Smc3-FRB, Scc1-FRB and FKBP-Smc1, or Smc1-int. FKBP and Smc3-int. FRB were transfected with *GL2*- or cohesin-directed siRNAs and incubated for 3 days in the absence (for *GL2* RNAi) or presence (for cohesin RNAi) of dox. Note that Smc3-FRB, Scc1-FRB, and Smc3-int. FRB migrate only slightly above the untagged proteins and, thus, are difficult to discern from the endogenous subunits in the mock-depleted samples. Note also that the western signals for Scc1-FRB and Smc3-FRB do not accurately reflect their expression levels because the corresponding antibodies display a greatly reduced sensitivity when their antigens are C-terminally tagged.
(C) Locking of the Scc1-Smc3 gate rescues premature loss of sister chromatid cohesion caused by Sgo1 RNAi. Analysis of chromosome spreads.
(D) Locking of the Scc1-Smc3 gate suppresses premature centriole disengagement caused by Sgo1 RNAi. Centrosomes were isolated and visualized by IFM using centrin 2 and C-Nap1 antibodies.
(C and D) Each column represents averages of three independent experiments (dots, 100 cells or centrosomes each). The amounts of chromatid separation and centriole disengagement of + rapa cells were normalized to - rapa cells (set to 100%).
Note: This experiment was done in collaboration with Johannes Buheitel (University of Bayreuth), who conducted the Western blot, chromosome spreads and quantification thereof.

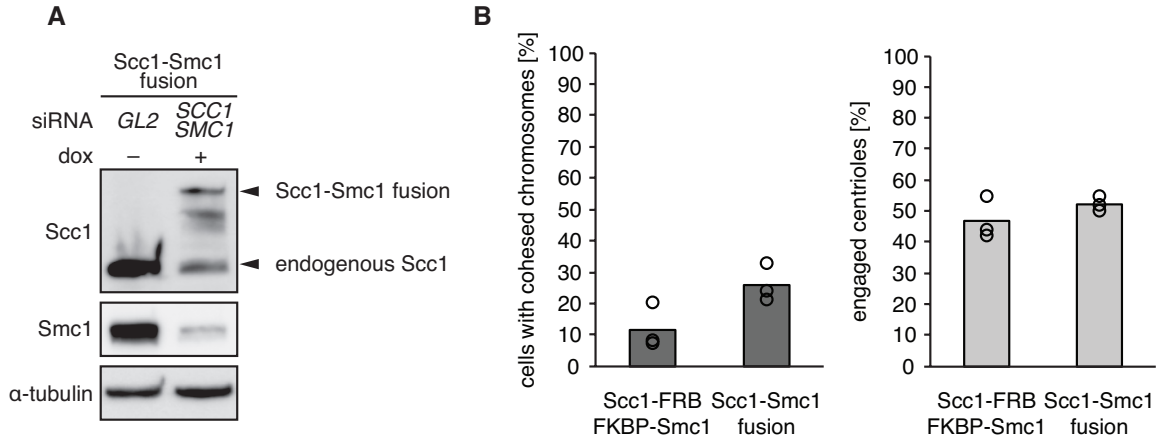

figure 35. Covalent fusion of Scc1 and Smc1 does not impair prophase pathway dependent centriole disengagement.
(A) Scc1 and Smc1 were knocked down in combination with dox-dependent expression of a covalent Scc1-Smc1 fusion construct and analyzed by Scc1 and Smc1 immunoblots. Anti-α-tubulin staining served as loading control.
(B) Shown are the absolute values of chromatid cohesion and centriole engagement of the rapamycin-treated double transgenic Scc1-FRB and FKBP-Smc1 cell line (from figure 34) and the Scc1-Smc1 fusion construct cell line.
Note: This experiment was done in collaboration with Johannes Buheitel (University of Bayreuth), who conducted the Western blot, chromosome spreads and quantification thereof.

2.6.3. Dissociation of cohesin from centrosomes in late mitosis requires separase activity

The previous results indicate that in order to cause centriole disengagement, cohesin has to be removed from the centrosome. Therefore, I wanted to test, if this removal could by visualized by IFM. To this end, HeLa cells were pre-synchronized with thymidine and then released into a taxol-mediated prometaphase-arrest. Addition of the aurora B kinase inhibitor ZM447439 (ZM) was used to release the cells from the arrest by overriding the spindle assembly checkpoint and synchronously drive them through late mitosis into G1 phase. Samples for Western blot and IFM were taken before (0 min), and 10, 30, 60 and 180 minutes after ZM addition (figure 36A). The success of the override can be seen by auto-cleavage of separase as well as degradation of cyclin B1 and securin, all of which occur about 30 minutes after ZM addition (figure 36B). I quantified the colocalization of cohesin with the centrosomes by using Smc1 and γ-tubulin antibodies for IFM (figure 36C). In the taxol-induced prometaphase arrest, Smc1 was present at the centrosomes in almost 100% of the cells (figure 36C and D). 10 minutes after the release, still 90% of the cells showed colocalization between Smc1 and γ-tubulin. 30 min after ZM addition however, Smc1

was no longer visible at 75% of the centrosomes and after 60 and 180 minutes it was absent from almost all centrosomes. Note that the taxol-ZM treatment prevents proper segregation of the separated chromatids (taxol) and inhibits cytokinesis (ZM), causing the decondensed DNA to form micronuclei visible in the 60 and 180 minutes time points. Unfortunately, whether Smc1 is reloaded onto centrosomes in telophase (as it is at chromosomes; (Buheitel and Stemmann, 2013 and figure 36C, 60 and 180 minutes after ZM), proved to be difficult to determine, as the prominent accumulation of Smc1 on DNA makes it difficult to discern any staining at the centrosome.

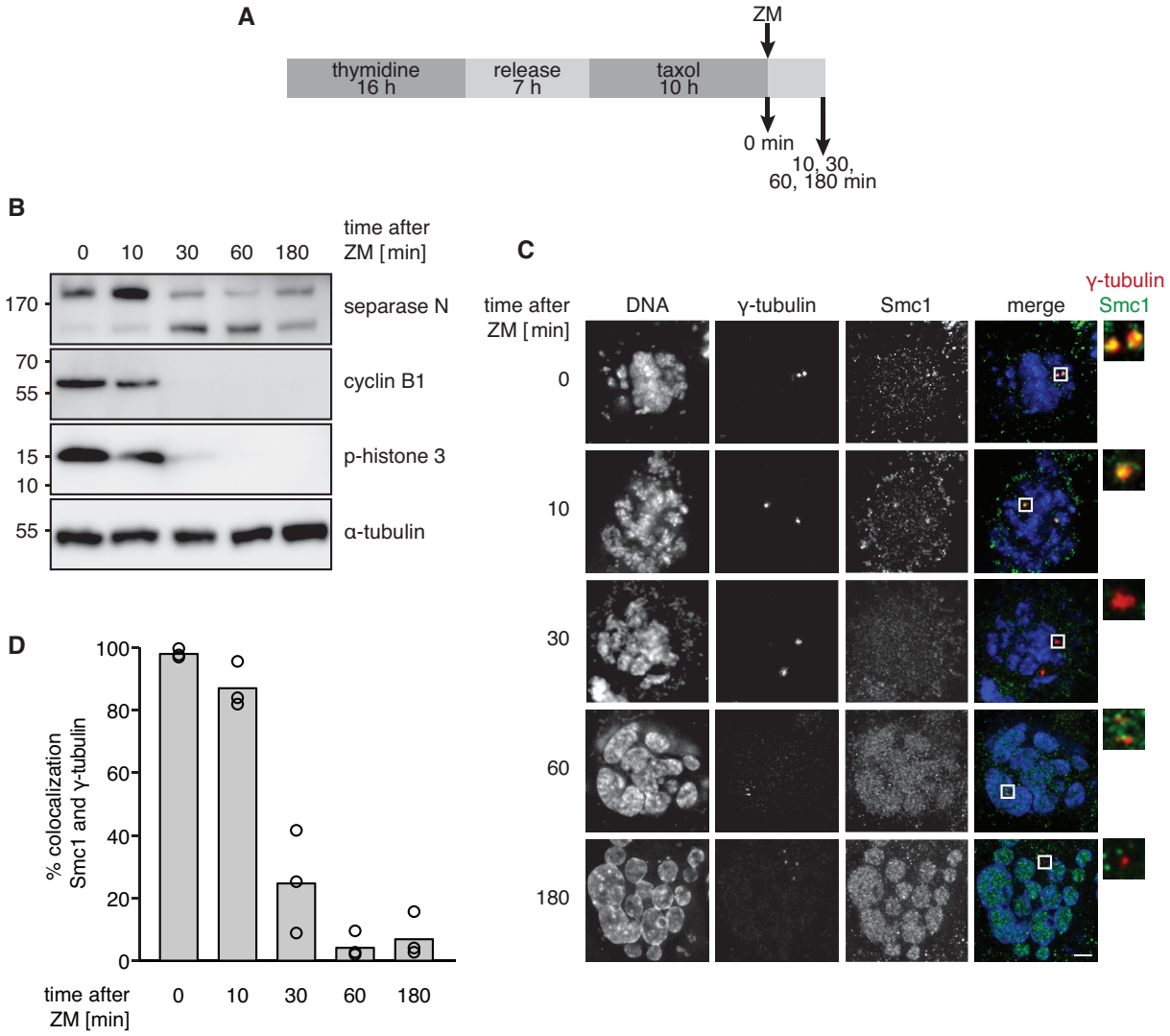

figure 36. Cohesin dissociates from centrosomes in late mitosis.
(A) Experimental setup of override of Taxol arrest by ZM447439 (ZM). HeLa cells were synchronized in early S phase by addition of thymidine. Cells were released into fresh medium and then arrested with taxol 10 hr prior to addition of ZM to override the prometaphase arrest. Directly before (0 min), 10 min, 30 min, 60 min and 180 min after ZM addition, samples were taken for western blotting and IFM.
(B) HeLa cells treated as described in (A) were analyzed in immunoblots for separase activation (auto-cleavage; anti-separase antibody raised against the N-terminus), degradation of cyclin B1 and dephosphorylation of histone 3 S10. Anti-α-tubulin staining served as loading control.

figure 36 continued:
(C) Cells treated as described in (A) were pre-extracted, fixed, and stained for Smc1, γ-tubulin, and DNA (Hoechst 33342). On the right, centrosomes are shown at 4-fold magnification. Scale bar: 5 μm.
(D) Co-localization of Smc1 and γ-tubulin as shown in C was quantified. Each column represents averages of three independent experiments (dots, 100 cells each).

While the previous experiment revealed that cohesin removal from centrosomes is seemingly timed with separase activation, it cannot provide clear evidence for a direct dependency. However, it has been shown that removal of Sgo1-PP2A-protected cohesin and, thus, ultimate centriole disengagement depends on the action of separase (Schöckel et al., 2011; Tsou and Stearns, 2006). To further corroborate this notion, I inactivated the prophase pathway by RNAi-mediated knockdown of its key player, Wapl.

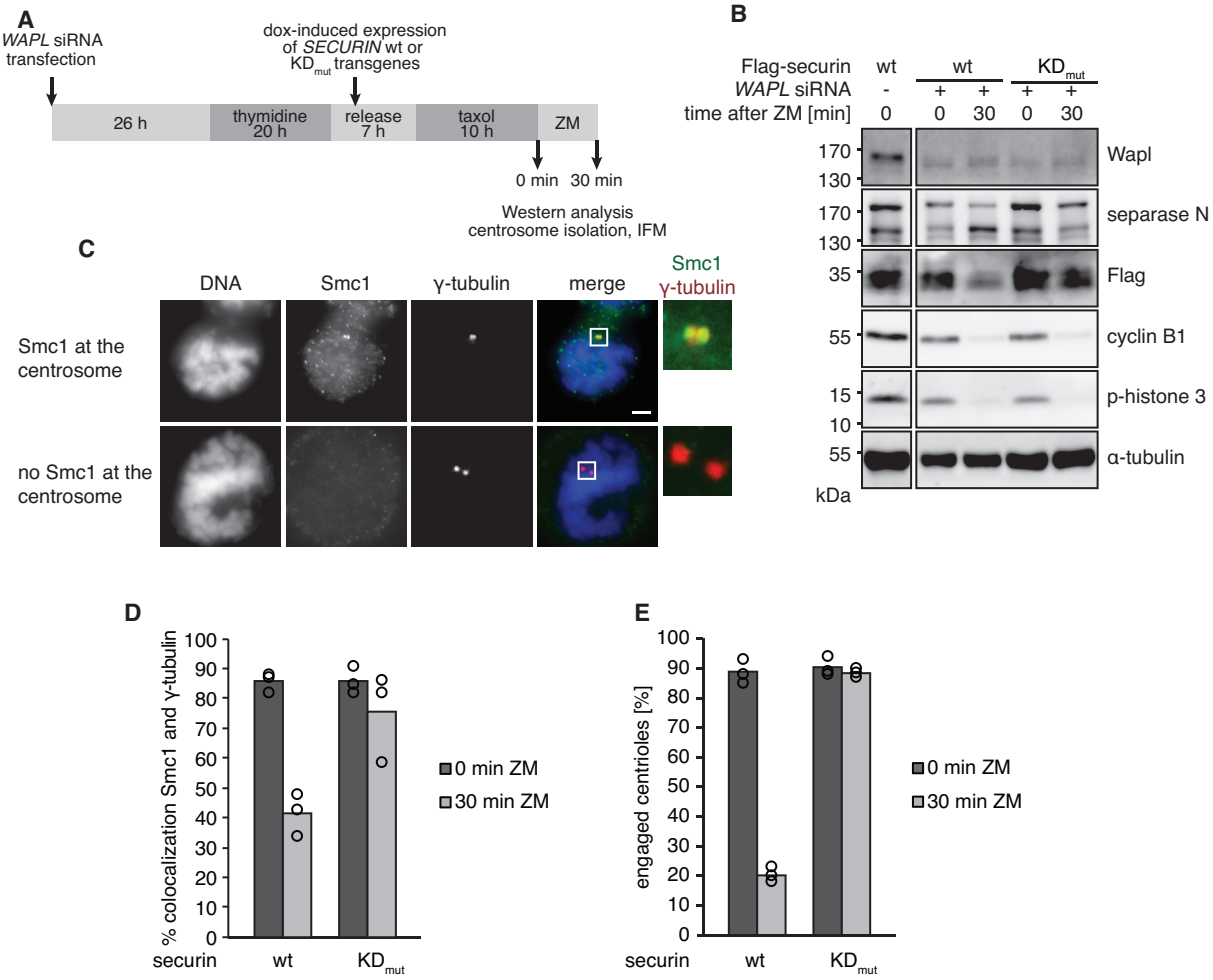

figure 37. Dissociation of cohesin from centrosomes and centriole disengagement in late mitosis require separase activity.
(A) Experimental setup of override of Taxol arrest by ZM447439 (ZM). Transgenic HeLa cell lines inducibly expressing Flag-tagged versions of wild type (WT) or non-degradable (KDmut) securin were depleted of Wapl by RNAi prior to synchronization in early S phase by addition of thymidine. Cells were released into fresh medium, induced to express the SECURIN transgenes, and then arrested

figure 37 continued: with taxol 10 h prior to addition of ZM to override the prometaphase arrest. Directly before (0 min) and 30 min after ZM addition, samples were taken for western blotting and IFM.
(B) HeLa cell lines treated as described in (A) were analyzed in immunoblots for transgene expression (anti-Flag), separase activation (auto-cleavage; anti-separase antibody raised against the N-terminus), degradation of cyclin B1, dephosphorylation of histone 3 S10, and Wapl depletion efficiency. Anti-α-tubulin staining served as loading control.
(C) Cells treated as described in (A) were pre-extracted, fixed, and stained for Smc1, γ-tubulin, and DNA (Hoechst 33342).
(D) Co-localization of Smc1 and γ-tubulin as shown in C was quantified. Each column represents averages of three independent experiments (circles, 100 cells each). Scale bar: 5 μm.
(E) Cells treated as described in (A) were analyzed by IFM on isolated centrosomes. Each column represents averages of three independent experiments (circles, 100 centrosomes each).

To show a dependency of cohesin removal on separase activity, I used transgenic HeLa cells that expressed the separase inhibitor securin either in its wild type form or as a non-degradable variant (KEN and D-box mutated = KD_{mut}; Hellmuth et al., 2014). Cells were depleted of Wapl by siRNA transfection before the taxol-ZM override, harvested before and 30 min after ZM-addition (figure 37A) and analyzed by immunoblotting (figure 37B) and IFM using γ-tubulin as a centrosomal and Smc1 as a cohesin marker (figures 37C and D). In parallel, centrosomes were isolated and assessed for their centriole engagement status (figure 37E). Quantification of cells displaying centrosomal Smc1 signals (figure 37C) revealed that inactivation of the prophase pathway by Wapl depletion does not abrogate the dissociation of cohesin from centrosomes during transition from prometaphase into late mitosis (figure 37C and D), which is hallmarked by separase auto-cleavage, cyclin B1 degradation and histone 3 serine 10-dephosphorylation (figure 37B). At the same time, centriole engagement was lost (figure 37E). In contrast, overexpression of non-degradable $securin_{KDmut}$, which cannot be degraded at the meta- to anaphase transition, keeps separase inactive. This is exemplified by lack of auto-cleavage, and resulted in continued association of cohesin with centrosomes (figure 37C and D) and engagement of centrioles (figure 37E). This phenotype was not caused by failure to resume cycling because cyclin B1 degradation and histone 3 serine 10-dephosphorylation occurred on schedule (figure 37B). Together, these results corroborate that, although the prophase pathway acts on centrosomes, the ultimate trigger of centriole disengagement is separase, which mediates removal of cohesin from centrosomes at a time when they are scheduled to undergo centriole disengagement.

3. DISCUSSION

The centrosomes' primary purpose is to nucleate and organize various microtubule arrays in interphase and mitosis. Their ability to form the mitotic spindle is crucial to ensure the correct distribution of the sister chromatids into the newly forming daughter cells. To ensure bipolarity of the mitotic spindle, and hence, faithful chromosome segregation, the centrosome cycle has to be coordinated with the chromosome cycle. The chromosome and centrosome cycles show striking parallels: (1) duplication of chromatids and centrosomes is limited to only once per cell cycle, (2) duplicated chromatids and centrosomes are evenly distributed to the newly forming daughter cells in mitosis, and (3) the regulation of both processes is marked by the dual use of several cell-cycle-coordinated key factors like Cdk1, Plk1, separase, and cohesin. Notably, Sgo1 has also been found to be involved in both processes: protecting cohesion of sister chromatids and centriole engagement (McGuinness et al., 2005; Schöckel et al., 2011; Tang et al., 2004; Wang et al., 2008; Yamada et al., 2012).

3.1 Localization of Sgo1 isoforms – dual function of Sgo1's CTS in mediating centrosomal, while abrogating centromeric recruitment

Extending a previous study (Wang et al., 2008; 2006), our group demonstrated that various splice variants of human Sgo1 exclusively localize to either centromeres or centrosomes (Mohr et al., 2015). Whereas Sgo1 A1 binds only to centromeres, Sgo1 A2 and C2 are exclusively found at centrosomes. How Sgo1 A1 is targeted to centromeres has been extensively studied in the past. It binds via its Sgo-C box to Bub1-phosphorylated histone 2A at kinetochores from where it is handed over to centromeric cohesin upon Cdk1-mediated phosphorylation of T346 (part of the polypeptide chain encoded by exon 6; (Liu et al., 2013a; 2015; 2013b). In this study, I identified the 40 C-terminal amino acids encoded by exon 9 of the A2 and C2 isoforms as the centrosomal targeting signal of human Sgo1 (CTS). Sgo1 A1 lacks the CTS, which readily explains why it is not found at centrosomes. Conversely,

centrosomal Sgo1 A2 and C2 do contain the major kinetochore targeting signal, the Sgo-C box, which strongly implies that the short CTS fulfills a dual function of mediating centrosomal targeting while simultaneously abolishing kinetochore/centromere localization. The underlying mechanisms, however, remain unclear. The CTS has no homologies to the centrosome-localizing PACT domain (PCNT-AKAP450-centrosomal targeting) of PCNT and AKAP450 (Gillingham and Munro, 2000) or the CLS (centrosomal localizing signal) of cyclin A and E (Ferguson and Maller, 2008; Matsumoto and Maller, 2004). With its 40 residues, of which we even know the last seven to be dispensable, it is also much shorter than the PACT domain (90 aa) but twice the size of the CLS (20 aa). Since the centrosome is not a membrane-enclosed organelle, recruitment to the huge multi-protein structure is unlikely to be mediated by a signal sequence utilizing special transport machineries as can be found for protein transport into the nucleus, mitochondria or endoplasmic reticulum (Dingwall and Laskey, 1991; Güttler et al., 2010; Neupert and Herrmann, 2007; Schatz and Dobberstein, 1996). In fact, recruitment to the centrosome must rather be mediated by binding to one or more components of the PCM or the centrioles. However, the identities of these recruiting factors are not known. This is true for the aforementioned PACT and CLS domains (Ferguson and Maller, 2008; Gillingham and Munro, 2000; Matsumoto and Maller, 2004) but unfortunately also for Sgo1's CTS. Due to the size and insoluble nature of the centrosome, co-immunoprecipitation as well as pulldown approaches are unlikely to produce high quality data, since interactions might be bridged by other factors or the network. A workaround for this problem might lie in utilizing a recently developed method called BioID. This proximity-dependent biotinylation technique is used to identify protein interactions in living cells (Roux et al., 2012). To this end, the protein of interest, in this case a centrosomal Sgo1 isoform or just the CTS, has to be fused to a mutated biotin-conjugating enzyme (BirA R118G or BirA*) from *E. coli* and expressed in human cell culture. Upon addition of biotin, proteins in the direct vicinity of the BirA*-tag are biotinylated. After cell lysis and complete denaturation, biotin-marked proteins can be affinity-purified using streptavidin beads and identified by mass spectrometry. The same approach was successfully used to generate a proximity map of the human centrosome-cilium interface, which confirmed the presence of cohesin and, interestingly, PP2A subunits at the centrosome (Gupta et al., 2015). However, it is

conceivable that centrosomal Sgo1 binds to a conserved, yet hitherto unknown protein in the PCM, since the CTS represents a transferrable centrosomal localization signal, which functions even in murine cells. The dominant anti-centromeric effect of the CTS might be explained by various models. One might envision that the CTS binds and thereby masks its own Sgo-C box. However, we could not detect such an interaction by genetic or biochemical assays (master's thesis Dorothea Karalus, University of Bayreuth, 2012). Alternatively, the CTS might serve as a nuclear export sequence (NES), thereby excluding those isoforms from the nucleus and preventing binding to the centromere. In fact, while Sgo1 A1 localizes to the nucleoplasm in interphase, the CTS-containing Sgo1 A2 and C2, as well as the mCherry-CTS fusion construct, are retained within the cytoplasm (this study; Kang et al., 2011). Furthermore, the CTS contains three sequence stretches weakly resembling a Crm1/exportin1-specific NES (Güttler et al., 2010). However, inhibition of Crm1-dependent nuclear export with leptomycin B did not result in altered localization of mCherry-CTS, which means that the CTS does not contain a functional NES (figure 19). Therefore, it seems likely that the CTS either alters Sgo1's three-dimensional structure in such a way that it is no longer accessible for binding to the centromere and/or that the affinity of the CTS for the centrosome exceeds that of the Sgo C-box to phosphorylated histone 2A.

3.2 Function of Sgo1 isoforms at the centrosome

Intriguingly, differential localization of human Sgo1 isoforms correlates with differential functions in that centromeric A1 protects sister chromatid cohesion, whereas centrosomal A2 and C2 sustain centriole engagement. Sgo1 at centromeres mediates the PP2A-dependent protection of cohesin ring complexes from prophase pathway signaling, which would otherwise result in premature opening of the Smc3-Scc1 gate (Buheitel and Stemmann, 2013; Kitajima et al., 2006; Riedel et al., 2006). However, the centrosomal mechanism of Sgo1-protection has remained enigmatic. Extending the parallels to the situation on chromosomes, I demonstrate here that Sgo1 recruits PP2A to the centrosomes, as exemplified by the inability of PP2A-binding-deficient A2 and C2 variants to functionally replace endogenous Sgo1 at centrosomes (figure 38). Sgo1 even becomes dispensable, when PP2A is artificially

tethered to the centrosome (figures 26 and 27). This strongly suggests that mitotic dephosphorylations at the centrosome are important for maintaining centriole engagement until separase is activated. But what is PP2As target at the centrosome? On the centromere, PP2A is known to act by reverting phosphorylations on cohesin's SA2 and sororin subunits set by Plk1 and possibly also Cdk1/Aurora B; (Dreier et al., 2011; Kitajima et al., 2006; Liu et al., 2013b; Zhang et al., 2011), thereby antagonizing the prophase pathway. This study now demonstrates that blocking the opening of the Smc3-Scc1 gate either indirectly via Wapl depletion or directly via rapamycin-mediated heterodimerization of FRB/FKBP-tagged cohesin subunits (partially) rescues the precocious loss of centriole engagement in Sgo1-depleted, prometaphase-arrested cells (figures 33-35). Thus, Sgo1-PP2A's centrosomal function consists at least partly, if not exclusively (see below), in protection of cohesin from the prophase pathway.

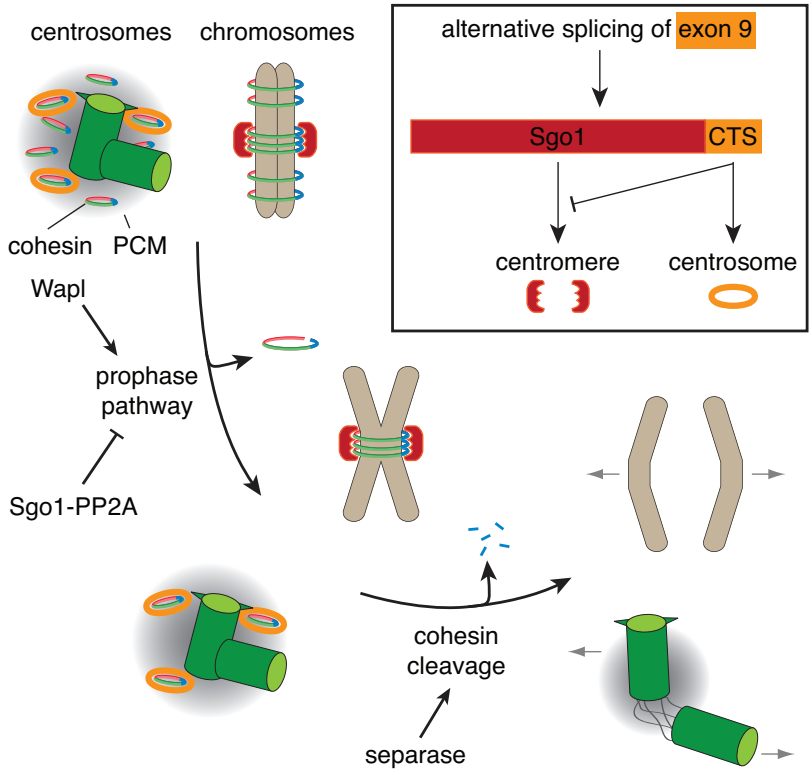

figure 38. Parallels between resolution of sister chromatid cohesion and centriole engagement. Several key players like cohesin, Wapl and separase are employed at both the chromosomes and the centrosomes. Cohesin is removed from chromosome arms as well as centrosomes by the prophase pathway (dependent on Wapl). Centromeric as well as some centrosomal cohesin rings are protected from the action of the prophase pathway by Sgo1-dependent recruitment of PP2A. The remaining cohesin is later removed by separase-dependent cleavage of its Scc1 subunit from centromeres and centrosomes. Alternative splicing gives rise to different isoforms of Sgo1, which lack or contain the exon 9-encoded CTS (centrsomal targeting signal of human Sgo1). Utilizing different isoforms of Sgo1 for protection of centromeric and centrosomal cohesin probably enables fine-tuning of both processes. For details see text.

While only one isoform of Sgo1 (A1) protects centromeric cohesin, I have demonstrated that both centrosomal Sgo1 isoforms (A2 and C2) are required to appreciably rescue centrioles from premature disengagement (figure 10). Strikingly, centrosomal Sgo1 C2 is still active in shielding centriole engagement despite the fact that (like the non-functional Sgo1 C1 isoform) it lacks T346, which is of crucial importance for the Sgo1 A1-dependent protection of chromosomal cohesin (see below). This might imply that Sgo1 does not need to bind centrosomal cohesin directly and that the tethering of PP2A in its proximity is sufficient to counteract phosphorylation-dependent opening of the ring. Consistent with this hypothesis, expression of PP2A-B'α in fusion with the CTS partially suppresses centriole disengagement in response to Sgo1 depletion (figures 26 and 27). Alternatively, centrosomal cohesin might be guarded only by (T346-containing) Sgo1 A2-PP2A, in which case Sgo1 C2-PP2A must have an as yet unidentified, different substrate. Of course, initial recruitment of both centrosomal Sgo1 variants would still be mediated by their respective CTS's. The near additive rescue effect of the simultaneous expression of both A2 and C2 in Sgo1-depleted cells would be consistent with this scenario. An attractive, yet highly speculative possibility is that this putative second substrate of centrosomal Sgo1 might be PCNT, which, next to cohesin, represents the other known centriole engagement factor and separase substrate. It should be emphasized that in this study, premature centriole disengagement was assessed in prometaphase-arrested, Sgo1-depleted cells, in which the prophase pathway is active but separase is not. Therefore, a corollary of this model would be that PCNT represents a hitherto-unappreciated second substrate of the prophase pathway.

3.3 Sgo2 – a new factor protecting centriole engagement

There is a clear division of labor between Sgo1 and Sgo2, which protect centromeric cohesion in early mitosis and meiosis I, respectively (Lee et al., 2008; Llano et al., 2012; McGuinness et al., 2005; Tang et al., 2004). Nevertheless, Sgo2 is also expressed in mitosis, where it has been associated with cohesion protection, spindle assembly and tension checkpoint (Huang et al., 2007; Kitajima et al., 2005; Orth et al., 2011; Tanno et al., 2010). However, Sgo2's role in protecting centromeric cohesin

form the prophase pathway in mitosis is highly controversial. Initially, it was reported that Sgo2 depletion causes premature loss of sister chromatid cohesion in mitotic cells similar to the effect of Sgo1 depletion (Kitajima et al., 2006). However, this observation could not be reproduced by three independent studies including this one, using different siRNAs for the Sgo2 knockdown, which suggests that the initially observed effect might have been the result of off-target effects of the siRNAs used (figure 29; Huang et al., 2007; Orth et al., 2011). Sgo2 was also reported to be involved in mitotic checkpoints by recruiting MCAK to the centromeres and thus facilitating the resolution of erroneous attachment of MTs to the kinetochores (Huang et al., 2007; Tanno et al., 2010). Furthermore, Sgo2 binds to Mad2 in a Mad1/Cdc20 like manner and has been implied as a negative regulator of spindle assembly checkpoint signaling (Orth et al., 2011; Rattani et al., 2013). However, these functions do not seem to be essential or even relevant for faithful mitosis, since Sgo2-less cells exhibit normal mitotic progression (Llano et al., 2012; Orth et al., 2011).

In this study, a new mitotic role for Sgo2 was found, surprisingly at the centrosome. Sgo2 is recruited to centrosomes in mitosis and its depletion leads to premature centriole disengagement to an extent almost as severe as depletion of Sgo1 (figure 29). The fact that combined depletion of both, Sgo1 and Sgo2, did only have a very small additional effect, suggests that they are involved in the same pathway. Overexpression of Sgo2 (but not of a PP2A-binding deficient variant thereof) not only suppresses premature centriole disengagement in Sgo2 depleted cells but to a lesser extent also in cells lacking Sgo1 (figures 31 and 32). Therefore, it is imaginable that Sgo2 functions downstream of Sgo1. In this scenario, a sufficiently high expression of Sgo2 should circumvent the requirement for Sgo1 function. To further test this hypothesis, one could try to rescue Sgo2 depletion by overexpression of Sgo1 A2 and/or C2. If Sgo2 indeed functions downstream of Sgo1, this rescue should not be possible. But what would be the target of Sgo2 at the centrosome? A direct protection of cohesin seems unlikely, since Sgo2 does not contain a known cohesin binding site. Sgo2 could nevertheless prevent premature opening of the cohesin ring by elevating the PP2A level in the vicinity of cohesin. If this was the case, combining Sgo2 depletion with Wapl knockdown or artificial closing of cohesin, should supress

the Sgo2 depletion phenotype. It should be noted, however, that Sgo2's peak recruitment to centromeres in late mitosis (where centriole disengagement should commence; figure 28) and it's apparent function in prometaphase are rather incompatible with a role solely based on centrosomal Sgo-PP2A levels. Instead, a more complex regulation of Sgo2 function is far more likely. Based on the previous hypothesis that Sgo1 C2, which is also incapable of binding cohesin, might have a different target, it is intuitive that Sgo2 might be downstream of Sgo1 C2 (figure 39).

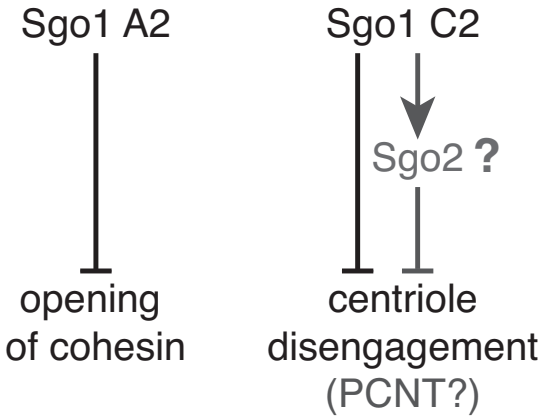

figure 39. Potential targets of Sgo1 and Sgo2 at the centrosome.
Black lines represent dependencies that have been demonstrated in this work, while gray lines stand for putative connections. For details see text.

If this is the case, what upstream effect could Sgo1 have on Sgo2? The fact that Sgo1 knockdown depletes PP2A from centrosomes (figure 22) suggests that Sgo2, for whose function PP2A-binding is also a requirement, cannot bind to centrosomes independently of Sgo1. However, to specifically address this hypothesis, one would have to investigate, whether Sgo2 is still recruited to the centrosomes in the absence of Sgo1.

3.4 How does cohesin mediate centriole engagement?

To hold the sister chromatids together, cohesin entraps the two DNA strands topologically within its ring structure (Gruber et al., 2003; Haering et al., 2002). Regarding the centrosomes, in contrast, it is impossible that cohesin, with a diameter of about 45 nm, can embrace both centrioles, each being around 200 nm in diameter and 500 nm in length. So how are the two centrioles held together by cohesin rings?

A recent electron microscopical study revealed that several cohesin subunits are located around the centrioles, i.e. in the PCM (unpublished observation Laura Schöckel, University of Bayreuth). Cohesin could therefore act indirectly, by crosslinking proteins within the PCM to form a net-like structure around the centrioles. This would be in agreement with two previous studies suggesting indirect, PCM-mediated centriole engagement (Cabral et al., 2013; Seo et al., 2015). Interestingly, the second factor known to be involved in centriole engagement, the long coiled-coil protein PCNT, spans through the highly structured PCM, with its C-terminal PACT domain directed towards the centriole and its N-terminus facing outwards (Lawo et al., 2012). It is conceivable that cohesin and PCNT form a rigid structure around the centrioles, thus holding them together. In this study, I showed that the separase-triggered centriole disengagement correlates with a removal of cohesin from the centrosome. I therefore suggest that cleavage of cohesin and/or PCNT leads to disengagement by loosening up the network around the centrioles.

Although there are many parallels between centriole disengagement and chromatid separation, there is one apparent difference: while chromatids are separated when separase becomes active at the transition form metaphase to anaphase, centrioles disengage rather late, i.e. in late mitosis or even early G1 phase (Chrétien et al., 1997; Kuriyama and Borisy, 1981; Vorobjev and Chentsov YuS, 1982). How can this discrepancy be explained? Interestingly, centriole disengagement depends not only on separase but also on Plk1 activity (Tsou et al., 2009). Strikingly, chemical inhibition of Plk1 causes centrioles to stay engaged even when separase becomes active, suggesting that Plk1 kinase activity is upstream from separase in centriole disengagement (Tsou et al., 2009). For both Scc1 and PCNT it has been shown that phosphorylation by Plk1 facilitates and enables cleavage by separase (Hauf et al., 2005; Kim et al., 2015). It is therefore conceivable that, analogous to its function in meiosis, Sgo-PP2A initially prevents cleavage of the centrosomal targets of separase. To enable disengagement, Scc1 and PCNT would then have to be deprotected by either Sgo-PP2A removal or inhibition to allow phosphorylations and therefore cleavage by separase. The timing discrepancy between cohesin cleavage at the centromere and the centrosome could be explained by several observations Hellmuth and colleagues made recently. They showed that after separase was

activated at the metaphase to anaphase transition, it becomes reinhibited by residual cyclin B (Hellmuth et al., 2014; 2015). This creates a late mitotic pool of cytosolic separase, which, upon complete cyclin B degradation at the end of mitosis, would then be able to trigger centriole disengagement.

3.5 Why does overexpression of Sgo1 C1 cause loss of sister chromatid cohesion?

At the centromeres, the mitotic kinase Bub1 phosphorylates T120 of centromeric Histone 2A, which subsequently recruits Sgo1-PP2A to the outer centromer via binding to the Sgo C-Box (Kawashima et al., 2010; Kitajima et al., 2005; Tang et al., 2006). Recent studies have found an additional histone-independent mechanism of recruitment, in which Sgo1 is phosphorylated in early mitosis at T346 (which is situated within the peptide encoded by exon 6) by Cdk1, which allows the Sgo1-PP2A complex to bind directly to cohesin (Liu et al., 2013b). While a T346A mutant is still able to localize to the outer centromere, Bub1 inactivation or a mutation (K492A) in the Sgo1 C-box delocalizes cohesin-bound Sgo1 to the chromosome arms. It has therefore been suggested that the histone 2A-dependent recruitment of Sgo1 acts as an initial step to ensure Sgo1's centromeric localization (Liu et al., 2013a). However, while the delocalized Sgo1 C-Box mutant (K492A) is still able to rescue a Sgo1 depletion phenotype, the T346A mutant fails to do so, which implies that the direct binding to cohesin is more crucial for Sgo1's centromeric function than the localization to the outer centromere (Liu et al., 2013a; 2013b). Taking this into consideration, it is not surprising that Sgo1 C1, which bears the Sgo C-box but lacks the peptide encoded by exon 6, including T346, localized to the centromere but was not able to rescue the chromosomal Sgo1 depletion phenotype (figure 10). Accordingly, overexpression of Sgo1 C1 had a dominant negative effect on chromatid cohesion, as cells arrested in mitosis due to premature loss of sister chromatid cohesin (figure 14). The same effect has previously been observed in cells overexpressing Sgo1 B1 (Matsuura et al., 2013). This isoform, potentially causing genomic instability, which is overexpressed in several non-small cell lung cancers, differs from Sgo1 C1 only in the presence of a short peptide derived from a small part of exon 6 (K492 also missing). It is therefore unlikely that Sgo1 C1 is expressed in

normal dividing cells. The overexpression of Sgo1 C1, similar to B1, could occur due to incorrect splicing and contribute to the development of cancer.

It was reported that defects in multiple factors of the splicing machinery (or spliceosome) resulted in aberrant mitotic progression (reviewed in Cooper et al., 2009). Moreover, four recent publications suggested that sister chromatid cohesion is particularly sensitive to mutations in spliceosome components, as defects in several core splicing components lead to premature loss of sister chromatid cohesion (Oka et al., 2014; Sundaramoorthy et al., 2014; van der Lelij et al., 2014; Watrin et al., 2014). In those studies, the defects in cohesion were explained by loss of sororin, due to intron retention in its transcripts, which caused frame shifts and inefficient translation. Without sororin, a key mediator of cohesion establishment and maintenance in vertebrates, its antagonist Wapl is able to prevent cohesion (Nishiyama et al., 2010; Schmitz et al., 2007). Strikingly however, the restoration of sororin levels did not completely restore normal mitotic progression, when spliceosome function was impaired. It seems therefore likely that additional targets of the spliceosome, which are involved in proper chromosome segregation, contribute to the observed phenotypes (Sundaramoorthy et al., 2014; Watrin et al., 2014). It is tempting to speculate these targets to at least include *SGO1*, potentially producing high levels of Sgo1 C1 or B1.

For many cancer types, wrongful splicing products of key factors, like the small GTPase Ras and the estrogen receptor, have been identified (Chung et al., 2016; Dong et al., 2015). For Sgo1, besides Sgo1 B1 and potentially C1, a third isoform has been described to be involved in the formation of cancer. Sgo1 P1, which consists only of the N-terminal 59 amino acids of Sgo1, is expressed only in tumors, where it drives malignancy in early stage colon cancers (Kahyo et al., 2011). Judging from its domain structure, this isoform is not able to bind Histone 2A, cohesin and probably not even PP2A, but still delays mitotic progression and causes extra γ-tubulin foci by an unknown mechanism. Please see chapter 3.7 for a more detailed discussion of Sgo1 function in cancer.

3.6 Why do humans employ specific isoforms of Sgo1?

In higher primates, the CTS specifies the localization of Sgo1, whereas mouse Sgo1 is targeted to centrosomes by other means. The signal's absence from murine Sgo1 might be explained by the high evolutionary plasticity of alternative splicing with only 28% of exons present in minor splice forms (<50% of transcripts) being conserved between human and mouse (Harr and Turner, 2010). Nevertheless, Sgo1's localization to the centrosome and its function in protecting centriole engagement are required also in mouse cells (figure 20 and 21; Wang et al., 2008). But why do higher primates employ differently specialized variants to fulfill the centromeric and centrosomal functions of Sgo1? The chromosome and centrosome cycles are usually strictly synchronized with each other, but this rule is violated on rare occasions as, for example, in male meiosis and after fertilization (reviewed in Avidor-Reiss et al., 2015; Cunha-Ferreira et al., 2009). During male meiosis, centrioles disengage and centrosomes duplicate between MI and MII, while DNA replication must not occur. Thus, the functional specialization of alternatively spliced Sgo1 variants might facilitate uncoupling of the centrosome cycle from the chromosome cycle in human spermatocytes.

Furthermore, after the second meiotic division human sperm harbor a centrosome containing two centrioles. The mother centriole functions as the basal body of the flagellum but becomes highly degenerated and loses its PCM and even 50% of its microtubule triplets, while the daughter centriole stays intact (Manandhar et al., 2000). Conversely, oocytes only contain strongly reduced, non-functional centrosomes, but still retain all the centriolar and pericentriolar components (Hertig and Adams, 1967; Sathananthan, 1997). Therefore, the sperm contributes the centrosome, but due to the reduction of the mother centriole, the daughter represents the only source of an intact centriole in the zygote (Sathananthan et al., 1996). It is not completely understood, how the second centriole is generated, but one hypothesis states that the remaining centriole undergoes two duplication cycles, one before and the second during the first replication. Thus, the cell possesses two centrosomes consisting of two centrioles to ensure a faithful bipolar division (reviewed in Avidor-Reiss et al., 2015). Since there is no separase activity after the first and until the second duplication, it is not known, how the centrioles are

disengaged and licensed for the second duplication. It is tempting to speculate that this is achieved by inactivation of Sgo-dependent protection of engagement.

3.7 Sgo1, centrosomes and cancer

Naturally, the division of labor between the Sgo1 isoforms requires exquisite regulation, as imbalanced expression ratios of centromeric *versus* centrosomal Sgo1 isoforms could result in abnormal numbers of chromosomes and/or centrosomes, both of which have been associated with the formation of cancer (Chan, 2011; Hanahan and Weinberg, 2011). As mentioned in chapter 3.5, specific isoforms of Sgo1 (B1 and P1) have been linked to cancer. It was furthermore reported that downregulation of Sgo1 leads to chromosomal instability (CIN) in colorectal cancer in humans and haploinsufficiency of Sgo1 was associated with enhanced colon tumorigenesis and development of hepatocellular carcinoma in mice (Iwaizumi et al., 2009; Yamada et al., 2012; 2015). Therefore Sgo1 has been suggested as a potential therapeutic target for cancer (Wang et al., 2015).

Interestingly, it was shown that premature centriole disengagement caused by Sgo1 depletion does not cause centriole overduplication in interphase (Wang et al., 2008). Nevertheless, maintenance of centriole engagement beyond S phase is reportedly of prime importance for mitotic fidelity. Failure to do so, while not resulting in centrosomal overduplication, does cause formation of multipolar spindles in mitosis due to separated centrioles serving as individual MTOCs (Di Fiore et al., 2003; Sluder and Rieder, 1985). Strikingly, virtually the same phenotype can be observed upon Sgo1 depletion, indicative of Sgo1's role in post-S phase maintenance of centriole engagement (Wang et al., 2008). Given this likely role of Sgo1 deficiency in cancer, it was surprising to us that the results of the Sgo1 expression study conducted in this thesis pointed towards the opposite direction. Sgo1, centromeric as well as centrosomal isoforms, were overexpressed in various cancer samples. It has to be noted that due to the design of the qPCR primers to specifically distinguish between all centromeric and centrosomal Sgo1 isoforms, it is quite possible that cancers, which featured high centromeric Sgo1 levels, were actually overexpressing Sgo1 B1 (or C1 and not A1) as it has been reported for lung cancer (Matsuura et al.,

2013). Since Sgo1 B1 and C1 are not only non-functional, but moreover, exert a dominant negative effect over A1, their overexpression would effectively phenocopy Sgo1 A1 deficiency, sufficiently explaining the observed correlation between Sgo1 overexpression and cancerogenesis. How the overexpression of centrosomal Sgo1 isoforms can be linked to cellular transformation is less intuitive. However, I showed that long-term overexpression of Sgo1 A2 and C2 causes the formation of aggregated centrosomes, with multiple daughter centrioles around one mother centriole. This “flower-like” phenotype was previously observed in cells overexpressing Plk4, the kinase inducing centriole duplication in S phase (Kleylein-Sohn et al., 2007). But why does long-term overexpression of centrosomal Sgo1 isoforms produce a similar phenotype as overduplication of daughter centrosomes? Since this phenotype did not occur after overexpression for a shorter span of time (2-3 days, data not shown) one can imagine that an overprotection of centriole engagement results in incomplete resolution of engagement by separase. And this could, in combination with several rounds of duplication without proper disengagement, lead to the observed “flower-like” phenotype. A similar process was already described at the DNA, where inactivation of the prophase pathway resulted in an excess of cohesin at the chromosomes, which in the long run could not be resolved by separase (Haarhuis et al., 2013). Since overexpression of Plk4 ultimately results in the formation of multipolar spindles (Ganem et al., 2009), it is imaginable that long-term overexpression of centrosomal Sgo1 isoforms has the same effect.

Interestingly, centrosome depletion as well as amplification have both been demonstrated to cause chromosomal instability (CIN): Depletion of the duplication factor STIL in chicken DT40 cells was shown to cause loss of centrosomes and, consequently, chromosomal instability (Sir et al., 2013). Centrosome amplification, as caused by SAS-6 or STIL overexpression, leads to supernumerary centrosomes (Kleylein-Sohn et al., 2007; Strnad et al., 2007; Tang et al., 2011) and one would assume that those cells would form multipolar spindles and therefore undergo multipolar divisions. However, Ganem and colleagues demonstrated that this only occurs rarely because spindles that are initially multipolar are usually corrected by bipolar clustering of the various MTOCs (Ganem et al., 2009). Importantly however, erroneous merotelic kinetochore-microtubule attachments, which are readily

generated during the multipolar stage, are particularly dangerous because they do not trigger the SAC (as these attachments are also capable to generate inter-kinetochore tension; Cimini, 2008; Salmon et al., 2005). Therefore, despite the bipolar clustering of the multipolar spindle, merotelic attachments are sufficient to promote missegregation of the chromatids and therefore cause CIN (Ganem et al., 2009). The small percentage of multipolar divisions results in unviable cells due to severe chromosomal missegregations.

The multiple connections between Sgo1 and the development of cancer emphasize how important it is for the cell to ensure homeostasis of Sgo1 variant levels to avoid chromosomal as well as centrosomal aberrations.

4. MATERIAL AND METHODS

4.1. Materials

4.1.1. Hard- and Software

This work was written on a MacBook Pro 13-inch, Late 2011 (Apple, Cupertino, CA, USA) running software “MacOS X” version 10.9.5 (Apple, Cupertino, CA, USA) using the text editing software "Microsoft Word 2008“ (Microsoft Corporation, Redmond, WA, USA). Diagrams were created with “Microsoft Excel 2008”. For details about IFM image acquisition see 4.5.19. Image editing was done with “ImageJ64“ (http://imagej.nih.gov/ij) with the "Bio-Formats" plugin (http://openmicroscopy.org/info/bio-formats) and „Adobe Photoshop CS4“ version 11.0 (Adobe Systems Inc., San Jose, CA, USA). Chemiluminescent signals were digitized using the "LAS-4000" system (FUJIFILM Europe GmbH, Düsseldorf, Germany). Figures were compiled in “Adobe Illustrator CS4” version 14.0 (Adobe Systems Inc., San Jose, CA, USA). "Lasergene" version 11.0.0 (DNASTAR, Madison, WI, USA) was used for analysis of DNA and protein sequences. Literature and database searches were conducted with the help of online tools provided by the National Center for Biotechnology Information (NCBI, http://www.ncbi.nlm.nih.gov/) and the European Bioinformatics Institute/Wellcome Trust Sanger Institute (EBI/WTSI, http://www.ensembl.org). “Papers2“ version 2.7.3 (Mekentosj, Dordrecht, The Netherlands) was used as bibliography software.

4.1.2. Chemicals and reagents

All chemicals and reagents were analytical grade and purchased from the following companies: Abcam (Cambridge, UK), AppliChem (Darmstadt, Germany), BD Biosciences (Heidelberg, Germany), Carl Roth (Karlsruhe, Germany), Fermentas/Fisher Scientific (Schwerte, Germany), GE Healthcare (Munich, Germany), Invitrogen/Life Technologies (Darmstadt, Germany), Merck (Darmstadt, Germany), Millipore/Merck (Schwalbach, Germany), New England Biosciences (NEB; Frankfurt a.M., Germany), Pierce/Thermo Fisher Scientific (Bonn, Germany), Roche

Diagnostics (Mannheim, Germany), Serva (Heidelberg, Germany), Sigma-Aldrich (Munich, Germany) and VWR (Darmstadt, Germany).

4.1.3. DNA oligonucleotides

DNA oligonucleotides were obtained from Sigma-Aldrich (Munich, Germany) or Eurofins Genomics (Ebersberg, Germany).

name	sequence
OS-Fse-hSGO	5'-AATGGCCGGCCAGGCATGGCCAAGGAAAGATGCCT-3'
hSgo1A1 rev -K196 stop 3'Asc	5'-GGCGCGCCTCACTTTAAACTGCTACGAACAGATAC-3'
hSgo1A2R522_5'F fwd	5'-ATAGGCCGGCCAAGAGCCCTGGAGGTATCA-3'
hSgo1_A2_Asc	5'-TTAGGCGCGCCTTACCTCAAGCAGATGTGGGTT-3'
B'ex9_Xba1long	5'-AAGCTCTAGAAAAACAGAATAGTGCTTACAACATGCACAGTATTC TCAGCAATACAAGTGCCGAACTGAGAAGAGGGGACCCTTTTACAG-3'
pcDNA_FArev_OS	5'-GCACGGGGGAGGGGCAAA-3'

4.1.4. RNA oligonucleotides (siRNAs)

All RNA oligonucleotides are 19mers with a 5'-dTdT-overhang and were obtained from Eurofins Genomics (Ebersberg, Germany)

target	name	sequence	final concentration
Luciferase	GL2	5'-CGUACGCGGAAUACUUCGA-3'	variable
hSgo1	BM_hSgo1	5'-CAGUAGAACCUGCUCAGAA-3'	50 nM each
	hSgo1 5'UTR1	5'-GAUAGCUGUUGCAGAAGUA-3'	
	LM_hSgo1	5'-GAUGACAGCUCCA GAAAUU-3'	50 nM
hSgo2	Sgo2 Yen3	5'-UCGGAAGUGUUAUUUCUUA-3'	80 nM
mSgo1	mSgo1 ORF1	5'-GCUACACUACUGAGAUAUU-3'	75 nm each
	mSgo1 ORF2	5'-GCAUUGAAAGAGAAGCUAA-3'	
Scc1	hScc13UTR1	5'-ACUCAGACUUCAGUGUAUA-3'	28.5 nM each
	hScc13UTR2	5'- AGGACAGACUGAUGGGAAA-3'	
Smc1	siSgo1_5'UTR	5'-GGAAG AAAGUAGAGACAGA-3'	57 nM
Smc3	hSmc3(3'UTR1)	5'-UGGGAGAUGUAUAUAGUAA-3'	28.5 nM each
	SMC3_3UTR_2	5'-UGUCAUGUUUGUACUGAUA-3'	
WAPL	Wapl1	5'-CGGACUACCCUUAGCACAA-3'	35 nM each
	Wapl2	5'-GGUUAAGUGUUCCUCUUAU-3'	

4.1.5. Plasmids

The multiple cloning sites of all plasmids used were replaced by FseI and AscI ("FA") sites to allow for rapid subcloning of genes by use of these rare 8-bp cutters.

name	insert	tag	backbone	origin
pBM2644	hSgo1 A1 siRNA resistant	N-Myc_6-	pcDNA5-FRT-TO	Bernd Mayer
pBM2645	hSgo1 A2 siRNA resistant	N-Myc_6-	pcDNA5-FRT-TO	Bernd Mayer
pBM2646	hSgo1 C2 siRNA resistant	N-Myc_6-	pcDNA5-FRT-TO	Bernd Mayer
pBM2740	hSgo1 C1 siRNA resistant	N-Myc_6-	pcDNA5-FRT-TO	Bernd Mayer
pLM3007	hSgo1 A2 siRNA resistant	N-$Flag_3$-Tev_2-	pcDNA3.1 attB-TO	this study
pMiS3205	hSgo1 A1 (aa1-196) siRNA resistant	N-Myc_6-	pcDNAL FRT TO Myc6 FA	this study
pLM3012	hSgo1-A2 part (aa522-end) = CTS	N-mCherry-	pCS2	this study
pLM3066	hSgo1-A2 part (aa522-end; I535A, L536A, Y537A) = CTS^{AAA}	N-mCherry-	pCS2	this study
pLM3134	hSgo1-A2 part (aa522-end) = CTS	N-FKBP-	pCS2	this study
pLM3135	hSgo1-A2 part (aa522-end; I535A, L536A, Y537A) = CTS^{AAA}	N-FKBP-	pCS2	this study
pMO2555	mSgo1	N-Myc_6-	pCS2	Michael Orth
pBM2648	hSgo1-$A2^{N61I}$ siRNA resistant	N-Myc_6-	pcDNA5-FRT-TO	Bernd Mayer
pDK2928	hSgo1-$A2^{Y57A, K26A}$ siRNA resistant	N-Myc_6-	pcDNA5-FRT-TO	Dorothea Karalus
pBM2649	hSgo1-$C2^{N61I}$ siRNA resistant	N-Myc_6-	pcDNA5-FRT-TO	Bernd Mayer
pJB3390	hSgo1-$C2^{Y57A, K26A}$ siRNA resistant	N-Myc_6-	pcDNA5-FRT-TO	Bernd Mayer
pLM3041	PP2A-B'α-fused to hSgo1-A2 part (aa522-end) = PP2A-B'α-CTS	N-Myc_6-	pcDNA5-FRT-TO	this study
pJB3319	PP2A-B'α-linker-exon9 = PP2A-B'α-CTS	N-Myc_6-	pCS2	Johannes Buheitel
pJB3323	PP2A-B'α-fused to hSgo1-A2 part (aa522-end) = PP2A-B'α-CTS^{AAA}	N-Myc_6-	pCS2	Johannes Buheitel
pMO1511	PP2A-B'α	N-Myc_6-	pCS2	Michael Orth
pAS1069	hSgo2	N-Myc_6-	pcDNA5-FRT-TO	Alexander Straßer

pLG2755	hSgo2 fused to C-terminus of Sgo1 A2 (D497-end) = Sgo2-CTS	N-Myc$_6$-	pcDNA5-FRT-TO	Laura Schöckel
pJB2304	hSgo2^{N58I} siRNA resistant (Yen3)	N-Myc$_6$-	pcDNA3.1-attB-TO	Johannes Buheitel
pJB2303	hSgo2 siRNA resistant (Yen3)	N-Myc$_6$-	pcDNA3.1-attB-TO	Johannes Buheitel
pLG2768	hSgo2^{N58I}	N-Myc$_6$-	pcDNA5-FRT-TO	Laura Schöckel
pFB2234	hSecurin	-His6-Flag-His6-Flag-C	pcDNA5-FRT-TO	Franziska Böttger
pFB2235	hSecurin mKEN + mDB	-His6-Flag-His6-Flag-C	pcDNA5-FRT-TO	Franziska Böttger
pJB2790	hScc1	N-FKBP-linker-	pcDNAL-FRT-TO	Johannes Buheitel
pJB2791	hScc1	-FRB-C	pcDNAL-FRT-TO	Johannes Buheitel
pJB2792	hSmc1 (siRNA resistant to siSmc1_ORF1)	N-FKBP-linker-	pcDNA5-loxP-TO	Johannes Buheitel
pJB2793	hSmc1 (siRNA resistant to siSmc1_ORF1)	internal FKBP-linker	pcDNA5-loxP-TO	Johannes Buheitel
pJB2897	Scc1-Smc1(siRNA resistant to siSmc1_ ORF1)-Fusion	-	pcDNAL-FRT-TO	Johannes Buheitel
pJB2794	hSmc3	-FRB-C	pcDNA5-loxP-TO	Johannes Buheitel
pJB2795	hSmc3	internal FRB	pcDNAL-FRT-TO	Johannes Buheitel
pAG1786	FLP recombinase	-	pCS2	Amelie Gutsmiedel
ΦC31	ΦC31 integrase	-	pCMV-Int	Michele P. Calos for details see (Groth et al., 2000)

4.1.6. Antibodies

Primary antibodies

target protein	species	clonality	dilution/ concentration	origin
C-Nap1	guinea pig	polyclonal	IFM: 1:2500	Self-made, for details see (Schöckel et al., 2011), affinity purified
centrin 2	rabbit	polyclonal	IFM: 1:5000	self-made, for details see (Schöckel et al., 2011), affinity purified, LG10 Run1
CREST (autoantibody against centromere)	human	polyclonal	IFM: 1:2000	Immunovision, hct-0100
cyclin B1	mouse	monoclonal	Western blot: 1:1000	Millipore, 05-373
FKBP	mouse	monoclonal	Western blot: 1:500	Abcam, ab58072
Flag	mouse	monoclonal	Western blot: 1:1000	Sigma-Aldrich, F3165
FRB	rabbit	polyclonal	Western blot: 0.34 µg/ml	self-made, for details see (Buheitel and Stemmann, 2013),

				affinity purified
Myc	mouse	monoclonal	IFM: 1:1500 Western blot: 1:2000	Millipore, clone 4A6, 05-724
p-histone 3	rabbit	polyclonal	Western blot: 1:2000	Millipore, 06-570
PP2A C	mouse	monoclonal	IFM: 1:50 Western blot: 1:1000	Millipore, clone 1D6, 05-421
RFP	rabbit	polyclonal	IFM: 1:3000	kindly provided by Stefan Heidmann
Scc1	mouse	monoclonal	Western blot: 1:1000	Millipore, 05-908
separase N	mouse	monoclonal	Western blot: 1:1000	Millipore, 05-908
Sgo1	rabbit	polyclonal	IFM: 1:50 Western blot 1:300	Abcam, ab21633
Sgo2	rabbit	polyclonal	IFM: 1:1000 Western blot: 1:2000	Bethyl Laboratories, A301-261A
Smc1	rabbit	polyclonal	IFM: 1:500 Western blot: 1:4000	Bethyl Laboratories, A300-055A
Smc3	rabbit	polyclonal	Western blot: 1 µg/ml	kindly provided by Susannah Rankin, affinity purified
survivin	rabbit	polyclonal	IFM:1:400	Santa Cruz, FL142, sc-10811
topoisomerase IIα	mouse	monoclonal	Western blot: 1:1000	Enzo, clone 1C5, ADI-KAM-CC210-E
WAPL	rabbit	polyclonal	Western blot: 1:1000	kindly provided by Susannah Rankin, affinity purified
α-tubulin	mouse	monoclonal	Western blot: 1:200	hybridoma supernatant, Developmental Studies Hybridoma Bank, 12G10
γ-tubulin	mouse	monoclonal	IFM: 1:1000	Sigma-Aldrich, T6657

Secondary antibodies

name	use	dilution	origin
HRP-conjugated goat anti-mouse-IgG	Western blot	1:20,000	Sigma-Aldrich
HRP-conjugated goat anti-rabbit IgG	Western blot	1:20,000	Sigma-Aldrich
AlexaFluor488 goat anti-mouse IgG	IFM	1:500	Invitrogen
AlexaFluor488 goat anti-rabbit IgG	IFM	1:500	Invitrogen
Cy3 goat anti-mouse IgG	IFM	1:500	Invitrogen
Cy3 goat anti-rabbit IgG	IFM	1:500	Invitrogen
Cy3 goat anti-guinea pig IgG	IFM	1:500	Jackson Immunoresearch Laboratories
Cy5 goat anti-mouse IgG	IFM	1:500	Jackson Immunoresearch Laboratories
Cy5 goat anti- human	IFM	1:500	Bethyl Laboratories

4.2. Microbiological methods

4.2.1. Strains

The *E. coli* stain XL1 blue was used for molecular cloning and plasmid production:

*E. coli sup*E44 *hsd*R17 *rec*A1 *gyr*A46 *thi rel*A1 *lac*$^-$*F'* [*pro*AB$^+$ *lac*I^q Δ(*lac*Z)M15 Tn*10*(*tet*^{r})] (Stratagene/Agilent Technologies, Santa Clara, CA, USA)

4.2.2. Media

LB medium	1% (w/v)	tryptone
	0.5% (w/v)	yeast extract
	1% (w/v)	NaCl
LB agar	LB medium	+ 1.5% (w/v) agar

4.2.3. Cultivation of *E. coli*

E. coli strains were grown at 37°C in LB medium in a vertical shaker at 200 rpm. Agar plates were incubated at 37°C. For selection of transformed bacteria ampicillin was added to the media at 100 µg/ml. Optical densities of cultures were determined at a wavelength of 600 nm (OD_{600}).

4.2.4. Preparation of chemically competent *E. coli* XL1-blue

SOB medium	0.5% (w/v)	NaCl
	0.5% (w/v)	yeast extract
	2% (w/v)	tryptone
	2.5 mM	KCl
		pH 7.0
Tbf1 buffer	30 mM	KAc
	50 mM	$MnCl_2$
	100 mM	KCl
	15% (v/v)	glycerol
		pH 5.8
Tbf2 buffer	10 mM	MOPS-NaOH
	75 mM	$CaCl_2$
	10 mM	KCl
	15% (v/v)	glycerol
		pH 7.0

To produce chemically competent bacteria, 300 ml SOB medium were inoculated with 4 ml of an overnight culture of XL1 blue with an OD_{600} of 0.5. The culture was chilled on ice for 15 min and cells were harvested by centrifugation (4°C, 3000 g, 15 min). All following steps were performed at 4°C. The pelleted bacteria were carefully resuspended in 90 ml Tbf1 buffer and incubated on ice for 15 minutes. After another centrifugation (4°C, 1500 g, 15 min) the cells were resuspended in 15 ml Tbf2 buffer and placed on ice for 5 min. Aliquots of this suspension were snap-frozen in liquid nitrogen and stored at -80°C.

4.2.5. Transformation of *E. coli*

To transform *E. coli* with Plasmid DNA, chemically competent cells were thawed on ice. 50 µl of the suspension were carefully mixed with 50 ng of plasmid DNA or 5 µl of ligation mix (see 4.3.7) and incubated on ice for 20 min. After a heatshock at 42°C for 45 s the suspension was chilled on ice for 2 min, followed by addition of 500 µl LB medium and incubation at 37°C for 30 min to allow the ampicillin resistance gene to be expressed. To select transformed cells, the suspension was plated on LB agar containing ampicillin.

4.3. Molecular biological methods

4.3.1. Isolation of plasmid DNA from *E. coli*

2 ml LB medium supplemented with ampicillin were inoculated with a single colony of transformed *E. coli*. After incubation at 37°C in a rotator, plasmid DNA was purified by alkaline lysis followed by DNA purification via silica columns according to the manufacturer's instructions (Fermentas/Thermo Scientific, Schwerte, Germany). Higher amounts of plasmid DNA for transfection of human cells were isolated out of 50-100 ml of over night culture using a plasmid midi preparation kit (QIAGEN, Hilden, Germany).

4.3.2. Determination of DNA concentrations in solutions

DNA concentrations in solutions were measured by determination of the optic density at a wavelength of 260 nm (OD_{260}) using a ND-1000 spectrophotometer (PeqLab, Erlangen, Germany). An OD_{260} of 1 corresponds to 50 μg/ml double-stranded DNA.

4.3.3. Restriction digestion of DNA

All used restriction enzymes were obtained from either NEB (Frankfurt a. M., Germany) or Fermentas/Thermo Scientific (Schwerte, Germany) and digestion was performed according to the manufacturer's instructions. Normally 1-5 units of enzyme were used to digest 1 μg DNA. Samples were incubated at the suggested temperatures for 1 h.

4.3.4. Dephosphorylation of DNA fragments

To prevent religation of digested vectors, the 5'-end of the vector DNA was dephosphorylated by addition of 1 unit of antarctic phosphatase (NEB, Frankfurt a. M., Germany) in the corresponding buffer at 37°C for 1 h.

4.3.5. Separation and analysis of DNA fragments by agarose gel electrophoresis

TPE buffer	50 mM	Tris
	0.13% (v/v)	H_3PO_4
	2 mM	EDTA
TBE buffer	90 mM	Tris
	90 mM	boric acid
	2.5 mM	EDTA
6x DNA loading buffer	50% (v/v)	glycerol
	0.1 M	EDTA
	0.02% (w/v)	xylene cyanol
	0.02% (w/v)	bromophenol
	0.02% (w/v)	SDS

For analysis or for preparative isolation, DNA fragments were electrophoretically separated on agarose gels. For this purpose, 1-2% agarose gels were prepared with TPE buffer (separation of fragments > 1 kb) or TBE buffer (separation of fragments <1 kb) and supplemented with ethidium bromide (final concentration: 0.5 µg/ml). The DNA samples were mixed with loading buffer (to 1x) and separated at 100 V in TBE or TPE buffer. The DNA fragments could be visualized due to the intercalation of ethidium bromide with the DNA using a UV transilluminator (324 nm). Size of the fragments was estimated using the standard size marker O'GeneRuler 1 kb DNALadder (Fermentas, St. Leon-Rot, Germany) or a self-made standard made from EcoRI-restriction digestion of SPP1 bacteriophage DNA.

4.3.6. Isolation of DNA from agarose gels

After gel electrophoresis, the band of the desired fragment was excised with a scalpel from the gel. The DNA was extracted using the GeneJet Gel Extraction Kit (Fermentas/Thermo Scientific, Schwerte, Germany) according to the manufacturer's instructions.

4.3.7. Ligation of DNA fragments

10x T4 DNA ligase buffer	50 mM	Tris-HCl, pH 7.5
	10 mM	$MgCl_2$
	1 mM	ATP
	10 mM	DTT

The amounts of insert and linearized, dephosphorylated vector and were estimated on an agarose gel. For the ligation, the molar ratio of vector to insert was adjusted to 1:3. The reaction mix of 10 µl usually additionally contained 1 µl of T4 DNA ligase (self-made in the lab) and 1 µl ligase buffer and was incubated at room temperature for 1 h.

4.3.8. Polymerase chain reaction (PCR)

For PCR reactions, a 50 µl mix containing 0.2 µl of 5'- and 3'- oligonucleotides (100 pmol/µl), 1 µl deoxyribonucleotide triphosphate mix (10 mM , NEB , Frankfurt a . M.) and 1 U DNA polymerase (Phusion, Fermentas/Thermo Scientific, Schwerte, German) in the corresponding PCR buffer (Phusion HF or GC buffer). As a template, 100 ng of plasmid DNA were used. Amplification was carried out in a TC-512 cycler (Techne, Burlington, NJ , USA).

step	temperature	duration	number of cycles
initial denaturation	98°C	1 min	1
denaturation	98°C	20 s	25
annealing	optimized for used oligonucleotides	20 s	
elongation	72°C	30 s/kb	
final elongation	72°C	5 min	1

4.3.9. Mutagenesis PCR

Site-directed mutagenesis was accomplished by a fusion PCR based method. To this end, two reverse-complement primers were used which carried the desired mutations. In two different PCR reactions using one of the mutagenesis primers an upstream and a downstream fragment generated. The respective outer primers were designed to carry additional restriction sites at their 5' ends. After gel purification, PCR was performed using the two PCR products (which anneal to and therefore prime each other) and the two outer primers to create a fused fragment. The resulting fragment was digested with the corresponding restriction enzymes and ligated into a identically digested vector carrying the wild-type ORF. The mutations were verified by sequencing (SeqLab, Göttingen, Germany).

4.3.10. Quantitative PCR (qPCR)

To quantify the amounts of SGO1 cDNA in different cancer tissues, I performed qPCR on commercial cDNA (brain, testis and fetal kidney, Takara/Clontech, Saint-Germain-en-Laye, France) and “TissueScan” cancer tissue cDNA arrays (Cancer survey I CSRT 101, OriGene, Rockville, MD, USA) containing 96 samples of cDNA,

which were obtained from 8 different tissues (breast, colon, kidney, liver, lung, ovaries, prostate and thyroid gland) at different stages of cancer. To quantify amounts of cDNA the TaqMan® system was used, which consists of a pair of unlabeled PCR primers and a probe with a fluorescent dye label on the 5' end and non-fluorescent quencher (NFQ) on the 3' end. During amplification, the polymerase reaches the probe and its endogenous 5' nuclease activity cleaves the probe, separating the dye from the quencher. The following forward and reverse primers were used in combination with a probe that was coupled to a FAM (6-carboxyfluorescein) reporter at the 5' end and a quencher (NFQ, non-fluorescent quencher) at the 3' end (designed with the Applied Biosystems software) targeting the unique 3' ends of either *SGO1* A1 or *SGO1* A2 and C2 cDNA).

name	sequence
SGO1 A1_fwd	5'-CTGGGATTACTGAGCCACTGT-3'
SGO1 A1_rev	5'-TGCCAGAAGCTTATAATTAAAAGATCTTATTTGAGTA-3'
SGO1 A1_probe	FAM-5'-CCCAAAATGTATCTTATACAAACAT-NFQ
SGO1 A2/C2_fwd	5'-AGCCCTTTAATTAGAGATAGCAACTTTCC-3'
SGO1 A2/C2_rev	5'-CAATCTCCAAGTGACACAACCAAAA-3'
SGO1 A2/C2_probe	FAM-5'-CTGATTCCTCGGTCACCC-3'-NFQ

To guarantee that identical amounts of template were used in all experiments, levels of *SGO1* cDNA had to bee normalized to cDNA levels of housekeeping genes. For initial optimization of the qPCR protocol, duplex-qPCR was performed with either SGO1 A1 or A2 and C2-primer mix in combination with a commercially available GAPDH primer mix, containing forward and reverse primers against GAPDH cDNA and a probe, coupled to a VIC reporter at the 5'-end and NFQ at the 3'-end (TaqMan® Gene expression Assays, GAPDH, no 4448484, Applied Biosystems/Thermo Scientific, Schwerte, Germany). The cDNAs of the cancer tissue array that were custom-plated on two 46-well plates were already normalized to β-actin expression. The qPCR reaction mix prepared as follows:

TaqMan universal master mix (no. 4324018, Applied Biosystems)	10 µl
primer mix SGO1	1 µl
primer mix GAPDH *	1 µl
cDNA *	0.5 or 1 µl
ddH_2O	ad 20 µl
	* only for initial studies

For expression studies of the cDNA array, the reaction mix was prepared without cDNA, vortexed, 20 µl were added to each well and the plates were sealed with adherent foil. The plates were then vortexed on the lowest speed, incubated on ice for 15 min, before being analyzed with a StepOne™ Real-Time PCR cycler (Applied Biosystems/Thermo Scientific, Schwerte, Germany).

4.4. Protein biochemical methods

4.4.1. Separation of proteins by denaturing SDS polyacrylamide gel electrophoresis (SDS-PAGE)

17% resolving gel (37.5 ml)	14 ml 1 M Tris-HCl, pH 8.8 21.3 ml 30% acryl amide-bisacryl amide (37.5:1) 2 ml 2.5 M sucrose 20 µl 20% SDS 160 µl 10% ammonium persulfate (APS) 11 µl TEMED
8% resolving gel (35 ml)	13.1 ml 1 M Tris-HCl, pH 8.8 9.3 ml 30% acryl amide-bisacryl amide (37.5:1) 12.4 ml ddH_2O 20 µl 20% SDS 160 µl 10% ammonium persulfate (APS) 11 µl TEMED
7% stacking gel (32.5 ml)	4.1 ml 1 M Tris-HCl, pH 6.8 7.6 ml 30% acryl amide-bisacryl amide (37.5:1) 20.6 ml ddH_2O 20 µl 20% SDS 160 µl 10% ammonium persulfate (APS) 11 µl TEMED
1x Laemmli running buffer	25 mM Tris 192 mM glycine 0.1% (w/v) SDS
4 x SDS sample buffer	40% glycerol 250 mM Tris-HCl, pH 6.8 8% (w/v) SDS 0.04% (w/v) bromophenol 2 M β-mercaptoethanol

Samples which were to be examined by SDS-PAGE, were mixed with SDS-sample buffer (to 1x) and denatured at 95°C for 5 to 15 min before they were loaded on self-poured 8-17% SDS gels. The gels ran at 25 mA in chambers with 1x Laemmli

running buffer for 75-90 min. Protein masses were estimated using the PageRuler prestained Molecular Weight Marker (Fermentas/Thermo Scientific, Schwerte, Germany).

4.4.2. Immunoblotting (Western blot)

Blotting buffer	25 mM	Tris
	192 mM	glycine
	0.01% (w/v)	SDS
	15% (v/v)	methanol
TBS/T	25 mM	Tris-HCl, pH 7.5
	137 mM	NaCl
	2.6 mM	KCl
	0.05% (v/v)	Tween-20
10x PBS	1.37 M	NaCl
	27 mM	KCl
	80 mM	Na_2HPO_4
	14 mM	KH_2PO_4
		pH 7.4

To identify proteins by Western blotting, after SDS-PAGE they were electrophoretically transferred on a PVDF (polyvinylidene fluoride) membrane (Serva, Heidelberg, Germany). For the applied semi-dry blotting method, gel and membrane were placed between two extra-thick blotting papers (BioRad, Munich, Germany), which had been pre-incubated in blotting buffer. The membrane had previously been activated in 100% methanol for 5 min, washed with ddH_2O and finally equilibrated in blotting buffer for 2 min. The proteins were transferred to the membrane in a semi-dry blotter (PeqLab, Erlangen, Germany) at 12 V and 120 mA for 1.5 h.

All subsequent steps were performed on a rocking shaker. After blotting, the membrane was blocked for 45 min in 5% (w/v) milk powder in 1x PBS and then washed 3 times for 10 min with TBS/T. Subsequently, the incubation with the primary antibody diluted in PBS/3% BSA was carried out for 1 h at RT or overnight at 4°C. After three 10-minute washes with TBS/T, the membrane was incubated with the secondary antibody diluted in 5% (w/v) milk powder in 1x PBS at RT for 1 h. Thereafter, the membrane was washed several times with TBS/T. The detection was carried out using electrochemiluminescence reagents (HRP-Juice, p.j.k,

Kleinblittersdorf, Germany or Lumigen ECL Ultra (TMA-6), Southfield, MI, USA) according to the manufacturer's instructions with an "LAS-4000" detection system (FUJIFILM Europe GmbH, Düsseldorf, Germany).

4.5. Cell biological methods

4.5.1. Basic mammalian lines

Hek293T human embryonic kidney cells (large T-antigen of SV40 transformed variant of the 293 cell line)

Hek293 FlpIn Flp-In™ T-REx™ 293 cell line (Invitrogen/Life Technologies (Darmstadt, Germany), containing a FLP site for Flp recombinase-directed integration of transgenes. Furthermore, cells express a tetracycline repressor, which binds to the tetracyclin operator sequence in the absence of tetra- or doxycycline to repress expression of subsequent genes. Addition of tetra- or doxycycline induces transgene expression.

HeLa K human cervix epithelial adenocarcinoma cells, subclone K

HeLa FlpIn Flp-In™ T-REx™ HeLa cell line (Thomas Mayer, University of Konstanz), containing a FLP site for Flp recombinase directed integration of transgenes. Furthermore cells express a tetracycline repressor, which binds to the tetracyclin operator sequence in the absence of tetra- or doxycycline to repress expression of subsequent genes. Addition of tetra- or doxycycline induces transgene expression.

U2OS human osteosarcoma cell line expressing wild type p53 and Rb, but lacking p16

NIH 3T3 mouse embryonic fibroblast cells, immortalized after the “3T3-protocol”

4.5.2. Stable cell lines

name	cell line	expressed protein 1	expressed protein 2	origin
1069	Hek293 FlpIn	Myc_6-hSgo2	-	this study
2234	HeLa FlpIn	hSecurin-His_6-Flag-His_6-Flag	-	Franziska Böttger
2235	HeLa FlpIn	hSecurin$^{mKEN + mDB}$-His_6-Flag-His_6-Flag	-	Franziska Böttger
2303	Hek293 FlpIn	Myc_6-hSgo2 siRNA resistant (Yen3)	-	this study

2304	Hek293 FlpIn	Myc_6-hSgo2^{N58I} siRNA resistant (Yen3)	-	this study
2644	Hek293 FlpIn	Myc_6-hSgo1 A1 siRNA resistant	-	Laura Schöckel
2645	Hek293 FlpIn	Myc_6-hSgo1 A2 siRNA resistant	-	Laura Schöckel
2646	Hek293 FlpIn	Myc_6-hSgo1 C2 siRNA resistant	-	Laura Schöckel
2646 + 3007	Hek293 FlpIn	Myc_6-hSgo1 C2 siRNA resistant	$Flag_3$-Tev_2-hSgo1 A2 siRNA resistant	this study
2648	Hek293 FlpIn	Myc_6-hSgo1-A2^{N61I} siRNA resistant	-	Laura Schöckel
2649	Hek293 FlpIn	Myc_6-hSgo1-C2^{N61I} siRNA resistant	-	this study
2740	Hek293 FlpIn	Myc_6-hSgo1 C1 siRNA resistant	-	this study
2755	Hek293 FlpIn	Myc_6-hSgo2-CTS	-	Laura Schöckel
2768	Hek293 FlpIn	Myc_6-hSgo2^{N58I}	-	this study
2790.4 + 2794.3	Hek293 FlpIn	FKBP-linker-Scc1	Smc3-FRB	this study
2791.6 + 2792.2	Hek293 FlpIn	Scc1-FRB	FKBP-linker-Smc1 (siRNA resistant)	this study
2795.7 + 2793.7	Hek293 FlpIn	Smc3-int. FRB	Smc1-int. FKBP	this study
2897.4	Hek293 FlpIn	Scc1-Smc1 fusion	-	this study
2928	Hek293 FlpIn	Myc_6-hSgo1-A2$^{Y57A, K26A}$ siRNA resistant	-	this study
3041	Hek293 FlpIn	Myc_6-PP2A-B'α-CTS	-	this study
3390	Hek293 FlpIn	Myc_6-hSgo1-C2$^{Y57A, K26A}$ siRNA resistant	-	this study

4.5.3. Cultivation of cell lines

All cell lines were cultured in DMEM (Dulbecco's modified eagle medium, PAA, Pasching, Östereich) supplemented with 10% fetal calf serum (FCS, Sigma-Aldrich (Munich, Germany) at 37°C and 5% CO_2. Adherent cultures grown in cell culture dishes (Greiner Bio-One, Kremsmünster, Austria) were split twice a week in the ratio 1:4 - 1:10. For this purpose, the medium was removed from the cell culture dishes, cells were washed with PBS (see 4.4.2) and subsequently incubated with Trypsin/EDTA solution (16 μl/cm^2, GIBCO/Thermo Fisher Scientific, Bonn, Germany) for 1 min (Hek and NIH 3T3 cells) or 5 min (HeLa and U2OS cells) to detach cells from the cell culture dish. By pipetting up and down in fresh medium, the cells were further detached from the tray and from each other. Cells were pelleted by centrifugation (300 g, 3 min, RT), and the pellet was resuspended in the required

volume of fresh medium. Exact numbers of cells were determined by the Vi-Cell Counter (Beckman Coulter, Krefeld, Germany).

4.5.4. Storage of cells

Cells were harvested by trypsinization (see 4.5.3) at a confluence of 80%, resuspended in storage medium (10% DMSO, 90% FCS) and aliquotted in cryo-tubes (Nalgene, Rochester, NY, USA). The cell suspension was then frozen slowly in a cardboard box at -80 ° C. For long time storage, the tubes were transferred into a tank of liquid nitrogen. For thawing, cryo-stocks were put into a water bath at 37°C. To remove the DMSO, the cell suspension was diluted with 10 ml medium and the cells centrifuged (300 g, 2 min). Finally, the pellet was resuspended in fresh medium and spread on cell culture dishes.

4.5.5. Transfection of Hek293 cells

2x HBS	800 mg	NaCl
	37 mg	KCl
	10.65 mg	Na_2HPO_4
	100 mg	glucose
	500 mg	HEPES
		adjust pH to 7.05 with NaOH, sterile filtered

Hek293T and Hek293 FlpIn cells were transfected with plasmid DNA or siRNA using the calcium phosphate method at a confluency of 40-60%. Shortly before transfection chloroquine was added to the medium (final concentration: 20 μM). The transfection mix was prepared as follows:

diameter of dish	**5.3 cm**	**10 cm**	**14.5 cm**
volume of medium	4 ml	10 ml	25 ml
amount of DNA	4 μg	16 μg	30 μg
ddH_2O (-volume of DNA and $CaCl_2$)	300 μl	800 μl	2000 μl
2 M $CaCl_2$	37.2 μl	99.2 μl	248 μl
2x HBS	300μl	800 μl	2000 μl

DNA or siRNA (for final concentrations see 4.1.4) was first mixed with ddH_2O, before sterile 2 M $CaCl_2$ was added. The HBS was then slowly dropped into the solution while vortexing. Finally, the transfection mix was added dropwise to the cells. After 8-12 h, the medium was changed. Depending on the experiments, cells grew and expressed the transgenes for 24 - 72 h.

4.5.6. Transfection of HeLa, U2OS and NIH 3T3 cells

For transfection of plasmid DNA into HeLa and NIH 3T3 cells, Lipofectamine 2000 (Invitrogen/Life Technologies, Darmstadt, Germany) was used. The following amounts refer to the transfection of cells on a 6-well plate. The transfection mix was prepared in two steps: First, 2 μg DNA were diluted in 250 μl OptiMEM (Invitrogen/Life Technologies, Darmstadt, Germany). In a separate reaction tube, 10 μl Lipofectamine 2000 were mixed with 250 μl OptiMEM. After 5 min incubation at RT, the DNA solution was added to the Lipofectamine solution and mixed well. After 20 min, the transfection mix was added to the cells. In order to keep the cytotoxicity as low as possible, the medium was changed after 4 - 8 hours.

Transfection of siRNA in HeLa, U2OS and NIH 3T3 cells was done using Lipofectamine RNAiMAX. For transfection of cells grown on a 8.6 cm dish, siRNA (for final concentrations see 4.1.4) was diluted in 1 ml OptiMEM. 20 μl Lipofectamine RNAiMAX were mixed with 1 ml OptiMEM and immediately added to the siRNA mix. After 20 min incubation at room temperature, the transfection mix was dropped on the cells and medium was changed 4 - 10 h later.

4.5.7. Generation of stable cell lines

To generate stable cell lines, Hek293 FlpIn cells were grown on a 14.5 cm dish. At 50% confluency, they were co-transfected with 3 μg of a plasmid containing the gene of interest (under control of a tetracyclin operator), a hygromycin resistance cassette and an FRT-site (which allows recombination into the FLP-site of the host genome), and 30 μg of a plasmid expressing the Flp recombinase (pAG1786). 48 h after transfection, hygromycin B was added (150 µg/ml, PAA) to select for clones with

stable integration of the transgene into the host genome. For 2 to 3 weeks, medium supplemented hygromycin B was changed every 2 - 4 days until clones were visible. They were isolated using small glass cylinders for trypsination (see 4.5.3). The clones were transferred into single wells of a multi-well cell culture dish and grew under selection until they were test-induced to verify expression of the transgene.

The doubly transgenic *SGO1* cell line was generated by ϕC31 integrase-mediated insertion of a $Flag_3$-Tev_2-Sgo1 A2 expression plasmid, which contained an *attB*-site and a neomycin resistance cassette into a cell line that already contained a Myc_6-Sgo1 C2 expressing transgene. To this end, 30 *µ*g of the ϕC31 plasmid and 3 *µ*g of the *SGO1*-plasmid were co-transfected and 48 h after transfection, clones were selected with 270 µg/ml G418 (GIBCO/Thermo Fisher Scientific, Bonn, Germany). The following steps were as described above.

The doubly transgenic Hek293 cell lines expressing FRB/FKBP-tagged cohesin subunits and the transgenic HeLa cell lines expressing securin wt and KD_{mut} have been previously described (Buheitel and Stemmann, 2013; Hellmuth et al., 2014).

4.5.8. Induction of transgene expression

All transgenes that were integrated into the host genome were under the control of a tetracycline operator. The initial Hek293 FlpIn and HeLa FlpIn cell lines express a tetracycline repressor, which binds to the operator and thereby blocks transgene expression. Transgene expression is induced only upon addition of tetracycline or doxycycline. Cell lines expressing Sgo1, variants thereof or securin were induced with 0.5 *µ*g/ml doxycycline. The (doubly) stable cell lines expressing cohesin subunits were induced with 0.05 *µ*g/ml doxycycline.

4.5.9. Synchronization of mammalian cells

For synchronization at the G1 / S transition thymidine was used, which interferes with the nucleoid metabolism of the cell and blocks DNA replication. For this purpose, the medium 2 mM thymidine (Sigma-Aldrich, Munich, Germany) was added. After 16 to

20 h, cells were released from the arrest by washing once with PBS (see 4.4.2) and addition of medium. After 30 min at 37°C, new medium was added for additional 20 min, followed by another medium exchange.

To arrest cells in prometaphase, either nocodazole (Sigma-Aldrich, Munich, Germany) which disassembles the microtubules of the cytoskeleton or taxol (Calbiochem/Merck, Darmstadt, Germany), which stabilizes the microtubules, was used, both at 0.2 *µ*g/ml. Nocodazole or taxol were added 4 h after a thymidine release or to unsynchronized cells for 16 h.

4.5.10. Taxol-ZM override

For the taxol-ZM override experiments, cells were transfected with *WAPL* or *GL2* siRNA (Wapl1 and Wapl2, 35 nM each or GL2, 70 nM) at ~70 % confluency 26 h prior to a thymidine block for 20 h. Cells were then released into fresh medium. Doxycyline and taxol were added 2 h and 5 h later, respectively, to induce transgene expression and arrest cells in prometaphase. 10 h later, cells were released for the indicated times by replating into medium supplemented with ZM 447439 (5 µM, Tocris Biosciences, Bristol, United Kingdom) and either harvested for Western blotting (see 4.4.2), centrosome isolation (see 4.5.17), or pre-extracted and fixed for IFM (see 4.5.19).

4.5.11. Inhibition of nuclear export by leptomycin B (LMB)

Hek 293T cells were transfected with plasmids encoding mCherry-CTS or mCherry-CTS^{AAA}. After 34 h, cells were trypsinized and plated in two wells of a 6-well containing poly-L-lysine coated cover slips. 12 h later, LMB (or a corresponding volume of ethanol) was added for 11 h (final concentration 20 ng/ml) to inhibit exporin 1-mediated nuclear export. Finally, cells on cover slips were washed once with PBS (see 4.4.2) and directly fixed with methanol (see 4.5.19) without any pre-extraction to preserve the soluble cytoplasmic proteins of the cells.

4.5.12. Myc-Immunoprecipitation (IP)

Lysis buffer 2 (LP2)	20 mM	Tris-HCl, pH 7.7
	100 mM	NaCl
	10 mM	NaF
	20 mM	β-glycerophosphate
	5 mM	$MgCl_2$
	0.1% (v/v)	Triton X-100
	5% (v/v)	glycerol
LP2*	LP2 supplemented with complete protease inhibitor cocktail minus EDTA (Roche, Mannheim, Germany)	

18 h after transfection of Hek293T at 70% confluency, cells expressing Myc_6-Sgo1 A2 or C2 (wt, N61I or Y57A K62A) were arrested in prometaphase using nocodazole. After 14 h mitotic cells were harvested by shake-off, washed once with PBS (see 4.4.2) and resuspended in 2 ml LP2* (for cells of a 14.5 cm dish). Cells were then lysed on ice by at least 10 strokes with a dounce homogenizer (Wheaton, Millville, NJ, USA). After 20 min incubation on ice, the lysates were centrifuged at 16,000 g and 4°C for 10 minutes. The supernatant was then divided in half and incubated with either rabbit anti-Myc beads (Sigma-Aldrich, Munich, Germany, A7470) or unspecific rabbit IgGs (Sigma-Aldrich, Munich, Germany) covalently cross-linked as described in (Herzog et al., 2013). The beads were washed 5 times with 1 ml LP2 (200 g, 1.5 min, 4°C), then supplemented with 2x SDS sample buffer and heated to 95°C to elute associated proteins. This suspension was transferred to Mobicol columns (MoBiTec, Göttingen, Germany) and centrifuged (200 g, 2 min, RT) to separate the eluate from the beads. Samples were analyzed by SDS-PAGE and subsequent Western blot.

4.5.13. Sgo1 depletion and rescue experiments

For the rescue experiments using the transgenic *SGO1* cell lines, expression of siRNA-resistant transgenes was induced at ~30% confluency by addition of doxycycline. After 8 h, cells were treated thymidine for synchronization at the G1/S boundary. 14 h later, cells were transfected with *SGO1* siRNA (Sgo1 5'UTR and Sgo1 ORF1), and after 7 h released into fresh medium (see 4.5.9). 4 h after release, cells were arrested in prometaphase by addition of taxol. 16 h later, cells were

harvested by shake-off and divided into samples for Western blot, chromosome spreads and centrosome preparation or IF on spreads (see below).

For rescue experiments using the doubly stable cohesin cell lines, expression of the FRB/FKBP-tagged transgenes was induced by addition of doxycycline. At the same time cells were depleted of the corresponding endogenous cohesin subunits by siRNA transfection. After 27.5 h, cells were synchronized using thymidine for 25.5 h before *SGO1* siRNA (*SGO1*_ORF2) was transfected. 6 h later, the cells were released from the thymidine block as described above. 8 h after release, taxol and 100 nM rapamycin (or the corresponding volume of DMSO) were added and cells were harvested 13 h later. Rescue of Sgo1 knockdown by PP2A B'α-CTS was carried out by first transfecting Hek293T cells with plasmids encoding for Myc6-PP2A-B'α (WT), Myc6-PP2A B'α-CTS or Myc6-PP2A B'α-CTS^{AAA}. 28.5 h later, thymidine was added to synchronize the cells for 24.5 h before endogenous Sgo1 was knocked down by transfection of siRNA (*SGO1*_5'UTR and *SGO1*_ORF1). After 6 h, cells were released from the thymidine block for 8 h before nocodazole was added to arrest cells in the following prometaphase. 13 h later cells were harvested for centrosome isolation and Western blot (see 4.4.2). For knockdown of murine Sgo1 in NIH 3T3, cells were treated for 14 h with thymidine for synchronization at the G1/S boundary at ~60% confluency, and then transfected with *M.m. SGO1* siRNA (ORF1 and ORF2). 7 h thereafter, cells were released into fresh medium and split into two wells (with and without poly-L-lysine coated cover slips). 4 h after release cells were arrested in prometaphase by addition of taxol. 16 h later cells were harvested by shake-off and divided into samples for Western blot, chromosome spreads and centrosome preparation.

4.5.14. Preparation of SDS-PAGE samples from cell culture

Cells were scraped off the culture dish, pelleted (300 g, 3 min, RT) and washed once with PBS (see 4.4.2). The cells of one well of a 12-well plate (corresponding to a volume of 1 ml medium) were resuspended in 150 µl PBS, supplemented with SDS sample buffer (to 1x, see 4.4.1) and denaturated at 95°C for 15 min before being analyzed by SDS-PAGE and Western blot.

4.5.15. Chromosome spreads

hypotonic medium	40% (v/v)	DMEM (without FCS)
	60% (v/v)	ddH_2O
	500 ng/ml	nocodazole
Carnoy's solution	75% (v/v)	methanol
	25% (v/v)	acedic acid
mounting medium	2.33% (w/v)	1,4-diazabicyclo-[2,2,2]-octaneglycerol
	20 mM	Tris-HCl, pH 8.0
	78% (v/v)	glycerol

For the chromosome spreading cell pellets were resuspended in 250 µl hypotonic medium and incubated for 3 min at RT. Subsequently, another 250 µl hypotonic medium was added followed by incubation for another 3 min. To swell the cells further, 2 ml hypotonic medium was added and the suspension was incubated for 5 min. The swollen cells were centrifuged gently at 100 g for 5 min and carefully resuspended in 20 µl hypotonic medium. Thereafter, 250 µl, 250 µl and 2 ml Carnoy's solution were added sequentially. In order to keep the loss of sticky cells as low as possible, the solution was added zestfully (and not pipetted up and down or vortexed). After 30 min incubation at RT, the cells were washed twice with 1 ml Carnoy's solution (300 g, 4 min), and finally resuspended in 120 - 250 µl Carnoy's solution. Cells were either directly processed or stored at -20°C.

For an optimal distribution of the chromosomes on the slides they were placed on a pre-cooled metal block. The slides were cooled to 0°C, then moistened by breath and 17 µl of the cell suspension was dropped in two aliquots on the slides, which were then dried at 60°C on a heating block covered with a wet paper towel. In order to stain the chromosomes, the dried slides were incubated in Hoechst 33342 (1 µg/ml in PBS) for 10 min, then washed 2 times with PBS and 4 times with ddH_2O. After drying at RT, 5 µl mounting medium was dropped on cover slips (22 x 22 mm), which were carefully placed on the spreads.

4.5.16. Chromosome spreads for additional immunostaining (IF on spreads)

hypotonic buffer 1 (HP1)	50 mM	sucrose
	30 mM	Tris-HCl, pH 8.2
	17 mM	Tri-sodium-citrate
	0.2 µg/ml	nocodazole
hypotonic buffer 2 (HP2)	100 mM	sucrose
fixing solution	1% (v/v)	para-formaldehyde
	5 mM	Na-borate, pH 9.2
	0.15% (v/v)	Triton X-100

Cells from 6-wells were harvested by shake off and pelleted (300 g, 3 min). The pellet was resuspended in 2 ml HP1 and incubated for 7 min at RT. Swollen cells were again centrifuged (100 g, 3 min) and carefully resuspended in 80 µl HP2. 7 µl of the cell suspension were pipetted on a poly-L-lysine coated cover slip (see 4.5.18) that had been immersed in fixing solution. Cells were spread over the cover slip by tilting. After the cover slips had been dried at RT, they were washed several times with PBS and finally submerged to blocking and IFM (see 4.5.19).

4.5.17. Isolation of centrosomes

5x BRB 80	400 mM	Pipes-KOH pH 6.8
	5 mM	$MgCl_2$
	5 mM	EGTA
sucrose cushion	1x	BRB 80
	20 mM	EDTA
	0.01%(v/v)	Triton X-100
	40% (w/v)	sucrose

To isolate centrosomes, mitotic cells from a 10 cm culture dish were harvested by mitotic shake-off. Of the 10 ml suspension, 0.5 ml were taken for analysis by Western blot (see 4.4.2), and when necessary, another 2 ml were processed for chromosome spreading (see 4.5.15). The remaining 9.5 or 7.5 ml of the cell suspension were centrifuged (300 g, 3 min). The cell pellet was washed once with PBS and resuspended in 1 ml LP2* (see 4.5.12) supplemented with DNaseI (20 µg/ml, Roche,

Mannheim, Germany) and nocodazole (1 μg/ml, Sigma-Aldrich, Munich, Germany). Lysis was performed on ice by 10 strokes with a tight dounce homogenizer (Wheaton, Millville, NJ, USA). After incubating on ice for 20 min, lysates were centrifuged at low speed to remove remaining chromatin and cell debris (3,800 g, 10 min, 4°C). Meanwhile, 13 mm round cover slips (Marienfeld, Lauda-Königshofen, Germany) were cleaned with 98% ethanol. The clean cover slips were placed into 15 ml COREX round bottom glass tubes on top of an appropriate adapter and ultimately submersed in 3.5 ml sucrose cushion. Supernatants containing the centrosomes were carefully loaded on top the sucrose cushion, and centrosomes were centrifuged directly onto cover slips (13,000 g, 25 min, 4°C, swing-out rotor). Specimens were fixed in -20°C methanol over night, and later subjected to blocking and IFM (see 4.5.19).

4.5.18. Preparation of poly-L-lysine coated cover slips

Cover slips were coated with poly-L-lysine to facilitate growth of adherent cells. To that end, 13 mm round cover slips (one pack of 100 pieces, Marienfeld, Lauda-Königshofen, Germany) were incubated with 100 ml of a poly-L-lysine solution (0.01% (w/v) in ddH_2O, Sigma-Aldrich, Munich, Germany) in a plastic beaker for 1 h on a horizontal shaker. Subsequently, they were washed 10 times with ddH_2O, before being incubated with 100% ethanol (p.A.) for another hour whilst shaking. Finally, under sterile conditions, they were individually placed inside a 14.5 cm cell culture dish, standing upright by leaning them against the side of the dish until they were properly dried.

4.5.19. Immunofluorescence microscopy (IFM)

CSK	100 mM	NaCl
	300 mM	sucrose
	3 mM	$MgCl_2$
	10 mM	Pipes-NaOH, pH 7.0
CSK-TX	CSK, supplemented with 0.1% (w/v) Triton X-100	
PBS-TX 0.3%	1x PBS	
	0.3% (w/v)	Triton X-100
PBS-FA	1x PBS	
	3.7% (v/v)	formaldehyde
quenching solution	1x PBS	
	50mM	NH_4Cl
blocking solution	1x PBS	
	3% (v/v)	BSA
PBS-TX 0.1%	1x PBS	
	0.1% (w/v)	Triton X-100

Cells grown on poly-L-lysine coated cover slips were washed once with PBS (see 4.4.2). For combinations of pre-extraction and fixation methods for the specific antibodies see table below. For pre-extraction, cells were carefully washed once with CSK buffer, incubated in CSK buffer for 5 min, again washed once with CSK and once with PBS. Alternatively, cells were pre-extracted by incubation with PBS-TX 0.3% for 3 min followed by washing once with PBS.

Cells were either fixed with 100% methanol (-20°C) overnight at -20°C or with formaldehyde (FA). For the latter, cells were incubated with freshly prepared PBS-FA for 15 min, washed once with PBS and treated with quenching solution for 5 min to quench residual fixative. After either method of fixation, cells were further permeabilized, by washing with PBS once, treating with PBS-TX 0.1% for 5 min, washing again with PBS and then incubating in blocking solution for 2 h at room temperature or overnight at 4°C. All following steps were performed at room temperature and PBS or PBS-TX 0.1% was used for all washing steps. Cover slips were incubated with primary antibodies diluted in blocking solution for 2 h, washed 2-3 times, treated with secondary antibodies (in blocking solution) for 1 h and washed again two times. DNA was stained using Hoechst 33342 (2 µg/ml in PBS) for 10 min, after 3 additional washing steps cover slips were mounted on glass slides, by

dropping 3 µl of mounting medium (see 4.5.15) on the slides and carefully placing the cover slips on top of it.

antibody	pre-extraction method	fixation method
C-Nap1	CSK	methanol
centrin 2	CSK	methanol or FA
Crest	CSK	methanol
Myc	CSK	methanol
PP2A C	CSK	FA
RFP	CSK or none	methanol
Sgo2	PBS-TX	FA
Smc1	CSK	FA
γ-tubulin	CSK or PBS-TX	methanol or FA

Centrosome preparations and chromosome spreads were analyzed and imaged on a Zeiss Axioplan 2 fluorescence microscope with a Plan-Apochromat 100x/1.40 Oil DICIII objective, an AxioCam MRm CCD camera and AxioVision software version 4.8.2.0. In all other cases, IFM was performed on a Leica DMI6000 B fluorescence microscope with a HCX PL APO 100x/1.40-0.70 Oil CS objective, a DFC360FX CCD camera and LAS AF software version 2.7.0.9329 (Z-stacks through the cells at 0.2 µm increments). For figures 8B, 11B, 15, 16B, 17, 20, 21B, 22, 24, 26A, 27A, 28, 30, 36C and 37C images were processed by digital 3D deconvolution of Z-axis image series using the LAS-AF software (5 iterations, blind deconvolution algorithm). In all cases, Z-stack series were projected onto one focus plane.

4.5.20. Quantitative analysis of cell cycle stages

To identify the distinct cell cycle stages, cells were trypsinized from the cell culture dish, collected in a 15 ml Falcon (Greiner Bio-One, Kremsmünster, Austria), pelleted (300 g, 3 min, RT) and washed once with PBS to remove residual medium. Cells were resuspended in 200 µl PBS (see 4.4.2) and fixed by dropwise addition of 5 ml -20°C cold 70% ethanol while vortexing. After incubation at 4°C for at least 1 h, cells were washed twice with PBS, 0.2% BSA (300 g, 5 min, RT) and resuspended in 0.5-1 ml 69 µM propidium iodide solution (in 38 mM tri-sodium citrate, Sigma-Aldrich, Munich, Germany) supplemented with 100 µg/ml RNase A (QIAGEN, Hilden,

Germany) to stain the DNA. After an incubation for 1 h at 37°C, cells were passed through a 35 µm nylon mesh cup of a FACS tube (BD Biosciences, Heidelberg, Germany). DNA content was determined using a Beckman Coulter Cytomics FC 500 flow cytometer and the corresponding software CXP Analysis (Beckman Coulter, Krefeld, Germany).

5. REFERENCES

Agircan, F.G., and Schiebel, E. (2014). Sensors at centrosomes reveal determinants of local separase activity. PLoS Genetics *10*, e1004672.

Alberts, A.S., Thorburn, A.M., Shenolikar, S., Mumby, M.C., and Feramisco, J.R. (1993). Regulation of cell cycle progression and nuclear affinity of the retinoblastoma protein by protein phosphatases. Proceedings of the National Academy of Sciences *90*, 388–392.

Andrews, P.D., Ovechkina, Y., Morrice, N., Wagenbach, M., Duncan, K., Wordeman, L., and Swedlow, J.R. (2004). Aurora B regulates MCAK at the mitotic centromere. Developmental Cell *6*, 253–268.

Arquint, C., Sonnen, K.F., Stierhof, Y.-D., and Nigg, E.A. (2012). Cell-cycle-regulated expression of STIL controls centriole number in human cells. Journal of Cell Science *125*, 1342–1352.

Arumugam, P., Gruber, S., Tanaka, K., Haering, C.H., Mechtler, K., and Nasmyth, K. (2003). ATP hydrolysis is required for cohesin's association with chromosomes. Current Biology *13*, 1941–1953.

Avidor-Reiss, T., Khire, A., Fishman, E.L., and Jo, K.H. (2015). Atypical centrioles during sexual reproduction. Frontiers in Cell and Developmental Biology *3*, 21.

Bahe, S., Stierhof, Y.-D., Wilkinson, C.J., Leiss, F., and Nigg, E.A. (2005). Rootletin forms centriole-associated filaments and functions in centrosome cohesion. Journal of Cell Biology *171*, 27–33.

Balestra, F.R., Strnad, P., Flückiger, I., and Gönczy, P. (2013). Discovering regulators of centriole biogenesis through siRNA-based functional genomics in human cells. Developmental Cell *25*, 555–571.

Basto, R., Brunk, K., Vinadogrova, T., Peel, N., Franz, A., Khodjakov, A., and Raff, J.W. (2008). Centrosome amplification can initiate tumorigenesis in flies. Cell *133*, 1032–1042.

Baudat, F., Imai, Y., and de Massy, B. (2013). Meiotic recombination in mammals: localization and regulation. Nature Reviews Genetics *14*, 794–806.

Beauchene, N.A., Diaz-Martinez, L.A., Furniss, K., Hsu, W.-S., Tsai, H.-J., Chamberlain, C., Esponda, P., Giménez-Abián, J.F., and Clarke, D.J. (2010). Rad21 is required for centrosome integrity in human cells independently of its role in chromosome cohesion. Cell Cycle *9*, 1774–1780.

Bernhard, W., and De Harven, E. (1956). [Electron microscopic study of the ultrastructure of centrioles in vertebra]. Zeitschrift für Zellforschung und mikroskopische Anatomie *45*, 378–398.

Bettencourt-Dias, M., and Glover, D.M. (2007). Centrosome biogenesis and function: centrosomics brings new understanding. Nature Reviews Molecular Cell Biology *8*, 451–463.

Boos, D., Kuffer, C., Lenobel, R., Körner, R., and Stemmann, O. (2008). Phosphorylation-dependent binding of cyclin B1 to a Cdc6-like domain of human separase. Journal of Biological Chemistry *283*, 816–823.

Bornens, M. (2002). Centrosome composition and microtubule anchoring mechanisms. Current Opinion in Cell Biology *14*, 25–34.

Buheitel, J., and Stemmann, O. (2013). Prophase pathway-dependent removal of cohesin from human chromosomes requires opening of the Smc3-Scc1 gate. EMBO Journal *32*, 666–676.

Buonomo, S.B., Clyne, R.K., Fuchs, J., Loidl, J., Uhlmann, F., and Nasmyth, K. (2000). Disjunction of homologous chromosomes in meiosis I depends on proteolytic cleavage of the meiotic cohesin Rec8 by separin. Cell *103*, 387–398.

Byers, B., Shriver, K., and Goetsch, L. (1978). The role of spindle pole bodies and modified microtubule ends in the initiation of microtubule assembly in Saccharomyces cerevisiae. Journal of Cell Science *30*, 331–352.

Cabral, G., Sans, S.S., Cowan, C.R., and Dammermann, A. (2013). Multiple mechanisms contribute to centriole separation in C. elegans. Current Biology *23*, 1380–1387.

Chambon, J.-P., Touati, S.A., Berneau, S., Cladière, D., Hebras, C., Groeme, R., McDougall, A., and Wassmann, K. (2013). The PP2A inhibitor I2PP2A is essential for sister chromatid segregation in oocyte meiosis II. Current Biology *23*, 485–490.

Chan, J.Y. (2011). A clinical overview of centrosome amplification in human cancers. International Journal of Biological Sciences *7*, 1122–1144.

Chan, K.-L., Roig, M.B., Hu, B., Beckouët, F., Metson, J., and Nasmyth, K. (2012). Cohesin's DNA exit gate is distinct from its entrance gate and is regulated by acetylation. Cell *150*, 961–974.

Chang, L., and Barford, D. (2014). Insights into the anaphase-promoting complex: a molecular machine that regulates mitosis. Current Opinion in Structural Biology *29*, 1–9.

Chen, R.H., Shevchenko, A., Mann, M., and Murray, A.W. (1998). Spindle checkpoint protein Xmad1 recruits Xmad2 to unattached kinetochores. Journal of Cell Biology *143*, 283–295.

Choi, Y.-K., Liu, P., Sze, S.K., Dai, C., and Qi, R.Z. (2010). CDK5RAP2 stimulates microtubule nucleation by the gamma-tubulin ring complex. Journal of Cell Biology *191*, 1089–1095.

Chrétien, D., Buendia, B., Fuller, S.D., and Karsenti, E. (1997). Reconstruction of the centrosome cycle from cryoelectron micrographs. Journal of Structural Biology *120*,

117–133.

Chung, S. I., Moon, H., Ju, H.-L., Kim, D. Y., Cho, K. J., Ribback, S., et al. (2016). Comparison of liver oncogenic potential among human RAS isoforms. Oncotarget *7*, 7354–7366.

Cimini, D. (2008). Merotelic kinetochore orientation, aneuploidy, and cancer. Biochimica et Biophysica Acta *1786*, 32–40.

Ciosk, R., Shirayama, M., Shevchenko, A., Tanaka, T., Toth, A., Shevchenko, A., and Nasmyth, K. (2000). Cohesin's binding to chromosomes depends on a separate complex consisting of Scc2 and Scc4 proteins. Molecular Cell *5*, 243–254.

Cohen-Fix, O., Peters, J.M., Kirschner, M.W., and Koshland, D. (1996). Anaphase initiation in Saccharomyces cerevisiae is controlled by the APC-dependent degradation of the anaphase inhibitor Pds1p. Genes & Development *10*, 3081–3093.

Cooper, T.A., Wan, L., and Dreyfuss, G. (2009). RNA and disease. Cell *136*, 777–793.

Cottee, M. A., Raff, J. W., Lea, S. M., & Roque, H. (2011). SAS-6 oligomerization: the key to the centriole? Nature Chemical Biology *7*, 650–653.

Csizmok, V., Felli, I.C., Tompa, P., Banci, L., and Bertini, I. (2008). Structural and dynamic characterization of intrinsically disordered human securin by NMR spectroscopy. Journal of the American Chemical Society *130*, 16873–16879.

Cunha-Ferreira, I., Bento, I., and Bettencourt-Dias, M. (2009a). From zero to many: control of centriole number in development and disease. Traffic *10*, 482–498.

Cunha-Ferreira, I., Rodrigues-Martins, A., Bento, I., Riparbelli, M., Zhang, W., Laue, E., Callaini, G., Glover, D.M., and Bettencourt-Dias, M. (2009b). The SCF/Slimb ubiquitin ligase limits centrosome amplification through degradation of SAK/PLK4. Current Biology *19*, 43–49.

Dammermann, A., Müller-Reichert, T., Pelletier, L., Habermann, B., Desai, A., and Oegema, K. (2004). Centriole assembly requires both centriolar and pericentriolar material proteins. Developmental Cell *7*, 815–829.

De Antoni, A., Pearson, C.G., Cimini, D., Canman, J.C., Sala, V., Nezi, L., Mapelli, M., Sironi, L., Faretta, M., Salmon, E.D., and Musacchio, A. (2005). The Mad1/Mad2 complex as a template for Mad2 activation in the spindle assembly checkpoint. Current Biology *15*, 214–225.

Delattre, M., Canard, C., and Gönczy, P. (2006). Sequential protein recruitment in C. elegans centriole formation. Current Biology *16*, 1844–1849.

Delattre, M., Leidel, S., Wani, K., Baumer, K., Bamat, J., Schnabel, H., Feichtinger, R., Schnabel, R., and Gönczy, P. (2004). Centriolar SAS-5 is required for centrosome duplication in C. elegans. Nature Cell Biology *6*, 656–664.

Di Fiore, B., Ciciarello, M., Mangiacasale, R., Palena, A., Tassin, A.-M., Cundari, E.,

and Lavia, P. (2003). Mammalian RanBP1 regulates centrosome cohesion during mitosis. Journal of Cell Science *116*, 3399–3411.

Dingwall, C., and Laskey, R.A. (1991). Nuclear targeting sequences - a consensus? Trends in Biochemical Sciences *16*, 478–481.

Dobbelaere, J., Josué, F., Suijkerbuijk, S., Baum, B., Tapon, N., and Raff, J. (2008). A genome-wide RNAi screen to dissect centriole duplication and centrosome maturation in Drosophila. PLoS Biology *6*, e224.

Dong, W., Li, J., Zhang, H., Huang, Y., He, L., Wang, Z., Shan, Z., and Teng, W. (2015). Altered expression of estrogen receptor β2 is associated with different biological markers and clinicopathological factors in papillary thyroid cancer. International Journal of Clinical and Experimental Pathology *8*, 7149–7156.

Dreier, M.R., Bekier, M.E., and Taylor, W.R. (2011). Regulation of sororin by Cdk1-mediated phosphorylation. Journal of Cell Science *124*, 2976–2987.

Eichinger, C.S., Kurze, A., Oliveira, R.A., and Nasmyth, K. (2013). Disengaging the Smc3/kleisin interface releases cohesin from Drosophila chromosomes during interphase and mitosis. EMBO Journal *32*, 656–665.

Ferguson, R.L., and Maller, J.L. (2008). Cyclin E-dependent localization of MCM5 regulates centrosome duplication. Journal of Cell Science *121*, 3224–3232.

Ferguson, R.L., Pascreau, G., and Maller, J.L. (2010). The cyclin A centrosomal localization sequence recruits MCM5 and Orc1 to regulate centrosome reduplication. Journal of Cell Science *123*, 2743–2749.

Firat-Karalar, E.N., Rauniyar, N., Yates, J.R., and Stearns, T. (2014). Proximity interactions among centrosome components identify regulators of centriole duplication. Current Biology *24*, 664–670.

Foley, E.A., Maldonado, M., and Kapoor, T.M. (2011). Formation of stable attachments between kinetochores and microtubules depends on the B56-PP2A phosphatase. Nature Cell Biology *13*, 1265–1271.

Fong, C.S., Kim, M., Yang, T.T., Liao, J.-C., and Tsou, M.-F.B. (2014). SAS-6 assembly templated by the lumen of cartwheel-less centrioles precedes centriole duplication. Developmental Cell *30*, 238–245.

Fry, A.M., Mayor, T., Meraldi, P., Stierhof, Y.D., Tanaka, K., and Nigg, E.A. (1998). C-Nap1, a novel centrosomal coiled-coil protein and candidate substrate of the cell cycle-regulated protein kinase Nek2. Journal of Cell Biology *141*, 1563–1574.

Fu, J., and Glover, D.M. (2012). Structured illumination of the interface between centriole and peri-centriolar material. Open Biology *2*, 120104.

Funabiki, H., Yamano, H., Kumada, K., Nagao, K., Hunt, T., and Yanagida, M. (1996). Cut2 proteolysis required for sister-chromatid seperation in fission yeast. Nature *381*, 438–441.

Gandhi, R., Gillespie, P.J., and Hirano, T. (2006). Human Wapl is a cohesin-binding protein that promotes sister-chromatid resolution in mitotic prophase. Current Biology *16*, 2406–2417.

Ganem, N.J., Godinho, S.A., and Pellman, D. (2009). A mechanism linking extra centrosomes to chromosomal instability. Nature *460*, 278–282.

Gerlich, D., Koch, B., Dupeux, F., Peters, J.-M., and Ellenberg, J. (2006). Live-cell imaging reveals a stable cohesin-chromatin interaction after but not before DNA replication. Current Biology *16*, 1571–1578.

Gillingham, A.K., and Munro, S. (2000). The PACT domain, a conserved centrosomal targeting motif in the coiled-coil proteins AKAP450 and pericentrin. EMBO Reports *1*, 524–529.

Glenn, G. M., & Eckhart, W. (1993). Mutation of a cysteine residue in polyomavirus middle T antigen abolishes interactions with protein phosphatase 2A, pp60c-src, and phosphatidylinositol-3 kinase, activation of c-fos expression, and cellular transformation. Journal of Virology *67*, 1945–1952.

Glotzer, M., Murray, A.W., and Kirschner, M.W. (1991). Cyclin is degraded by the ubiquitin pathway. Nature *349*, 132–138.

Gomez-Ferreria, M.A., Rath, U., Buster, D.W., Chanda, S.K., Caldwell, J.S., Rines, D.R., and Sharp, D.J. (2007). Human Cep192 is required for mitotic centrosome and spindle assembly. Current Biology *17*, 1960–1966.

Gorr, I.H., Boos, D., and Stemmann, O. (2005). Mutual inhibition of separase and Cdk1 by two-step complex formation. Molecular Cell *19*, 135–141.

Gómez, R., Valdeolmillos, A., Parra, M.T., Viera, A., Carreiro, C., Roncal, F., Rufas, J.S., Barbero, J.L., and Suja, J.A. (2007). Mammalian SGO2 appears at the inner centromere domain and redistributes depending on tension across centromeres during meiosis II and mitosis. EMBO Reports *8*, 173–180.

Gregson, H.C., Schmiesing, J.A., Kim, J.S., Kobayashi, T., Zhou, S., and Yokomori, K. (2001). A potential role for human cohesin in mitotic spindle aster assembly. Journal of Biological Chemistry *276*, 47575–47582.

Groth, A.C., Olivares, E.C., Thyagarajan, B., and Calos, M.P. (2000). A phage integrase directs efficient site-specific integration in human cells. Proceedings of the National Academy of Sciences *97*, 5995–6000.

Gruber, S., Arumugam, P., Katou, Y., Kuglitsch, D., Helmhart, W., Shirahige, K., and Nasmyth, K. (2006). Evidence that loading of cohesin onto chromosomes involves opening of its SMC hinge. Cell *127*, 523–537.

Gruber, S., Haering, C.H., and Nasmyth, K. (2003). Chromosomal cohesin forms a ring. Cell *112*, 765–777.

Guan, J., Ekwurtzel, E., Kvist, U., and Yuan, L. (2008). Cohesin protein SMC1 is a centrosomal protein. Biochemical and Biophysical Research Communications *372*,

761–764.

Guo, H., Reddy, S. A., & Damuni, Z. (1993). Purification and characterization of an autophosphorylation-activated protein serine threonine kinase that phosphorylates and inactivates protein phosphatase 2A. Journal of Biological Chemistry *268*, 11193–11198.

Gupta, G.D., Coyaud, É., Gonçalves, J., Mojarad, B.A., Liu, Y., Wu, Q., Gheiratmand, L., Comartin, D., Tkach, J.M., Cheung, S.W.T., Bashkurov, M., Hasegan, M., Knight, J.D., Lin, Z.Y., Schueler, M., Hildebrandt, F., Moffat, J., Gingras, A.C., Raught, B., and Pelletier, L. (2015). A Dynamic Protein Interaction Landscape of the Human Centrosome-Cilium Interface. Cell *163*, 1484–1499.

Gutiérrez-Caballero, C., Herrán, Y., Sánchez-Martín, M., Angel Suja, J., Luis Barbero, J., Llano, E., and Pendás, A.M. (2011). Identification and molecular characterization of the mammalian alpha-kleisin RAD21L. Cell Cycle *10*, 1477–1487.

Güttler, T., Madl, T., Neumann, P., Deichsel, D., Corsini, L., Monecke, T., Ficner, R., Sattler, M., and Görlich, D. (2010). NES consensus redefined by structures of PKI-type and Rev-type nuclear export signals bound to CRM1. Nature Structural & Molecular Biology *17*, 1367–1376.

Haarhuis, J.H.I., Elbatsh, A.M.O., van den Broek, B., Camps, D., Erkan, H., Jalink, K., Medema, R.H., and Rowland, B.D. (2013). WAPL-mediated removal of cohesin protects against segregation errors and aneuploidy. Current Biology *23*, 2071–2077.

Habedanck, R., Stierhof, Y.-D., Wilkinson, C.J., and Nigg, E.A. (2005). The Polo kinase Plk4 functions in centriole duplication. Nature Cell Biology *7*, 1140–1146.

Haering, C.H., Löwe, J., Hochwagen, A., and Nasmyth, K. (2002). Molecular architecture of SMC proteins and the yeast cohesin complex. Molecular Cell *9*, 773–788.

Hanahan, D., and Weinberg, R.A. (2011). Hallmarks of cancer: the next generation. Cell *144*, 646–674.

Hara, K., Zheng, G., Qu, Q., Liu, H., Ouyang, Z., Chen, Z., Tomchick, D.R., and Yu, H. (2014). Structure of cohesin subcomplex pinpoints direct shugoshin-Wapl antagonism in centromeric cohesion. Nature Structural & Molecular Biology *21*, 864–870.

Hardwick, K.G., Johnston, R.C., Smith, D.L., and Murray, A.W. (2000). MAD3 encodes a novel component of the spindle checkpoint which interacts with Bub3p, Cdc20p, and Mad2p. Journal of Cell Biology *148*, 871–882.

Harr, B., and Turner, L.M. (2010). Genome-wide analysis of alternative splicing evolution among Mus subspecies. Molecular Ecology *19*, 228–239.

Hauf, S., Roitinger, E., Koch, B., Dittrich, C.M., Mechtler, K., and Peters, J.-M. (2005). Dissociation of cohesin from chromosome arms and loss of arm cohesion during early mitosis depends on phosphorylation of SA2. PLoS Biology *3*, e69.

Hellmuth, S., Böttger, F., Pan, C., Mann, M., and Stemmann, O. (2014). PP2A delays APC/C-dependent degradation of separase-associated but not free securin. EMBO Journal *33*, 1134–1147.

Hellmuth, S., Pöhlmann, C., Brown, A., Böttger, F., Sprinzl, M., and Stemmann, O. (2015a). Positive and negative regulation of vertebrate separase by cdk1-cyclin b1 may explain why securin is dispensable. Journal of Biological Chemistry *290*, 8002–8010.

Hellmuth, S., Rata, S., Brown, A., Heidmann, S., Novak, B., & Stemmann, O. (2015). Human chromosome segregation involves multi-layered regulation of separase by the peptidyl-prolyl-isomerase Pin1. Molecular Cell *58*, 495–506.

Helps, N.R., Luo, X., Barker, H.M., and Cohen, P.T. (2000). NIMA-related kinase 2 (Nek2), a cell-cycle-regulated protein kinase localized to centrosomes, is complexed to protein phosphatase 1. Biochemical Journal *349*, 509–518.

Hemerly, A.S., Prasanth, S.G., Siddiqui, K., and Stillman, B. (2009). Orc1 controls centriole and centrosome copy number in human cells. Science *323*, 789–793.

Hertig, A.T., and Adams, E.C. (1967). Studies on the human oocyte and its follicle. I. Ultrastructural and histochemical observations on the primordial follicle stage. Journal of Cell Biology *34*, 647–675.

Herzog, S., Nagarkar Jaiswal, S., Urban, E., Riemer, A., Fischer, S., and Heidmann, S.K. (2013). Functional dissection of the Drosophila melanogaster condensin subunit Cap-G reveals its exclusive association with condensin I. PLoS Genetics *9*, e1003463.

Holland, A.J., and Taylor, S.S. (2006). Cyclin-B1-mediated inhibition of excess separase is required for timely chromosome disjunction. Journal of Cell Science *119*, 3325–3336.

Holland, A.J., Böttger, F., Stemmann, O., and Taylor, S.S. (2007). Protein phosphatase 2A and separase form a complex regulated by separase autocleavage. Journal of Biological Chemistry *282*, 24623–24632.

Holland, A.J., Fachinetti, D., Zhu, Q., Bauer, M., Verma, I.M., Nigg, E.A., and Cleveland, D.W. (2012). The autoregulated instability of Polo-like kinase 4 limits centrosome duplication to once per cell cycle. Genes & Development *26*, 2684–2689.

Howell, B.J., McEwen, B.F., Canman, J.C., Hoffman, D.B., Farrar, E.M., Rieder, C.L., and Salmon, E.D. (2001). Cytoplasmic dynein/dynactin drives kinetochore protein transport to the spindle poles and has a role in mitotic spindle checkpoint inactivation. Journal of Cell Biology *155*, 1159–1172.

Hu, B., Itoh, T., Mishra, A., Katoh, Y., Chan, K.-L., Upcher, W., Godlee, C., Roig, M.B., Shirahige, K., and Nasmyth, K. (2011). ATP hydrolysis is required for relocating cohesin from sites occupied by its Scc2/4 loading complex. Current Biology *21*, 12–24.

Huang, H., Feng, J., Famulski, J., Rattner, J.B., Liu, S.T., Kao, G.D., Muschel, R.,

Chan, G.K.T., and Yen, T.J. (2007). Tripin/hSgo2 recruits MCAK to the inner centromere to correct defective kinetochore attachments. Journal of Cell Biology *177*, 413–424.

Ishiguro, K.-I., Kim, J., Shibuya, H., Hernández-Hernández, A., Suzuki, A., Fukagawa, T., Shioi, G., Kiyonari, H., Li, X.C., Schimenti, J., Höög, C., and Watanabe, I. (2014). Meiosis-specific cohesin mediates homolog recognition in mouse spermatocytes. Genes & Development *28*, 594–607.

Ishiguro, T., Tanaka, K., Sakuno, T., and Watanabe, Y. (2010). Shugoshin-PP2A counteracts casein-kinase-1-dependent cleavage of Rec8 by separase. Nature Cell Biology *12*, 500–506.

Iwaizumi, M., Shinmura, K., Mori, H., Yamada, H., Suzuki, M., Kitayama, Y., Igarashi, H., Nakamura, T., Suzuki, H., Watanabe, Y., Hishida, A., Ikuma, M., Sugimura, H. (2009). Human Sgo1 downregulation leads to chromosomal instability in colorectal cancer. Gut *58*, 249–260.

Izquierdo, D., Wang, W.-J., Uryu, K., and Tsou, M.-F.B. (2014). Stabilization of cartwheel-less centrioles for duplication requires CEP295-mediated centriole-to-centrosome conversion. Cell Reports *8*, 957–965.

Jallepalli, P.V., Waizenegger, I.C., Bunz, F., Langer, S., Speicher, M.R., Peters, J.M., Kinzler, K.W., Vogelstein, B., and Lengauer, C. (2001). Securin is required for chromosomal stability in human cells. Cell *105*, 445–457.

Jäger, H., Herzig, B., Herzig, A., Sticht, H., Lehner, C.F., and Heidmann, S. (2004). Structure predictions and interaction studies indicate homology of separase N-terminal regulatory domains and Drosophila THR. Cell Cycle *3*, 182–188.

Kahyo, T., Iwaizumi, M., Shinmura, K., Matsuura, S., Nakamura, T., Watanabe, Y., Yamada, H., and Sugimura, H. (2011). A novel tumor-derived SGOL1 variant causes abnormal mitosis and unstable chromatid cohesion. Oncogene *30*, 4453–4463.

Kang, J., Chaudhary, J., Dong, H., Kim, S., Brautigam, C.A., and Yu, H. (2011). Mitotic centromeric targeting of HP1 and its binding to Sgo1 are dispensable for sister-chromatid cohesion in human cells. Molecular Biology of the Cell *22*, 1181–1190.

Kapoor, T.M., Mayer, T.U., Coughlin, M.L., and Mitchison, T.J. (2000). Probing spindle assembly mechanisms with monastrol, a small molecule inhibitor of the mitotic kinesin, Eg5. Journal of Cell Biology *150*, 975–988.

Karamysheva, Z., Diaz-Martinez, L.A., Crow, S.E., Li, B., and Yu, H. (2009). Multiple anaphase-promoting complex/cyclosome degrons mediate the degradation of human Sgo1. Journal of Biological Chemistry *284*, 1772–1780.

Kashina, A.S., Baskin, R.J., Cole, D.G., Wedaman, K.P., Saxton, W.M., and Scholey, J.M. (1996). A bipolar kinesin. Nature *379*, 270–272.

Kastan, M.B., and Bartek, J. (2004). Cell-cycle checkpoints and cancer. Nature *432*, 316–323.

Katis, V.L., Gálová, M., Rabitsch, K.P., Gregan, J., and Nasmyth, K. (2004). Maintenance of cohesin at centromeres after meiosis I in budding yeast requires a kinetochore-associated protein related to MEI-S332. Current Biology *14*, 560–572.

Katis, V.L., Lipp, J.J., Imre, R., Bogdanova, A., Okaz, E., Habermann, B., Mechtler, K., Nasmyth, K., and Zachariae, W. (2010). Rec8 phosphorylation by casein kinase 1 and Cdc7-Dbf4 kinase regulates cohesin cleavage by separase during meiosis. Developmental Cell *18*, 397–409.

Kawashima, S.A., Yamagishi, Y., Honda, T., Ishiguro, K.-I., and Watanabe, Y. (2010). Phosphorylation of H2A by Bub1 prevents chromosomal instability through localizing shugoshin. Science *327*, 172–177.

Keeling, J., Tsiokas, L., and Maskey, D. (2016). Cellular Mechanisms of Ciliary Length Control. Cells *5*.

Kemp, C.A., Kopish, K.R., Zipperlen, P., Ahringer, J., and O'Connell, K.F. (2004). Centrosome maturation and duplication in C. elegans require the coiled-coil protein SPD-2. Developmental Cell *6*, 511–523.

Kerrebrock, A.W., Miyazaki, W.Y., Birnby, D., and Orr-Weaver, T.L. (1992). The Drosophila mei-S332 gene promotes sister-chromatid cohesion in meiosis following kinetochore differentiation. Genetics *130*, 827–841.

Kerrebrock, A.W., Moore, D.P., Wu, J.S., and Orr-Weaver, T.L. (1995). Mei-S332, a Drosophila protein required for sister-chromatid cohesion, can localize to meiotic centromere regions. Cell *83*, 247–256.

Kim, J., Lee, K., and Rhee, K. (2015). PLK1 regulation of PCNT cleavage ensures fidelity of centriole separation during mitotic exit. Nature Communications *6*, 10076.

Kim, Y., Holland, A.J., Lan, W., and Cleveland, D.W. (2010). Aurora kinases and protein phosphatase 1 mediate chromosome congression through regulation of CENP-E. Cell *142*, 444–455.

Kirkham, M., Müller-Reichert, T., Oegema, K., Grill, S., and Hyman, A.A. (2003). SAS-4 is a C. elegans centriolar protein that controls centrosome size. Cell *112*, 575–587.

Kitagawa, D., Vakonakis, I., Olieric, N., Hilbert, M., Keller, D., Olieric, V., Bortfeld, M., Erat, M.C., Flückiger, I., Gönczy, P., and Steinmetz, M.O. (2011). Structural basis of the 9-fold symmetry of centrioles. Cell *144*, 364–375.

Kitajima, T.S., Hauf, S., Ohsugi, M., Yamamoto, T., and Watanabe, Y. (2005). Human Bub1 defines the persistent cohesion site along the mitotic chromosome by affecting Shugoshin localization. Current Biology *15*, 353–359.

Kitajima, T.S., Kawashima, S.A., and Watanabe, Y. (2004). The conserved kinetochore protein shugoshin protects centromeric cohesion during meiosis. Nature *427*, 510–517.

Kitajima, T.S., Sakuno, T., Ishiguro, K.-I., Iemura, S.-I., Natsume, T., Kawashima,

S.A., and Watanabe, Y. (2006). Shugoshin collaborates with protein phosphatase 2A to protect cohesin. Nature *441*, 46–52.

Klein, F., Mahr, P., Galova, M., Buonomo, S.B., Michaelis, C., Nairz, K., and Nasmyth, K. (1999). A central role for cohesins in sister chromatid cohesion, formation of axial elements, and recombination during yeast meiosis. Cell *98*, 91–103.

Kleylein-Sohn, J., Westendorf, J., Le Clech, M., Habedanck, R., Stierhof, Y.-D., and Nigg, E.A. (2007). Plk4-induced centriole biogenesis in human cells. Developmental Cell *13*, 190–202.

Kline-Smith, S.L., Khodjakov, A., Hergert, P., and Walczak, C.E. (2004). Depletion of centromeric MCAK leads to chromosome congression and segregation defects due to improper kinetochore attachments. Molecular Biology of the Cell *15*, 1146–1159.

Knauer, S.K., Bier, C., Habtemichael, N., and Stauber, R.H. (2006). The Survivin-Crm1 interaction is essential for chromosomal passenger complex localization and function. EMBO Reports *7*, 1259–1265.

Kogut, I., Wang, J., Guacci, V., Mistry, R.K., and Megee, P.C. (2009). The Scc2/Scc4 cohesin loader determines the distribution of cohesin on budding yeast chromosomes. Genes & Development *23*, 2345–2357.

Kohlmaier, G., Loncarek, J., Meng, X., McEwen, B.F., Mogensen, M.M., Spektor, A., Dynlacht, B.D., Khodjakov, A., and Gönczy, P. (2009). Overly long centrioles and defective cell division upon excess of the SAS-4-related protein CPAP. Current Biology *19*, 1012–1018.

Kong, X., Ball, A.R., Sonoda, E., Feng, J., Takeda, S., Fukagawa, T., Yen, T.J., and Yokomori, K. (2009). Cohesin associates with spindle poles in a mitosis-specific manner and functions in spindle assembly in vertebrate cells. Molecular Biology of the Cell *20*, 1289–1301.

Krantz, I.D., McCallum, J., DeScipio, C., Kaur, M., Gillis, L.A., Yaeger, D., Jukofsky, L., Wasserman, N., Bottani, A., Morris, C.A., Nowaczyk, M.J.M., Toriello, H., Bamshad, M.J., Carey, J.C. Rappaport, E., Kawauchi, S., Lander, A.D., Calof, AnL., Li, H.-H., Devoto, M., and Jackson, L.G. (2004). Cornelia de Lange syndrome is caused by mutations in NIPBL, the human homolog of Drosophila melanogaster Nipped-B. Nature Genetics *36*, 631–635.

Kudo, N.R., Anger, M., Peters, A.H.F.M., Stemmann, O., Theussl, H.-C., Helmhart, W., Kudo, H., Heyting, C., and Nasmyth, K. (2009). Role of cleavage by separase of the Rec8 kleisin subunit of cohesin during mammalian meiosis I. Journal of Cell Science *122*, 2686–2698.

Kueng, S., Hegemann, B., Peters, B.H., Lipp, J.J., Schleiffer, A., Mechtler, K., and Peters, J.-M. (2006). Wapl controls the dynamic association of cohesin with chromatin. Cell *127*, 955–967.

Kuriyama, R., and Borisy, G.G. (1981). Centriole cycle in Chinese hamster ovary cells as determined by whole-mount electron microscopy. Journal of Cell Biology *91*,

814–821.

Ladurner, R., Bhaskara, V., Huis in 't Veld, P.J., Davidson, I.F., Kreidl, E., Petzold, G., and Peters, J.-M. (2014). Cohesin's ATPase activity couples cohesin loading onto DNA with Smc3 acetylation. Current Biology *24*, 2228–2237.

Lan, W., Zhang, X., Kline-Smith, S.L., Rosasco, S.E., Barrett-Wilt, G.A., Shabanowitz, J., Hunt, D.F., Walczak, C.E., and Stukenberg, P.T. (2004). Aurora B phosphorylates centromeric MCAK and regulates its localization and microtubule depolymerization activity. Current Biology *14*, 273–286.

Lawo, S., Hasegan, M., Gupta, G.D., and Pelletier, L. (2012). Subdiffraction imaging of centrosomes reveals higher-order organizational features of pericentriolar material. Nature Cell Biology *14*, 1148–1158.

Lechward, K., Awotunde, O.S., Swiatek, W., and Muszyńska, G. (2001). Protein phosphatase 2A: variety of forms and diversity of functions. Acta Biochimica Polonica *48*, 921–933.

Lee, J.Y., Hayashi-Hagihara, A., and Orr-Weaver, T.L. (2005). Roles and regulation of the Drosophila centromere cohesion protein MEI-S332 family. Philosophical Transactions of the Royal Society B: Biological Sciences *360*, 543–552.

Lee, J., Kitajima, T.S., Tanno, Y., Yoshida, K., Morita, T., Miyano, T., Miyake, M., and Watanabe, Y. (2008). Unified mode of centromeric protection by shugoshin in mammalian oocytes and somatic cells. Nature Cell Biology *10*, 42–52.

Lee, K., and Rhee, K. (2011). PLK1 phosphorylation of pericentrin initiates centrosome maturation at the onset of mitosis. Journal of Cell Biology *195*, 1093–1101.

Lee, K., and Rhee, K. (2012). Separase-dependent cleavage of pericentrin B is necessary and sufficient for centriole disengagement during mitosis. Cell Cycle *11*, 2476–2485.

Lee, S., and Rhee, K. (2010). CEP215 is involved in the dynein-dependent accumulation of pericentriolar matrix proteins for spindle pole formation. Cell Cycle *9*, 774–783.

Leidel, S., and Gönczy, P. (2003). SAS-4 is essential for centrosome duplication in C elegans and is recruited to daughter centrioles once per cell cycle. Developmental Cell *4*, 431–439.

Leidel, S., Delattre, M., Cerutti, L., Baumer, K., and Gönczy, P. (2005). SAS-6 defines a protein family required for centrosome duplication in C. elegans and in human cells. Nature Cell Biology *7*, 115–125.

Leismann, O., Herzig, A., Heidmann, S., and Lehner, C.F. (2000). Degradation of Drosophila PIM regulates sister chromatid separation during mitosis. Genes & Development *14*, 2192–2205.

Lingle, W.L., Barrett, S.L., Negron, V.C., D'Assoro, A.B., Boeneman, K., Liu, W.,

Whitehead, C.M., Reynolds, C., and Salisbury, J.L. (2002). Centrosome amplification drives chromosomal instability in breast tumor development. Proceedings of the National Academy of Sciences *99*, 1978–1983.

Liu, H., Jia, L., and Yu, H. (2013a). Phospho-H2A and cohesin specify distinct tension-regulated Sgo1 pools at kinetochores and inner centromeres. Current Biology *23*, 1927–1933.

Liu, H., Qu, Q., Warrington, R., Rice, A., Cheng, N., and Yu, H. (2015). Mitotic Transcription Installs Sgo1 at Centromeres to Coordinate Chromosome Segregation. Molecular Cell *59*, 426–436.

Liu, H., Rankin, S., and Yu, H. (2013b). Phosphorylation-enabled binding of SGO1-PP2A to cohesin protects sororin and centromeric cohesion during mitosis. Nature Cell Biology *15*, 40–49.

Llano, E., Gómez, R., Gutiérrez-Caballero, C., Herrán, Y., Sánchez-Martín, M., Vázquez-Quiñones, L., Hernández, T., de Álava, E., Cuadrado, A., Barbero, J.L., Suja, J.A., and Pendàs, A.M. (2008). Shugoshin-2 is essential for the completion of meiosis but not for mitotic cell division in mice. Genes & Development *22*, 2400–2413.

Llano, E., Herrán, Y., García-Tuñón, I., Gutiérrez-Caballero, C., de Álava, E., Barbero, J.L., Schimenti, J., de Rooij, D.G., Sánchez-Martín, M., and Pendás, A.M. (2012). Meiotic cohesin complexes are essential for the formation of the axial element in mice. Journal of Cell Biology *197*, 877–885.

Losada, A., Hirano, M., and Hirano, T. (1998). Identification of Xenopus SMC protein complexes required for sister chromatid cohesion. Genes & Development *12*, 1986–1997.

Lu, F., Lan, R., Zhang, H., Jiang, Q., and Zhang, C. (2009). Geminin is partially localized to the centrosome and plays a role in proper centrosome duplication. Biology of the Cell *101*, 273–285.

Luo, X., Tang, Z., Rizo, J., and Yu, H. (2002). The Mad2 spindle checkpoint protein undergoes similar major conformational changes upon binding to either Mad1 or Cdc20. Molecular Cell *9*, 59–71.

Luo, X., Tang, Z., Xia, G., Wassmann, K., Matsumoto, T., Rizo, J., and Yu, H. (2004). The Mad2 spindle checkpoint protein has two distinct natively folded states. Nature Structural & Molecular Biology *11*, 338–345.

Lüders, J., and Stearns, T. (2007). Microtubule-organizing centres: a re-evaluation. Nature Reviews Molecular Cell Biology *8*, 161–167.

Lüders, J., Patel, U.K., and Stearns, T. (2006). GCP-WD is a gamma-tubulin targeting factor required for centrosomal and chromatin-mediated microtubule nucleation. Nature Cell Biology *8*, 137–147.

Manandhar, G., Simerly, C., and Schatten, G. (2000). Highly degenerated distal centrioles in rhesus and human spermatozoa. Human Reproduction *15*, 256–263.

Mapelli, M., Filipp, F.V., Rancati, G., Massimiliano, L., Nezi, L., Stier, G., Hagan, R.S., Confalonieri, S., Piatti, S., Sattler, M., and Musacchio, A. (2006). Determinants of conformational dimerization of Mad2 and its inhibition by p31comet. EMBO Journal *25*, 1273–1284.

Mardin, B.R., Agircan, F.G., Lange, C., and Schiebel, E. (2011). Plk1 controls the Nek2A-PP1γ antagonism in centrosome disjunction. Current Biology *21*, 1145–1151.

Mardin, B.R., Lange, C., Baxter, J.E., Hardy, T., Scholz, S.R., Fry, A.M., and Schiebel, E. (2010). Components of the Hippo pathway cooperate with Nek2 kinase to regulate centrosome disjunction. Nature Cell Biology *12*, 1166–1176.

Marshall, W.F. (2009). Centriole evolution. Current Opinion in Cell Biology *21*, 14–19.

Marston, A.L. (2015). Shugoshins: tension-sensitive pericentromeric adaptors safeguarding chromosome segregation. Molecular and Cellular Biology *35*, 634–648.

Marston, A.L., Tham, W.-H., Shah, H., and Amon, A. (2004). A genome-wide screen identifies genes required for centromeric cohesion. Science *303*, 1367–1370.

Matsumoto, Y., Hayashi, K., and Nishida, E. (1999). Cyclin-dependent kinase 2 (Cdk2) is required for centrosome duplication in mammalian cells. Current Biology *9*, 429–432.

Matsumoto, Y., and Maller, J.L. (2004). A centrosomal localization signal in cyclin E required for Cdk2-independent S phase entry. Science *306*, 885–888.

Matsuo, K., Ohsumi, K., Iwabuchi, M., Kawamata, T., Ono, Y., and Takahashi, M. (2012). Kendrin is a novel substrate for separase involved in the licensing of centriole duplication. Current Biology *22*, 915–921.

Matsuura, S., Kahyo, T., Shinmura, K., Iwaizumi, M., Yamada, H., Funai, K., Kobayashi, J., Tanahashi, M., Niwa, H., Ogawa, H., Takahashi, T., Inui, N., Suda, T., Chida, K., Watanabe, Y, and Sugimura, H. (2013). SGOL1 variant B induces abnormal mitosis and resistance to taxane in non-small cell lung cancers. Scientific Reports *3*, 3012.

McGuinness, B.E., Hirota, T., Kudo, N.R., Peters, J.-M., and Nasmyth, K. (2005). Shugoshin prevents dissociation of cohesin from centromeres during mitosis in vertebrate cells. PLoS Biology *3*, e86.

Mei, J., Huang, X., and Zhang, P. (2001). Securin is not required for cellular viability, but is required for normal growth of mouse embryonic fibroblasts. Current Biology *11*, 1197–1201.

Melby, T.E., Ciampaglio, C.N., Briscoe, G., and Erickson, H.P. (1998). The symmetrical structure of structural maintenance of chromosomes (SMC) and MukB proteins: long, antiparallel coiled coils, folded at a flexible hinge. Journal of Cell Biology *142*, 1595–1604.

Mennella, V., Keszthelyi, B., McDonald, K.L., Chhun, B., Kan, F., Rogers, G.C., Huang, B., and Agard, D.A. (2012). Subdiffraction-resolution fluorescence

microscopy reveals a domain of the centrosome critical for pericentriolar material organization. Nature Cell Biology *14*, 1159–1168.

Meraldi, P., Lukas, J., Fry, A.M., Bartek, J., and Nigg, E.A. (1999). Centrosome duplication in mammalian somatic cells requires E2F and Cdk2-cyclin A. Nature Cell Biology *1*, 88–93.

Mohr, L., Buheitel, J., Schöckel, L., Karalus, D., Mayer, B., and Stemmann, O. (2015). An Alternatively Spliced Bifunctional Localization Signal Reprograms Human Shugoshin 1 to Protect Centrosomal Instead of Centromeric Cohesin. Cell Reports *12*, 2156–2168.

Moritz, M., Braunfeld, M.B., Guénebaut, V., Heuser, J., and Agard, D.A. (2000). Structure of the gamma-tubulin ring complex: a template for microtubule nucleation. Nature Cell Biology *2*, 365–370.

Moyer, T.C., Clutario, K.M., Lambrus, B.G., Daggubati, V., and Holland, A.J. (2015). Binding of STIL to Plk4 activates kinase activity to promote centriole assembly. Journal of Cell Biology *209*, 863–878.

Murayama, Y., and Uhlmann, F. (2015). DNA Entry into and Exit out of the Cohesin Ring by an Interlocking Gate Mechanism. Cell *163*, 1628–1640.

Murray, A.W. (2004). Recycling the cell cycle: cyclins revisited. Cell *116*, 221–234.

Nasmyth, K. (2011). Cohesin: a catenase with separate entry and exit gates? Nature Cell Biology *13*, 1170–1177.

Neupert, W., and Herrmann, J.M. (2007). Translocation of proteins into mitochondria. Annual Review of Biochemistry *76*, 723–749.

Nishiyama, T., Ladurner, R., Schmitz, J., Kreidl, E., Schleiffer, A., Bhaskara, V., Bando, M., Shirahige, K., Hyman, A.A., Mechtler, K., and Peters, J.M. (2010). Sororin mediates sister chromatid cohesion by antagonizing Wapl. Cell *143*, 737–749.

Nishiyama, T., Sykora, M.M., Huis in 't Veld, P.J., Mechtler, K., and Peters, J.-M. (2013). Aurora B and Cdk1 mediate Wapl activation and release of acetylated cohesin from chromosomes by phosphorylating Sororin. Proceedings of the National Academy of Sciences *110*, 13404–13409.

Nogales, E., Whittaker, M., Milligan, R.A., and Downing, K.H. (1999). High-resolution model of the microtubule. Cell *96*, 79–88.

Nogales, E., Wolf, S.G., and Downing, K.H. (1998). Structure of the alpha beta tubulin dimer by electron crystallography. Nature *391*, 199–203.

O'Connell, K.F., Caron, C., Kopish, K.R., Hurd, D.D., Kemphues, K.J., Li, Y., and White, J.G. (2001). The C. elegans zyg-1 gene encodes a regulator of centrosome duplication with distinct maternal and paternal roles in the embryo. Cell *105*, 547–558.

Oka, Y., Varmark, H., Vitting-Seerup, K., Beli, P., Waage, J., Hakobyan, A., Mistrik,

M., Choudhary, C., Rohde, M., Bekker-Jensen, S., and Mailand, N. (2014). UBL5 is essential for pre-mRNA splicing and sister chromatid cohesion in human cells. EMBO Reports *15*, 956–964.

Orth, M., Mayer, B., Rehm, K., Rothweiler, U., Heidmann, D., Holak, T.A., and Stemmann, O. (2011). Shugoshin is a Mad1/Cdc20-like interactor of Mad2. EMBO Journal *30*, 2868–2880.

Palazzo, R.E., Vogel, J.M., Schnackenberg, B.J., Hull, D.R., and Wu, X. (2000). Centrosome maturation. Current Topics in Developmental Biology *49*, 449–470.

Palframan, W.J., Meehl, J.B., Jaspersen, S.L., Winey, M., and Murray, A.W. (2006). Anaphase inactivation of the spindle checkpoint. Science *313*, 680–684.

Pelletier, L., O'Toole, E., Schwager, A., Hyman, A.A., and Müller-Reichert, T. (2006). Centriole assembly in Caenorhabditis elegans. Nature *444*, 619–623.

Pelletier, L., Ozlü, N., Hannak, E., Cowan, C., Habermann, B., Ruer, M., Müller-Reichert, T., and Hyman, A.A. (2004). The Caenorhabditis elegans centrosomal protein SPD-2 is required for both pericentriolar material recruitment and centriole duplication. Current Biology *14*, 863–873.

Pezzi, N., Prieto, I., Kremer, L., Pérez Jurado, L.A., Valero, C., Del Mazo, J., Martínez-A, C., and Barbero, J.L. (2000). STAG3, a novel gene encoding a protein involved in meiotic chromosome pairing and location of STAG3-related genes flanking the Williams-Beuren syndrome deletion. FASEB Journal *14*, 581–592.

Pfleger, C.M., Lee, E., and Kirschner, M.W. (2001). Substrate recognition by the Cdc20 and Cdh1 components of the anaphase-promoting complex. Genes & Development *15*, 2396–2407.

Pfleghaar, K., Heubes, S., Cox, J., Stemmann, O., and Speicher, M.R. (2005). Securin is not required for chromosomal stability in human cells. PLoS Biology *3*, e416.

Pihan, G.A., Purohit, A., Wallace, J., Malhotra, R., Liotta, L., and Doxsey, S.J. (2001). Centrosome defects can account for cellular and genetic changes that characterize prostate cancer progression. Cancer Research *61*, 2212–2219.

Polakova, S., Cipak, L., and Gregan, J. (2011). RAD21L is a novel kleisin subunit of the cohesin complex. Cell Cycle *10*, 1892–1893.

Prieto, I., Suja, J.A., Pezzi, N., Kremer, L., Martínez-A, C., Rufas, J.S., and Barbero, J.L. (2001). Mammalian STAG3 is a cohesin specific to sister chromatid arms in meiosis I. Nature Cell Biology *3*, 761–766.

Rabitsch, K.P., Gregan, J., Schleiffer, A., Javerzat, J.P., Eisenhaber, F., and Nasmyth, K. (2004). Two fission yeast homologs of Drosophila Mei-S332 are required for chromosome segregation during meiosis I and II. Current Biology *14*, 287–301.

Rattani, A., Wolna, M., Ploquin, M., Helmhart, W., Morrone, S., Mayer, B., Godwin,

J., Xu, W., Stemmann, O., Pendas, A., and Nasmyth, K. (2013). Sgol2 provides a regulatory platform that coordinates essential cell cycle processes during meiosis I in oocytes. eLife *2*, e01133.

Reddy, S.K., Rape, M., Margansky, W.A., and Kirschner, M.W. (2007). Ubiquitination by the anaphase-promoting complex drives spindle checkpoint inactivation. Nature *446*, 921–925.

Revenkova, E., Eijpe, M., Heyting, C., Gross, B., and Jessberger, R. (2001). Novel meiosis-specific isoform of mammalian SMC1. Molecular and Cellular Biology *21*, 6984–6998.

Revenkova, E., Eijpe, M., Heyting, C., Hodges, C.A., Hunt, P.A., Liebe, B., Scherthan, H., and Jessberger, R. (2004). Cohesin SMC1 beta is required for meiotic chromosome dynamics, sister chromatid cohesion and DNA recombination. Nature Cell Biology *6*, 555–562.

Riedel, C.G., Katis, V.L., Katou, Y., Mori, S., Itoh, T., Helmhart, W., Gálová, M., Petronczki, M., Gregan, J., Cetin, B., Mudrak, I., Ogris, E., Mechtler, K., Pelletier, L., Buchholz, F., Shirahige, K., and Nasmyth, K. (2006). Protein phosphatase 2A protects centromeric sister chromatid cohesion during meiosis I. Nature *441*, 53–61.

Rodriguez-Bravo, V., Maciejowski, J., Corona, J., Buch, H.K., Collin, P., Kanemaki, M.T., Shah, J.V., and Jallepalli, P.V. (2014). Nuclear pores protect genome integrity by assembling a premitotic and Mad1-dependent anaphase inhibitor. Cell *156*, 1017–1031.

Rogers, G.C., Rusan, N.M., Roberts, D.M., Peifer, M., and Rogers, S.L. (2009). The SCF Slimb ubiquitin ligase regulates Plk4/Sak levels to block centriole reduplication. Journal of Cell Biology *184*, 225–239.

Roig, M.B., Löwe, J., Chan, K.-L., Beckouët, F., Metson, J., and Nasmyth, K. (2014). Structure and function of cohesin's Scc3/SA regulatory subunit. FEBS Letters *588*, 3692–3702.

Rolef Ben-Shahar, T., Heeger, S., Lehane, C., East, P., Flynn, H., Skehel, M., and Uhlmann, F. (2008). Eco1-dependent cohesin acetylation during establishment of sister chromatid cohesion. Science *321*, 563–566.

Ronne, H., Carlberg, M., Hu, G.Z., and Nehlin, J.O. (1991). Protein phosphatase 2A in Saccharomyces cerevisiae: effects on cell growth and bud morphogenesis. Molecular and Cellular Biology *11*, 4876–4884.

Roux, K.J., Kim, D.I., Raida, M., and Burke, B. (2012). A promiscuous biotin ligase fusion protein identifies proximal and interacting proteins in mammalian cells. Journal of Cell Biology *196*, 801–810.

Rowland, B.D., Roig, M.B., Nishino, T., Kurze, A., Uluocak, P., Mishra, A., Beckouët, F., Underwood, P., Metson, J., Imre, R., Mechtler, K., Katis, V.L., and Nasmyth, K. (2009). Building sister chromatid cohesion: smc3 acetylation counteracts an antiestablishment activity. Molecular Cell *33*, 763–774.

Rumpf, C., Cipak, L., Dudas, A., Benko, Z., Pozgajova, M., Riedel, C.G., Ammerer, G., Mechtler, K., and Gregan, J. (2010). Casein kinase 1 is required for efficient removal of Rec8 during meiosis I. Cell Cycle *9*, 2657–2662.

Salic, A., Waters, J.C., and Mitchison, T.J. (2004). Vertebrate shugoshin links sister centromere cohesion and kinetochore microtubule stability in mitosis. Cell *118*, 567–578.

Salmon, E.D., Cimini, D., Cameron, L.A., and DeLuca, J.G. (2005). Merotelic kinetochores in mammalian tissue cells. Philosophical Transactions of the Royal Society B: Biological Sciences *360*, 553–568.

Santaguida, S., and Amon, A. (2015). Short- and long-term effects of chromosome mis-segregation and aneuploidy. Nature Reviews Molecular Cell Biology *16*, 473–485.

Santaguida, S., Tighe, A., D'Alise, A.M., Taylor, S.S., and Musacchio, A. (2010). Dissecting the role of MPS1 in chromosome biorientation and the spindle checkpoint through the small molecule inhibitor reversine. Journal of Cell Biology *190*, 73–87.

Santaguida, S., Vernieri, C., Villa, F., Ciliberto, A., and Musacchio, A. (2011). Evidence that Aurora B is implicated in spindle checkpoint signalling independently of error correction. EMBO Journal *30*, 1508–1519.

Sathananthan, A.H. (1997). Ultrastructure of the human egg. Human Cell *10*, 21–38.

Sathananthan, A.H., Ratnam, S.S., Ng, S.C., Tarín, J.J., Gianaroli, L., and Trounson, A. (1996). The sperm centriole: its inheritance, replication and perpetuation in early human embryos. Human Reproduction *11*, 345–356.

Schatz, G., and Dobberstein, B. (1996). Common principles of protein translocation across membranes. Science *271*, 1519–1526.

Schmidt, T.I., Kleylein-Sohn, J., Westendorf, J., Le Clech, M., Lavoie, S.B., Stierhof, Y.-D., and Nigg, E.A. (2009). Control of centriole length by CPAP and CP110. Current Biology *19*, 1005–1011.

Schmitz, J., Watrin, E., Lénárt, P., Mechtler, K., and Peters, J.-M. (2007). Sororin is required for stable binding of cohesin to chromatin and for sister chromatid cohesion in interphase. Current Biology *17*, 630–636.

Schöckel, L., Möckel, M., Mayer, B., Boos, D., and Stemmann, O. (2011). Cleavage of cohesin rings coordinates the separation of centrioles and chromatids. Nature Cell Biology *13*, 966–972.

Schönthal, A.H. (2001). Role of serine/threonine protein phosphatase 2A in cancer. Cancer Letters *170*, 1–13.

Schuldt, A. (2011). Cytoskeleton: SAS-6 turns a cartwheel trick. Nature Reviews Molecular Cell Biology *12*, 137.

Seo, M.Y., Jang, W., and Rhee, K. (2015). Integrity of the Pericentriolar Material Is

Essential for Maintaining Centriole Association during M Phase. PLoS ONE *10*, e0138905.

Seshacharyulu, P., Pandey, P., Datta, K., and Batra, S.K. (2013). Phosphatase: PP2A structural importance, regulation and its aberrant expression in cancer. Cancer Letters *335*, 9–18.

Shannon, K.B., Canman, J.C., and Salmon, E.D. (2002). Mad2 and BubR1 function in a single checkpoint pathway that responds to a loss of tension. Molecular Biology of the Cell *13*, 3706–3719.

Sir, J.-H., Pütz, M., Daly, O., Morrison, C.G., Dunning, M., Kilmartin, J.V., and Gergely, F. (2013). Loss of centrioles causes chromosomal instability in vertebrate somatic cells. Journal of Cell Biology *203*, 747–756.

Sluder, G., and Rieder, C.L. (1985). Centriole number and the reproductive capacity of spindle poles. Journal of Cell Biology *100*, 887–896.

Sonnen, K.F., Gabryjonczyk, A.-M., Anselm, E., Stierhof, Y.-D., and Nigg, E.A. (2013). Human Cep192 and Cep152 cooperate in Plk4 recruitment and centriole duplication. Journal of Cell Science *126*, 3223–3233.

Sonnen, K.F., Schermelleh, L., Leonhardt, H., and Nigg, E.A. (2012). 3D-structured illumination microscopy provides novel insight into architecture of human centrosomes. Biology Open *1*, 965–976.

Stemmann, O., Zou, H., Gerber, S.A., Gygi, S.P., and Kirschner, M.W. (2001). Dual inhibition of sister chromatid separation at metaphase. Cell *107*, 715–726.

Strnad, P., Leidel, S., Vinogradova, T., Euteneuer, U., Khodjakov, A., and Gönczy, P. (2007). Regulated HsSAS-6 levels ensure formation of a single procentriole per centriole during the centrosome duplication cycle. Developmental Cell *13*, 203–213.

Sudakin, V., Chan, G.K., and Yen, T.J. (2001). Checkpoint inhibition of the APC/C in HeLa cells is mediated by a complex of BUBR1, BUB3, CDC20, and MAD2. Journal of Cell Biology *154*, 925–936.

Sundaramoorthy, S., Vázquez-Novelle, M.D., Lekomtsev, S., Howell, M., and Petronczki, M. (2014). Functional genomics identifies a requirement of pre-mRNA splicing factors for sister chromatid cohesion. EMBO Journal *33*, 2623–2642.

Sveshnikova, I. (1952). [Comparative analysis of centrosomes in animal and plant cell]. Doklady Akademii nauk SSSR *84*, 797–800.

Tachibana, K.-E.K., Gonzalez, M.A., Guarguaglini, G., Nigg, E.A., and Laskey, R.A. (2005). Depletion of licensing inhibitor geminin causes centrosome overduplication and mitotic defects. EMBO Reports *6*, 1052–1057.

Takahashi, M., Yamagiwa, A., Nishimura, T., Mukai, H., and Ono, Y. (2002). Centrosomal proteins CG-NAP and kendrin provide microtubule nucleation sites by anchoring gamma-tubulin ring complex. Molecular Biology of the Cell *13*, 3235–3245.

Tang, C.-J.C., Fu, R.-H., Wu, K.-S., Hsu, W.-B., and Tang, T.K. (2009). CPAP is a cell-cycle regulated protein that controls centriole length. Nature Cell Biology *11*, 825–831.

Tang, C.-J.C., Lin, S.-Y., Hsu, W.-B., Lin, Y.-N., Wu, C.-T., Lin, Y.-C., Chang, C.-W., Wu, K.-S., and Tang, T.K. (2011). The human microcephaly protein STIL interacts with CPAP and is required for procentriole formation. EMBO Journal *30*, 4790–4804.

Tang, Z., Shu, H., Qi, W., Mahmood, N.A., Mumby, M.C., and Yu, H. (2006). PP2A is required for centromeric localization of Sgo1 and proper chromosome segregation. Developmental Cell *10*, 575–585.

Tang, Z., Sun, Y., Harley, S.E., Zou, H., and Yu, H. (2004). Human Bub1 protects centromeric sister-chromatid cohesion through Shugoshin during mitosis. Proceedings of the National Academy of Sciences *101*, 18012–18017.

Tanno, Y., Kitajima, T.S., Honda, T., Ando, Y., Ishiguro, K.-I., and Watanabe, Y. (2010). Phosphorylation of mammalian Sgo2 by Aurora B recruits PP2A and MCAK to centromeres. Genes & Development *24*, 2169–2179.

Teichner, A., Eytan, E., Sitry-Shevah, D., Miniowitz-Shemtov, S., Dumin, E., Gromis, J., and Hershko, A. (2011). p31comet Promotes disassembly of the mitotic checkpoint complex in an ATP-dependent process. Proceedings of the National Academy of Sciences *108*, 3187–3192.

Teixidó-Travesa, N., Villén, J., Lacasa, C., Bertran, M.T., Archinti, M., Gygi, S.P., Caelles, C., Roig, J., and Lüders, J. (2010). The gammaTuRC revisited: a comparative analysis of interphase and mitotic human gammaTuRC redefines the set of core components and identifies the novel subunit GCP8. Molecular Biology of the Cell *21*, 3963–3972.

Tonkin, E.T., Wang, T.-J., Lisgo, S., Bamshad, M.J., and Strachan, T. (2004). NIPBL, encoding a homolog of fungal Scc2-type sister chromatid cohesion proteins and fly Nipped-B, is mutated in Cornelia de Lange syndrome. Nature Genetics *36*, 636–641.

Tsou, M.-F.B., and Stearns, T. (2006). Mechanism limiting centrosome duplication to once per cell cycle. Nature *442*, 947–951.

Tsou, M.-F.B., Wang, W.-J., George, K.A., Uryu, K., Stearns, T., and Jallepalli, P.V. (2009). Polo kinase and separase regulate the mitotic licensing of centriole duplication in human cells. Developmental Cell *17*, 344–354.

Tsukahara, T., Tanno, Y., and Watanabe, Y. (2010). Phosphorylation of the CPC by Cdk1 promotes chromosome bi-orientation. Nature *467*, 719–723.

Tung, H.Y.L., Alemany, S., and Cohen, P. (1985). The protein phosphatases involved in cellular regulation. European Journal of Biochemistry *148*, 253–263.

Uhlmann, F., Lottspeich, F., and Nasmyth, K. (1999). Sister-chromatid separation at anaphase onset is promoted by cleavage of the cohesin subunit Scc1. Nature *400*, 37–42.

van Breugel, M., Hirono, M., Andreeva, A., Yanagisawa, H.-A., Yamaguchi, S., Nakazawa, Y., Morgner, N., Petrovich, M., Ebong, I.-O., Robinson, C.V., Johnson, C.M., Veprintsev, D., and Zuber, B. (2011). Structures of SAS-6 suggest its organization in centrioles. Science *331*, 1196–1199.

van der Lelij, P., Stocsits, R.R., Ladurner, R., Petzold, G., Kreidl, E., Koch, B., Schmitz, J., Neumann, B., Ellenberg, J., and Peters, J.-M. (2014). SNW1 enables sister chromatid cohesion by mediating the splicing of sororin and APC2 pre-mRNAs. EMBO Journal *33*, 2643–2658.

Vázquez-Novelle, M.D., Sansregret, L., Dick, A.E., Smith, C.A., McAinsh, A.D., Gerlich, D.W., and Petronczki, M. (2014). Cdk1 inactivation terminates mitotic checkpoint surveillance and stabilizes kinetochore attachments in anaphase. Current Biology *24*, 638–645.

Venkatesan, S., Natarajan, A.T., and Hande, M.P. (2015). Chromosomal instability—mechanisms and consequences. Insights Into Formation and Consequences of Chromosome Aberrations: Report on the 11th International Symposium on Chromosomal Aberrations (ISCA 11), Rhodes , Greece, September 12-14, 2014 *793*, 176–184.

Viadiu, H., Stemmann, O., Kirschner, M.W., and Walz, T. (2005). Domain structure of separase and its binding to securin as determined by EM. Nature Structural & Molecular Biology *12*, 552–553.

Vink, M., Simonetta, M., Transidico, P., Ferrari, K., Mapelli, M., De Antoni, A., Massimiliano, L., Ciliberto, A., Faretta, M., Salmon, E.D., and Musacchio, A. (2006). In vitro FRAP identifies the minimal requirements for Mad2 kinetochore dynamics. Current Biology *16*, 755–766.

Vorobjev, I.A., and Chentsov YuS (1982). Centrioles in the cell cycle. I. Epithelial cells. Journal of Cell Biology *93*, 938–949.

Vulprecht, J., David, A., Tibelius, A., Castiel, A., Konotop, G., Liu, F., Bestvater, F., Raab, M.S., Zentgraf, H., Izraeli, and Krämer, A. (2012). STIL is required for centriole duplication in human cells. Journal of Cell Science *125*, 1353–1362.

Waizenegger, I.C., Hauf, S., Meinke, A., and Peters, J.M. (2000). Two distinct pathways remove mammalian cohesin from chromosome arms in prophase and from centromeres in anaphase. Cell *103*, 399–410.

Waizenegger, I., Giménez-Abián, J.F., Wernic, D., and Peters, J.-M. (2002). Regulation of human separase by securin binding and autocleavage. Current Biology *12*, 1368–1378.

Wang, L.-H., Yen, C.-J., Li, T.-N., Elowe, S., Wang, W.-C., and Wang, L.H.-C. (2015). Sgo1 is a potential therapeutic target for hepatocellular carcinoma. Oncotarget *6*, 2023–2033.

Wang, W.J., Soni, R.K., Uryu, K., and Bryan Tsou, M.F. (2011). The conversion of centrioles to centrosomes: essential coupling of duplication with segregation. Journal of Cell Biology *193*, 727–739.

Wang, X., Yang, Y., and Dai, W. (2006). Differential subcellular localizations of two human Sgo1 isoforms: implications in regulation of sister chromatid cohesion and microtubule dynamics. Cell Cycle *5*, 635–640.

Wang, X., Yang, Y., Duan, Q., Jiang, N., Huang, Y., Darzynkiewicz, Z., and Dai, W. (2008). sSgo1, a major splice variant of Sgo1, functions in centriole cohesion where it is regulated by Plk1. Developmental Cell *14*, 331–341.

Watanabe, Y., and Nurse, P. (1999). Cohesin Rec8 is required for reductional chromosome segregation at meiosis. Nature *400*, 461–464.

Watrin, E., Demidova, M., Watrin, T., Hu, Z., and Prigent, C. (2014). Sororin pre-mRNA splicing is required for proper sister chromatid cohesion in human cells. EMBO Reports *15*, 948–955.

Watrin, E., Schleiffer, A., Tanaka, K., Eisenhaber, F., Nasmyth, K., and Peters, J.-M. (2006). Human Scc4 is required for cohesin binding to chromatin, sister-chromatid cohesion, and mitotic progression. Current Biology *16*, 863–874.

Weitzer, S., Lehane, C., and Uhlmann, F. (2003). A model for ATP hydrolysis-dependent binding of cohesin to DNA. Current Biology *13*, 1930–1940.

Welburn, J.P.I., Vleugel, M., Liu, D., Yates, J.R., Lampson, M.A., Fukagawa, T., and Cheeseman, I.M. (2010). Aurora B phosphorylates spatially distinct targets to differentially regulate the kinetochore-microtubule interface. Molecular Cell *38*, 383–392.

Wiese, C., and Zheng, Y. (2000). A new function for the gamma-tubulin ring complex as a microtubule minus-end cap. Nature Cell Biology *2*, 358–364.

Wong, R.W., and Blobel, G. (2008). Cohesin subunit SMC1 associates with mitotic microtubules at the spindle pole. Proceedings of the National Academy of Sciences *105*, 15441–15445.

Xu, Z., Cetin, B., Anger, M., Cho, U.S., Helmhart, W., Nasmyth, K., and Xu, W. (2009). Structure and function of the PP2A-shugoshin interaction. Molecular Cell *35*, 426–441.

Yamada, H.Y., Yao, Y., Wang, X., Zhang, Y., Huang, Y., Dai, W., and Rao, C.V. (2012). Haploinsufficiency of SGO1 results in deregulated centrosome dynamics, enhanced chromosomal instability and colon tumorigenesis. Cell Cycle *11*, 479–488.

Yamada, H.Y., Zhang, Y., Reddy, A., Mohammed, A., Lightfoot, S., Dai, W., and Rao, C.V. (2015). Tumor-promoting/progressing role of additional chromosome instability in hepatic carcinogenesis in Sgo1 (Shugoshin 1) haploinsufficient mice. Carcinogenesis *36*, 429–440.

Yamagishi, Y., Honda, T., Tanno, Y., and Watanabe, Y. (2010). Two histone marks establish the inner centromere and chromosome bi-orientation. Science *330*, 239–243.

Yamamoto, A., Guacci, V., and Koshland, D. (1996). Pds1p, an inhibitor of anaphase

in budding yeast, plays a critical role in the APC and checkpoint pathway(s). Journal of Cell Biology *133*, 99–110.

Yang, J., Adamian, M., and Li, T. (2006). Rootletin interacts with C-Nap1 and may function as a physical linker between the pair of centrioles/basal bodies in cells. Molecular Biology of the Cell *17*, 1033–1040.

Zhang, J., Shi, X., Li, Y., Kim, B.-J., Jia, J., Huang, Z., Yang, T., Fu, X., Jung, S.Y., Wang, Y., Zhang, P., Kim, S-T., Pan, X., and Qin, J. (2008). Acetylation of Smc3 by Eco1 is required for S phase sister chromatid cohesion in both human and yeast. Molecular Cell *31*, 143–151.

Zhang, N., Panigrahi, A.K., Mao, Q., and Pati, D. (2011). Interaction of Sororin protein with polo-like kinase 1 mediates resolution of chromosomal arm cohesion. Journal of Biological Chemistry *286*, 41826–41837.

Zhu, F., Lawo, S., Bird, A., Pinchev, D., Ralph, A., Richter, C., Müller-Reichert, T., Kittler, R., Hyman, A.A., and Pelletier, L. (2008). The mammalian SPD-2 ortholog Cep192 regulates centrosome biogenesis. Current Biology *18*, 136–141.

Zimmerman, W., and Doxsey, S.J. (2000). Construction of centrosomes and spindle poles by molecular motor-driven assembly of protein particles. Traffic *1*, 927–934.

Zimmerman, W.C., Sillibourne, J., Rosa, J., and Doxsey, S.J. (2004). Mitosis-specific anchoring of gamma tubulin complexes by pericentrin controls spindle organization and mitotic entry. Molecular Biology of the Cell *15*, 3642–3657.

Zolnierowicz, S., Csortos, C., Bondor, J., Verin, A., Mumby, M.C., and DePaoli-Roach, A.A. (1994). Diversity in the regulatory B-subunits of protein phosphatase 2A: identification of a novel isoform highly expressed in brain. Biochemistry *33*, 11858–11867.

Zou, H., McGarry, T.J., Bernal, T., and Kirschner, M.W. (1999). Identification of a vertebrate sister-chromatid separation inhibitor involved in transformation and tumorigenesis. Science *285*, 418–422.

6. ABBREVIATIONS

3D-SIM	3 dimensional structured illumination microscopy
aa	amino acid(s)
APC/C	anaphase promoting complex / cyclosome
ATP	Adenosine triphosphate
bp	base pairs
BSA	bovine serum albumine
C-	carboxy-
C. elegans	*Caenorhabditis elegans*
Cdk	cyclin-dependent kinase
cDNA	copy DNA
CIN	chromosomal instability
CLS	centrosomal localization signal (of cyclin A and cyclin E)
CPC	chromosomal passenger complex
CTS	centrosomal targeting signal of human Sgo1
Da	Dalton
DNA	deoxyribonucleic acid
dNTP	deoxyribonucleotide triphosphate
dox	doxycycline
DTT	dithiothreitol
E. coli	*Escherichia coli*
Eco1	establishment of cohesion 1
EDTA	ethylenediamine tetraacetic acid
EGTA	ethylene glycol tetraacetic acid
FKBP	FK506 binding protein
FRB	FKBP-rapamycin binding domain of mTOR
GAPDH	Glyceraldehyde 3-phosphate dehydrogenase
GCP	γ-tubulin complex protein
GTP	Guanosine triphosphate
GTPase	Guanosine triphosphate hydrolase

h	human
H2A	histone 2 A
HBS	HEPES buffered saline
Hek	human embryonic kidney
HeLa	Henrietta Lacks (patient from whom cell line is derived)
HEPES	4-(2-hydroxyethyl)-1-piperazineethanesulfonic acid
HRP	horse radish peroxidase
IFM	immunofluorescence microscopy
IgG	immunoglobulin G
IP	Immunoprecipitation
kb	kilobase pairs
LB	lysogeny broth
LMB	leptomycin B
m	mouse
MCC	mitotic checkpoint complex
MCS	multiple cloning site
MEF	mouse embryonic fibroblast
mRNA	messenger RNA
MT	microtubule
MTOC	microtubule organizing center
N-	amino-
NEBD	nuclear envelope breakdown
NES	nuclear export sequence
noc	nocodazole
OD	optical density
ORF	open reading frame
PAGE	polyacrylamide gel electrophoresis
PBS	phosphate buffered saline
PCM	pericentriolar material
PCNT	pericentrin
PCR	polymerase chain reaction
Pds5	precocious dissociation of sisters
Pipes	piperazine-N,N'-bis(2-ethanesulfonic acid)

Plk	Polo-like kinase
Pol II	RNA polymerase II
PP1	protein phosphatase 1
PP2A	protein phosphatase 2A
PVDF	polyvinylidene fluorid
qPCR	quantitative PCR
rapa	rapamycin
RNA	ribonucleic acid
RNAi	RNA interference
RT	room temperature
SA	stromalin antigen
SAC	spindle assembly checkpoint
Scc	sister chromatid cohesion
SCF	Skp-cullin-F-box class ubiquitin ligase
SDS	sodium dodecyl sulfate
Sgo	shugoshin
siRNA	small interfering RNA
Smc	structural maintenance of cohesin
snRNA	small nuclear RNA
tax	taxol
TEMED	Tetramethylethylenediamine
Tris	tris(hydroxymethyl)aminomethane
U	unit(s)
UTR	untranslated region
v/v	volume per volume
w/v	weight per volume
Wapl	wings apart-like
WB	Western blot
WT	wild type
X. laevis	*Xenopus laevis*
ZM	ZM447439
γTuRC	γ-tubulin ring complex

7. PUBLIKATION

Im Rahmen dieser Arbeit ist die folgende Veröffentlichung entstanden:

Mohr, L., Buheitel, J., Schöckel, L., Karalus, D., Mayer, B., Stemmann, O., 2015. An Alternatively Spliced Bifunctional Localization Signal Reprograms Human Shugoshin 1 to Protect Centrosomal Instead of Centromeric Cohesin. Cell Rep 12, 2156–2168. doi:10.1016/j.celrep.2015.08.045

8. DANKSAGUNG

Ich möchte mich an erster Stelle bei Olaf Stemmann für die Bereitstellung des äußerst interessanten Themas bedanken. Seine Unterstützung, seine Ideen und unsere wissenschaftlichen Diskussion haben mich stets motiviert. Außerdem möchte ich ihm dafür danken, dass er es mir ermöglicht hat an zahlreichen Meetings teilzunehmen.

Weiterhin gilt mein Dank allen Mitgliedern des Prüfungsausschusses, für ihr Interesse und ihre Zeit. Ein besonderer Dank geht außerdem an die weiteren Mitglieder meines Ph.D. Mentorats Stefan Geimer und Kaus Ersfeld. Außerdem möchte ich mich bei Susannah Rankin für die Bereitstellung von Antikörpern bedanken.

Bei allen ehemaligen und aktuellen Mitgliedern der Arbeitsgruppe Stemmann, Franziska Böttger, Andreas Brown, Johannes Buheitel, Heike Haase, Doris Heidmann, Petra Helies, Susanne Hellmuth, Markus Herrmann, Jutta Hübner, Philip Kahlen, Juliane Karich, Bernd Mayer, Michaela Meyerholz, Brigitte Neumann, Moni Ohlraun, Michael Orth, Laura Schöckel, Markus Schuster, Petra Seidler und Peter Wolf bedanke ich mich für die Hilfestellungen im Labor und die angenehme Arbeitsatmosphäre. Außerdem gedankt sei allen Mitgliedern der Arbeitsgruppen Heidmann und Ersfeld: Karin Angermann, Sabine Herzog, Brigitte Jaunich, Anna Riemer, Krisina Seel und Evelin Urban. Unsere gemeinsamen Grillpartys, Feuerzangenbowlen- und Filmabende waren eine angenehme Abwechslung zum Laboralltag.

Philip, dem besten Labor-Mitbewohner aller Zeiten möchte ich für seine Aufmunterungen, Denkanstöße, unsere fachlichen Diskussionen, seine Unkompliziertheit, Freundschaft und gute Musik danken. Bei Susi möchte ich mich für die gemeinsame Zeit am Lehrstuhl voller Hochs und Tiefs und ihr Vertrauen bedanken und für ihre Freundschaft. Besonderer Dank geht an Petra Helies, deren, Hilfsbereitschaft und allzeit moralische Unterstützung mir Vieles erleichtert hat.

Meinen Bachelor und Master Studenten Sevn Becker, Michi Schulz, Christian Lips danke ich für ich für ihren Einsatz und die gute Zusammenarbeit.

Meinen Eltern, meinem Bruder Florian und meiner ganzen Familie möchte ich dafür danken, dass sie mir immer den Rücken gestärkt und an mich geglaubt haben.

Abschließend bedanke ich mich bei meinem Freund Johannes Buheitel für das Korrekturlesen dieser Arbeit und die Unterstützung und Zusammenarbeit bei unserem Paper und während des Studiums und der Doktorarbeit. Danke, dass du immer für mich da bist. Ohne dich wäre ich nicht so weit gekommen.

(Eidesstattliche) Versicherungen und Erklärungen

(§ 8 S. 2 Nr. 6 PromO)

Hiermit erkläre ich mich damit einverstanden, dass die elektronische Fassung meiner Dissertation unter Wahrung meiner Urheberrechte und des Datenschutzes einer gesonderten Überprüfung hinsichtlich der eigenständigen Anfertigung der Dissertation unterzogen werden kann.

(§8 S. 2 Nr. 8 PromO)

Hiermit erkläre ich eidesstattlich, dass ich die Dissertation selbständig verfasst und keine anderen als die von mir angegebenen Quellen und Hilfsmittel benutzt habe.

(§8 S. 2 Nr. 9 PromO)

Ich habe die Dissertation nicht bereits zur Erlangung eines akademischen Grades anderweitig eingereicht und habe auch nicht bereits diese oder eine gleichartige Doktorprüfung endgültig nicht bestanden.

(§8 S. 2 Nr. 10 PromO)

Hiermit erkläre ich, dass ich keine Hilfe von gewerblichen Promotionsberatern bzw. –vermittlern in Anspruch genommen habe und auch künftig nicht nehmen werde.

Bayreuth, den 04.07.2016 _____

Lisa Mohr